

DISSERTATION

Intranasal soluble ACE2 improves organ histopathology and survival in k18hACE2 mice infected with SARS-CoV-2

Intranasales lösliches ACE2 Protein verbessert Überleben und Organhistopathologie in SARS-CoV-2 infizierten k18hACE2 Mäusen

zur Erlangung des akademischen Grades  
Doctor medicinae (Dr. med.)

vorgelegt der Medizinischen Fakultät  
Charité – Universitätsmedizin Berlin

von

Hassler, Luise

Erstbetreuung: Prof. Dr. Michael Bader

Datum der Promotion: 28.02.2025



## Table of Contents

<b>List of tables</b> .....	<b>iii</b>
<b>List of figures</b> .....	<b>iv</b>
<b>List of abbreviations</b> .....	<b>v</b>
<b>Abstract (German)</b> .....	<b>1</b>
<b>Abstract (English)</b> .....	<b>3</b>
<b>1 Introduction</b> .....	<b>4</b>
<b>1.1 Angiotensin-converting enzyme 2: enzyme of the Renin-Angiotensin-system and cell entry receptor for SARS-CoV-2</b> .....	<b>4</b>
<b>1.2 ACE2 decoy proteins for SARS-CoV-2 infection</b> .....	<b>5</b>
<b>1.3 ACE2 618-DDC-ABD protects k18hACE2 infected with SARS-CoV-2</b> .....	<b>7</b>
<b>1.4 Intranasal versus intraperitoneal and pre- versus post viral inoculation administration of ACE2 618-DDC-ABD in k18hACE2 mice infected with SARS-CoV-2</b> .....	<b>7</b>
<b>2 Methods</b> .....	<b>9</b>
<b>2.1 SARS-CoV-2 Infectivity studies in A549 and Vero E6 cells</b> .....	<b>9</b>
<b>2.2 SARS-CoV-2 Infectivity studies in k18hACE2 mice</b> .....	<b>10</b>
2.2.1 Pre-treatment protocol .....	11
2.2.2 Post-treatment protocol .....	11
<b>2.3 Sample analysis</b> .....	<b>12</b>
2.3.1 Hematoxylin and eosin staining .....	12
2.3.2 Immunofluorescence staining .....	13
2.3.3 Plaque assay for infectious virus .....	13
<b>2.4 ACE2 enzymatic activity in the brain</b> .....	<b>14</b>
<b>2.5 Statistics</b> .....	<b>14</b>
<b>3 Results</b> .....	<b>16</b>
<b>3.1 ACE2 618-DDC-ABD neutralizes SARS-CoV-2 infection in A549 and Vero E6 cells</b> .....	<b>16</b>
<b>3.2 SARS-CoV-2 infection in k18hACE2 mice</b> .....	<b>18</b>
3.2.1 ACE2 618-DDC-ABD administration pre- and post-viral inoculation .....	18

---

3.2.2 ACE2 618-DDC-ABD administration only post-viral inoculation.....	18
3.2.3 SARS-CoV-2 titers in brains and lungs .....	20
3.2.4 ACE2 618-DDC-ABD can be detected in the brain after intranasal administration.....	21
3.2.5 Brain histopathology in SARS-CoV-2 infected k18hACE2 mice that received ACE2 618-DDC-ABD pre- and post-viral inoculation .....	22
3.2.6 Brain histopathology in SARS-CoV-2 infected k18hACE2 mice that received ACE2 618-DDC-ABD only post-viral inoculation .....	26
3.2.7 Lung histopathology in SARS-CoV-2 infected k18hACE2 mice that received ACE2 618-DDC-ABD pre- and post-viral inoculation .....	28
3.2.8 Lung histopathology in SARS-CoV-2 infected k18hACE2 mice that received ACE2 618-DDC-ABD only post-viral inoculation .....	30
<b>4 Discussion.....</b>	<b>32</b>
<b>4.1 Main findings.....</b>	<b>32</b>
<b>4.2 State of research of soluble ACE2 proteins for SARS-CoV-2 .....</b>	<b>35</b>
<b>4.3 Universality of ACE2 proteins for SARS-CoV-2 infection .....</b>	<b>36</b>
<b>4.4 Conclusion .....</b>	<b>37</b>
<b>References .....</b>	<b>39</b>
<b>Eidesstattliche Versicherung .....</b>	<b>49</b>
<b>Declaration of contribution .....</b>	<b>50</b>
<b>Printed copy of the publication.....</b>	<b>52</b>
<b>CV .....</b>	<b>65</b>
<b>Complete list of publications .....</b>	<b>67</b>
<b>Acknowledgements.....</b>	<b>69</b>

---

**List of tables**

<b>Table 1.</b> Scoring system for health evaluation of SARS-CoV-2 infected k18hACE2 mice.....	Page 10
<b>Table 2.</b> Scoring system for lung histopathology in k18hACE2 mice infected with SARS-CoV-2.....	Page 12
<b>Table 3.</b> Scoring system for brain histopathology in k18hACE2 mice infected with SARS-CoV-2.....	Page 13

---

## List of figures

- Figure 1.** Hypothesized mechanism of action of soluble ACE2 proteins in SARS-CoV-2 infection..... Page 5
- Figure 2.** Binding affinity for the SARS-CoV-2 S1-RBD protein and duration of action of soluble ACE2 proteins..... Page 6
- Figure 3.** Treatment scheme for SARS-CoV-2 inoculated k18hACE2 mice... Page 11
- Figure 4.** ACE2 618-DDC-ABD neutralizes wildtype and omicron SARS-CoV-2 infection *in vitro*. .... Page 17
- Figure 5.** Survival, body weight change and clinical score in k18hACE2 mice infected with SARS-CoV-2..... Page 19
- Figure 6.** Brain and lung SARS-CoV-2 titers in k18hACE2 mice infected with SARS-CoV-2..... Page 21
- Figure 7.** Brain histopathology and immunofluorescence staining for GFAP and IBA1 in k18hACE2 mice infected with SARS-CoV-2 that received ACE2 618-DDC-ABD pre- and post-viral inoculation..... Page 23
- Figure 8.** GFAP and IBA1 immunofluorescence in k18hACE2 mice infected with SARS-CoV-2 that received ACE2 618-DDC-ABD pre- and post-viral inoculation..... Page 25
- Figure 9.** Brain histopathology in k18hACE2 mice infected with SARS-CoV-2 that received ACE2 618-DDC-ABD only post-viral inoculation..... Page 27
- Figure 10.** Lung histopathology in k18hACE2 mice infected with SARS-CoV-2 that received ACE2 618-DDC-ABD pre- and post-viral inoculation..... Page 29
- Figure 11.** Lung histopathology in k18hACE2 mice infected with SARS-CoV-2 that received ACE2 618-DDC-ABD post viral inoculation only..... Page 31

---

## List of abbreviations

ACE2 = Angiotensin converting enzyme 2  
SARS-CoV = Severe acute respiratory syndrome coronavirus  
COVID-19 = Coronavirus disease 2019  
PFU = plaque forming units  
BSA = Bovine serum albumin  
PBS = Phosphate-buffered saline  
RAS = Renin-Angiotensin-system  
Ang = Angiotensin  
RBD = Receptor binding domain  
TMPRSS2 = transmembrane serine protease 2  
ABD = albumin binding domain  
DDC = dodecapeptide  
RFU = relative fluorescence  
IN = Intranasal(ly)  
IP = Intraperitoneal(ly)  
BSL-3 = Biosafety safety level 3  
CDC = Centers for Disease Control and Prevention  
IACUC = Institutional Animal Care and Use Committees  
BW = body weight  
H&E = hematoxylin and eosin  
PMN = polymorphonuclear neutrophils  
IBA1 = ionized calcium binding adapter molecule 1  
GFAP = glial fibrillary acidic protein  
DMEM = Dulbeccos Modified Eagle Medium  
FBS = fetal bovine serum  
ACE2KO = ACE2 knockout mice  
PRCP = prolylcarboxypeptidase  
RIPA = Radioimmunoprecipitation assay  
BCA = Bicinchoninic acid  
TBS = Tris-buffered saline  
mACE2 = mouse ACE2  
SEM = standard error of the mean  
Fc = fragment crystallizable

## Abstract (German)

Angiotensin converting enzyme 2 (ACE2) ist der wichtigste Rezeptor für severe acute respiratory syndrome coronavirus 2 (SARS-CoV-2), das Coronavirus verantwortlich für die Coronavirus disease 2019 (COVID-19) Pandemie. ACE2 existiert in zwei verschiedenen physiologischen Zuständen: membrangebunden und frei löslich zirkulierend. Lösliche ACE2 Proteine können als “decoy” genutzt werden, um die Bindung von SARS-CoV-2 an membrangebundenes ACE2 zu verhindern und dadurch den Zelleintritt von SARS-CoV-2 und die nachfolgende Replikation in der Zelle zu unterbinden. ACE2 618-DDC-ABD ist ein modifiziertes, lösliches ACE2 Protein mit verlängerter Aktivität *in vivo* und verbesserter Affinität für SARS-CoV-2. Diese Dissertation basiert auf meiner Arbeit mit ACE2 618-DDC-ABD in k18hACE2 Mäusen infiziert mit SARS-CoV-2, mit Fokus auf eine Publikation, in welcher die Effektivität verschiedener Anwendungsmodalitäten von ACE2 618-DDC-ABD verglichen wurde. Dabei wurden die Effekte auf Überleben, Organtiter und Lungen- und Hirnhistopathologie untersucht. ACE2 618-DDC-ABD wurde entweder intranasal oder intraperitoneal verabreicht. Der Zeitpunkt der Verabreichung war entweder sowohl vor als auch nach viraler Inokulation oder nur nach viraler intranasaler Inokulation (je  $2 \times 10^4$  Plaque forming units (PFU) SARS-CoV-2 (Wildtyp)). Die Kontrollgruppe welche ebenfalls mit SARS-CoV-2 inokuliert wurde erhielt bovine serum albumin (BSA) in Phosphate-buffered saline (PBS). An Tag 5 hatten 0% der Mäuse in der Kontrollgruppe überlebt und die SARS-CoV-2 Titer in Lunge und Hirn waren hoch. Die intranasale Applikation von ACE2 618-DDC-ABD sowohl vor als auch nach viraler Inokulation war den anderen Anwendungsmodalitäten überlegen. An Tag 5 betrug das Überleben in dieser Gruppe 90%, Hirn SARS-CoV-2-Titer waren nicht detektierbar, und Lungen SARS-CoV-2-Titer reduziert. Verabreichung von ACE2 618-DDC-ABD intraperitoneal oder nur nach viraler Inokulation erzielte nur partiellen Schutz vor der hohen Letalität. Zusätzlich waren die SARS-CoV-2 Hirntiter in diesen Gruppen hoch. Zusammenfassend zeigen diese Studien, dass die intranasale Applikation von ACE2 618-DDC-ABD der intraperitonealen Applikation deutlich überlegen ist. Des Weiteren ist die Anwendung bereits vor viraler Inokulation der alleinigen Anwendung nach viraler Inokulation überlegen. Die intranasale Applikation von ACE2 618-DDC-ABD sowohl vor als auch nach viraler Inokulation führte zu einem beinahe vollständigen Überleben der SARS-CoV-2 infizierten Mäuse in dieser Gruppe. Therapien basierend auf löslichen ACE2 Proteinen werden weiterhin erforscht und sind

ein potentieller Baustein in der Prävention und/oder Therapie von zukünftigen SARS-CoV-2 Varianten sowie anderen Coronaviren, welche ACE2 als Rezeptor verwenden.

---

## Abstract (English)

Angiotensin-converting enzyme 2 (ACE2) is the main cell entry receptor for SARS-CoV-2, the coronavirus responsible for the COVID-19 pandemic. ACE2 exists in two different forms: membrane-bound and soluble. Soluble ACE2 proteins have been proposed as decoys to intercept SARS-CoV-2 from cell entry via membrane-bound ACE2 preventing subsequent viral replication. ACE2 618-DDC-ABD is a bioengineered soluble ACE2 protein with a prolonged duration of action and improved binding affinity for SARS-CoV-2. This dissertation is based on my work testing ACE2 618-DDC-ABD in k18hACE2 mice, a model of lethal SARS-CoV-2 infection, focusing in particular on my latest publication comparing different administration modes of ACE2 618-DDC-ABD to improve survival, decrease viral organ titers, and protect from organ injury. ACE2 618-DDC-ABD was administered either intranasally or intraperitoneally and either pre- and post-viral inoculation or only post-viral inoculation with  $2 \times 10^4$  PFU ancestral SARS-CoV-2. In infected untreated control mice that received BSA in PBS, survival on day 5 was 0% and brain and lung viral titers were high. Lung injury was found to be severe; brain injury was subtle but consistent. The best outcomes in terms of protection from lethality were achieved by intranasal administration of ACE2 618-DDC-ABD when given both pre- and post-viral inoculation. This resulted in 90% survival on day 5, the complete absence of brain viral titers, decreased lung viral titers, and near-normal brain and lung histopathology. By contrast, when ACE2 618-DDC-ABD was administered intraperitoneally or only post-viral inoculation, there was only partial protection from lethality, brain viral titers were high in most mice, and organ histopathology was improved only partially. In conclusion, this work shows that intranasal administration of ACE2 618-DDC-ABD is superior to intraperitoneal administration, and that combined pre- and post-viral inoculation dosing is more effective than only post-viral inoculation dosing. When administered intranasally already before viral inoculation, ACE2 618-DDC-ABD provided almost complete protection from lethality in k18hACE2 mice infected with SARS-CoV-2. This supports the potential development of soluble ACE2-based therapies for preventative/therapeutic use against current and future variants of SARS-CoV-2 and other emerging coronaviruses that use ACE2 as their main cell entry receptor.

## 1 Introduction

This work aims to contextualize the background, methods, results and potential implications of the following publication (1):

Hassler, L., Wysocki, J., Ahrendsen, J. T., Ye, M., Gelarden, I., Nicolaescu, V., Tomatsidou, A., Gula, H., Cianfarini, C., Forster, P., Khurram, N., Singer, B.D., Randall, G., Missiakas, D., Henkin, J., & Battle, D. (2023). Intranasal soluble ACE2 improves survival and prevents brain SARS-CoV-2 infection. *Life Science Alliance*, 6(7)

### 1.1 Angiotensin-converting enzyme 2: enzyme of the Renin-Angiotensin-system and cell entry receptor for SARS-CoV-2

Angiotensin-converting enzyme 2 (ACE2), discovered in 2000, is an enzyme of the Renin-Angiotensin-system (RAS) that functions as a monocarboxypeptidase, cleaving the C-terminus of Angiotensin (Ang) II to form Ang-(1-7) (2, 3). Other substrates of ACE2 include des-Arg<sup>9</sup> Bradykinin, Apelin 13, and Dynorphin 13 (4). The catalytical domain of ACE2 shares 42% homology with that of ACE, the enzyme that cleaves Ang I to form Ang II (3). While the ACE/Ang II axis exerts mainly pro-inflammatory, pro-fibrotic and vasoconstrictive effects, the ACE2/Ang-(1-7) axis acts as its counterpart with anti-inflammatory, anti-fibrotic and vasodilatory effects and is considered a potential therapeutic target for diabetes, cardiovascular and renal disease (5-8). In 2003, ACE2 was reported to be the main cell entry receptor for SARS-CoV, the coronavirus responsible for the SARS outbreak that started in the fall of 2002 (9, 10). When SARS-CoV-2 emerged at the end of 2019, ACE2 was soon found to be the main cell-entry receptor for this coronavirus responsible for the COVID-19 pandemic (11-13). Binding of ACE2 to the receptor binding domain (RBD) of the SARS-CoV-2 S1 spike protein induces conformational changes in the S1 spike protein (14-17). Transmembrane serine protease 2 (TMPRSS2) then cleaves S2' within the S2 spike protein initiating membrane fusion and therefore cell entry (11, 14, 18). In the absence of TMPRSS2, SARS-CoV-2 can still enter the cell via clathrin mediated endocytosis followed by S2' cleavage by Cathepsins (11, 14, 19, 20).

ACE2 exists in two different forms: membrane-bound and as soluble proteins (2, 3). Membrane-bound ACE2 consists of 805 amino acids and is anchored into the cell membrane by a hydrophobic transmembrane region (2, 3, 21). Soluble ACE2 consists of 740 or less amino acids, lacks the transmembrane domain and circulates in the blood in very small amounts (2, 3, 22, 23). The membrane bound and the 740 amino acid soluble ACE2

protein contain a collectrin-like domain, located C-terminally just before the transmembrane domain, that mediates dimerization of two ACE2 proteins (21, 24-26). Soluble and membrane bound ACE2 are both enzymatically active and can bind the S1 spike protein of SARS-CoV-2 (2, 3, 13). Because soluble ACE2 is lacking the transmembrane domain (2, 3), it cannot anchor into the cell membrane to mediate entry of SARS-CoV-2, as demonstrated in human kidney organoids generated from an ACE2 knockout cell line that does not express membrane bound ACE2 (27, 28). In the absence of membrane bound ACE2 and presence of soluble ACE2, SARS-CoV-2 infection did not occur in the ACE2 knockout kidney organoids (28).

## 1.2 ACE2 decoy proteins for SARS-CoV-2 infection

The decoy effect of ACE2 was first demonstrated using SARS-CoV pseudovirus infection in 293T cells permissive for SARS-CoV (29). ACE2 was reported as cell entry receptor for SARS-CoV-2 in early 2020 (11-13). Shortly after, the use of soluble ACE2 proteins as a decoy was proposed to prevent SARS-CoV-2 cell entry and subsequent replication (30, 31) (**Figure 1**). By administering a sufficient amount of soluble ACE2, the binding of the S1 spike protein of SARS-CoV-2 to membrane-bound ACE2 can be intercepted, preventing cell entry and subsequent replication of SARS-CoV-2 (30) (**Figure 1**).

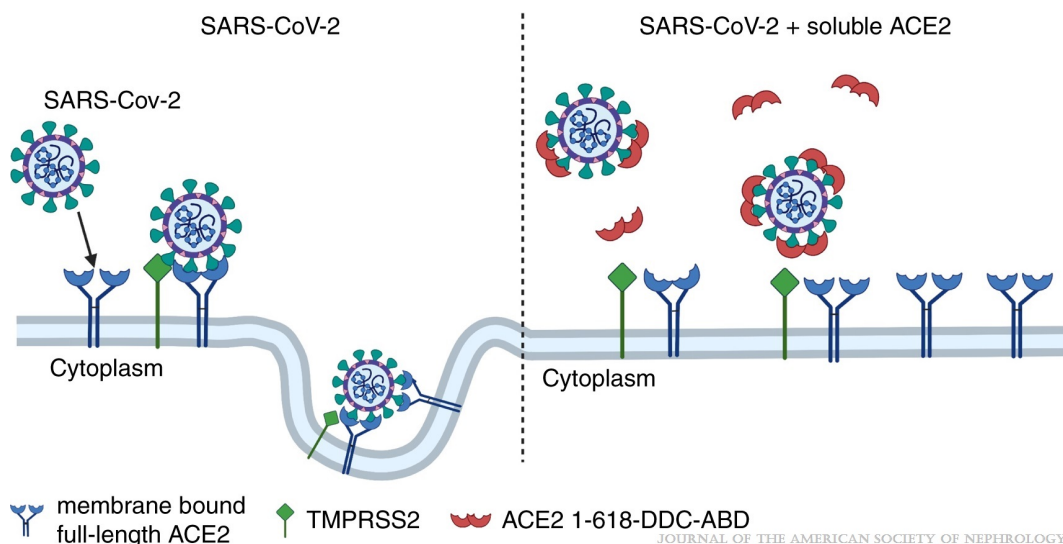


**Figure 1.** Hypothesized mechanism of action of soluble ACE2 proteins in SARS-CoV-2 infection. From: Hassler et al (32), A novel soluble ACE2 protein provides lung and kidney protection in mice susceptible to lethal SARS-CoV-2 infection, *Journal of the American Society of Nephrology (JASN)* volume 33, issue 7, page 1303, figure 5 (not modified) [https://journals.lww.com/jasn/Fulltext/2022/07000/A\\_Novel\\_Soluble\\_ACE2\\_Protein\\_Provides\\_Lung\\_and.16.aspx](https://journals.lww.com/jasn/Fulltext/2022/07000/A_Novel_Soluble_ACE2_Protein_Provides_Lung_and.16.aspx) license number 5704060091141

Neutralization of SARS-CoV-2 infection by soluble ACE2 was then confirmed in Vero E6 cells and human vascular and kidney organoids (33, 34). Different variants of soluble ACE2 proteins were used in these experiments: the native soluble ACE2 protein with 740 amino acids (ACE2 740) that naturally forms a dimer mediated by the collectrin-like-domain (21, 24, 33, 34) and a monomeric soluble ACE2 protein that was shortened to 618 amino acids, thus lacking the C-terminal collectrin domain but retaining full ACE2 enzymatic activity (34). To achieve prolonged *in vivo* duration of action, this shorter protein was fused with an Albumin binding domain (ABD) and the resulting protein was termed ACE2 618-ABD (34). Both native soluble ACE2 740 and the bioengineered ACE2 618-ABD protein neutralized SARS-CoV-2 infection in Vero E6 cells and human kidney organoids when tested at high concentrations (34). To improve the binding affinity of monomeric ACE2 618-ABD for SARS-CoV-2, a dodecapeptide (DDC) motif was then inserted mediating dimerization via disulfide bond formation (35). The resulting dimeric protein was termed ACE2 618-DDC-ABD (32). ACE2 618-DDC-ABD has preserved ACE2 enzymatic activity, a higher binding affinity for the SARS-CoV-2 S1-RBD protein, as shown by a significantly lower EC<sub>50</sub> concentration compared to both native ACE2 740 and ACE2 618-ABD (**fig 2A**) and prolonged *in vivo* duration of action as compared to native soluble ACE2 740 (**fig 2B**) (32).

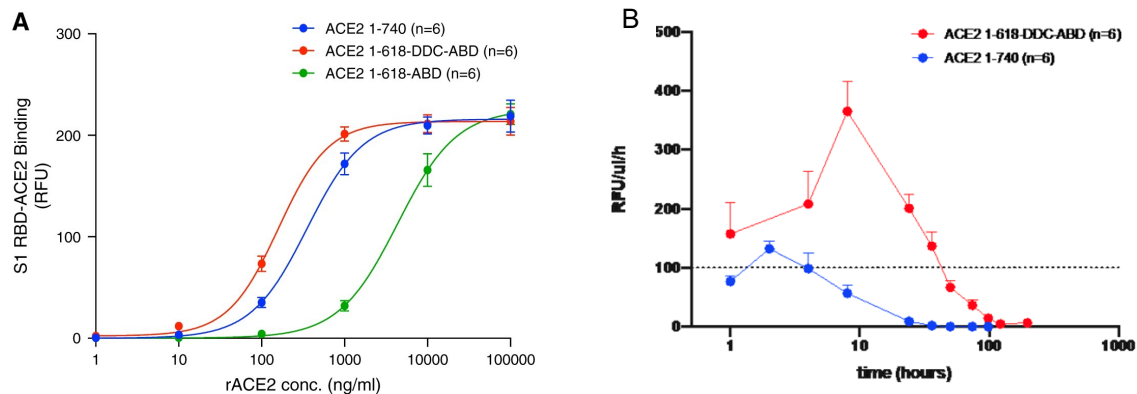


**Figure 2.** Binding affinity for the SARS-CoV-2 S1-RBD protein and duration of action of soluble ACE2 proteins.

**Panel A.** The binding affinity of ACE2 740 (blue), ACE2 618-DDC-ABD (red) and ACE2 618-ABD (green) for the S1-RBD of SARS-CoV-2 was tested using an *in vitro* assay for the detection of ACE2-RBD interaction (34). The EC<sub>50</sub> concentration of ACE2 618-DDC-ABD (red, 158ng/ml) was markedly lower than that of both ACE2 740 (blue, 352ng/ml) and ACE2 618-ABD (green, 4359ng/ml). **Panel B.** ACE2 618-DDC-ABD (red) has longer duration of action than the native soluble ACE2 740 (blue). RFU = relative fluorescence units. From: Hassler et al (32), A novel

soluble ACE2 protein provides lung and kidney protection in mice susceptible to lethal SARS-CoV-2 infection, *Journal of the American Society of Nephrology (JASN)* volume 33, issue 7, page 1297 figure 1A and supplement page 2 figure 1 (not modified). [https://journals.lww.com/jasn/Fulltext/2022/07000/A\\_Novel\\_Soluble\\_ACE2\\_Protein\\_Provides\\_Lung\\_and.16.aspx](https://journals.lww.com/jasn/Fulltext/2022/07000/A_Novel_Soluble_ACE2_Protein_Provides_Lung_and.16.aspx) license number 5704060964514

### **1.3 ACE2 618-DDC-ABD protects k18hACE2 infected with SARS-CoV-2**

To test the efficacy of ACE2 618-DDC-ABD to neutralize SARS-CoV-2 infection *in vivo*, we used the transgenic k18hACE2 mouse model expressing human ACE2 driven by the human keratin 18 promoter (36, 37). Normal wildtype mice are not susceptible to SARS-CoV-2 infection as mouse ACE2 does not recognize wildtype SARS-CoV-2 (38). The k18hACE2 mouse model is a commonly used model for SARS-CoV and SARS-CoV-2 infection, developed by McCray et al (36). When infected with a high dose of wildtype SARS-CoV-2, k18hACE2 mice develop rapid weight loss and the lethality rate is almost 100% by days 5-9 post-viral inoculation (32, 37, 39-41). In a first *in vivo* proof of concept study, ACE2 618-DDC-ABD was administered combined intranasally (IN) and intraperitoneally (IP) 1 hour prior- and 24 and 48 hours post-viral inoculation of k18hACE2 mice with  $2 \times 10^4$  PFU SARS-CoV-2 (32). Infected control mice received PBS at the same timepoints (32). All mice in the control group had to be humanely euthanized by days 6-7, lung and brain SARS-CoV-2 titers were high, and lung histopathology showed extensive alveolar hemorrhage and mononuclear infiltrates (32). In the ACE2 618-DDC-ABD treated group, by contrast, all but one mice survived until day 14, lung and brain viral titers were markedly decreased or undetectable, and lung histopathology was near normal (32). Because ACE2 618-DDC-ABD was administered combined intranasally and intraperitoneally and both before and after viral inoculation, however, my prior study was not able to discern the differences between these administration modalities (32).

### **1.4 Intranasal versus intraperitoneal and pre- versus post viral inoculation administration of ACE2 618-DDC-ABD in k18hACE2 mice infected with SARS-CoV-2**

The objective of the publication forming the base of this thesis was to compare the effect of intranasal against intraperitoneal administration of ACE2 618-DDC-ABD in SARS-CoV-2 infected k18hACE2 mice (1). Moreover, different times of administration of ACE2 618-DDC-ABD were tested, with k18hACE2 mice receiving ACE2 618-DDC-ABD either pre-

and post-viral inoculation, or only post-viral inoculation to investigate the effect on survival, SARS-CoV-2 organ titers and lung and brain histopathology (1).

## 2 Methods

### 2.1 SARS-CoV-2 Infectivity studies in A549 and Vero E6 cells

All experiments with live SARS-CoV-2 in cell lines susceptible to SARS-CoV-2 infection were performed in the Biosafety safety level 3 (BSL-3) facility of the Howard T. Ricketts Regional Biocontainment Laboratory at The University of Chicago. Two different cell lines susceptible to SARS-CoV-2 infection were used: hACE2-A549 cells derived from human lung adenocarcinoma cells, and Vero E6 cells, derived from African green monkey kidney epithelial cells (42). Two different strains of SARS-CoV-2 were used for these experiments: Wildtype (novel coronavirus/Washington/1/2020, provided by N. Thornburg (Centers for Disease Control and Prevention (CDC)) via the World Reference Center for Emerging Viruses and Arboviruses) and omicron BA.1 (BEI NR- 56481, obtained through BEI Resources, NIAID, NIH: SARS-related coronavirus 2, Isolate hCoV-19/USA/GA-EHC-2811C/2021 (Lineage B.1.1.529; omicron variant), contributed by Mehul Suthar) (1). Both the wildtype and omicron BA.1 variant of SARS-CoV-2 were incubated with different concentrations of two different soluble ACE2 proteins (human ACE2 618-DDC-ABD or mouse ACE2 740) for 1 hour at 37°C (1). This mixture was then used to infect the A549 cells (ACE2 concentrations of 0.0128, 0.064, 0.32, 1.6, 8.0, 40.0, 200ug/ml) and Vero E6 cells (ACE2 concentrations of 5.626, 11.25, 22.5, 45, 90, 180ug/ml) (1). Cells were infected and incubated until a noticeable cytopathic effect was seen in the untreated control wells (0ug/ml of ACE2 proteins) (1). Specifically, cells infected with wildtype SARS-CoV-2 were incubated for 3-4 days, whereas cells infected with the omicron BA.1 variant were incubated for 5 days (1). Cells infected with the omicron BA.1 variant, therefore, required a longer incubation period than cells infected with wildtype SARS-CoV-2, which may be contributed to by reduced syncytia formation and overall lower cytopathic effect of omicron (43, 44). To assess the cell viability at the end of the incubation period, crystal violet staining was followed by reading the absorbance of each well at 595 nm (1). The values were then normalized to the 0 ug/ml control wells and were expressed as percentage of uninfected (no virus) control wells (1).

## 2.2 SARS-CoV-2 Infectivity studies in k18hACE2 mice

All experiments with live SARS-CoV-2 in k18hACE2 mice were performed in the BSL-3 facility of the Ricketts Regional Biocontainment Laboratory, University of Chicago. The protocol for these studies was approved by the Institutional Animal Care and Use Committees (IACUC) of both Northwestern University (IS00004795) and the University of Chicago (72642) (1). K18hACE2 mice (8-13 weeks old) with an estimated standardized human ACE2 gene copy number of 8, with human ACE2 expression driven by the human keratin 18 promoter were purchased from Jackson Laboratory (1). Mice were inoculated intranasally with  $2 \times 10^4$  plaque forming units (PFU) SARS-CoV-2 in 20  $\mu$ l (novel coronavirus/Washington/1/2020 was provided by N Thornburg (CDC) via the World Reference Center for Emerging Viruses and Arboviruses) (1). Two different protocols were used to compare the pretreatment and posttreatment effects of soluble ACE2 618-DDC-ABD (see below). Infected mice were weighed once daily and monitored twice daily for health using a clinical score (**Table 1**) (1).

**Table 1.** Scoring system for health evaluation of SARS-CoV-2 infected k18hACE2 mice. Modified from Hassler et al, Life Science Alliance, 2023 (1).

Score	Description
0	Pre-inoculation: mice are bright, alert, active, normal fur coat and posture
1	Post-inoculation: mice are bright, alert, active, normal fur coat and posture, no weight loss
1.5	Mice present with slightly ruffled fur but are active, or weight loss might occur but <2.5, recovery can be expected
2	Ruffled fur or less active or weight loss <5%, recovery might occur
2.5	Ruffled fur or not active but moves when touched or hunched posture or difficulty breathing or weight loss 5-10%, recovery is unlikely but still might occur
3	Ruffled fur or inactive but moves when touched or difficulty breathing or weight loss at 11-20%, recovery is not expected
4	Ruffled fur or positioned on its side or back or dehydrated or difficulty breathing or weight loss >20% or labored breathing, recovery is not expected
5	death

Per protocol approved by the IACUCs, mice that reached a clinical score of 3 or more or lost more than 20% of their baseline body weight were euthanized for humane reasons, this was considered a mortality event (1). Mice that did not reach these endpoints were monitored until day 14. Euthanasia was performed using CO<sub>2</sub>-forced inhalation, followed by cervical dislocation after the last breathing movement (1). Parts of lungs and brains were collected for plaque assays to measure SARS-CoV-2 titers (see below) (1). The remaining parts were fixed in 10% formalin to be safely released from the BSL-3 facility

and shipped to the Batlle laboratory where the formalin was replaced by 70% Ethanol (1). The Northwestern University Mouse Histology and Phenotyping Laboratory Center embedded these organs in paraffin and generated slides for histopathology and immunofluorescence studies (see below) (1).

### 2.2.1 Pre-treatment protocol

ACE2 618-DDC-ABD was administered to k18hACE2 mice 1 hour prior to viral inoculation with  $2 \times 10^4$  PFU SARS-CoV-2, with additional doses at 24 and 48 hours post-viral inoculation (1). The pretreatment groups received ACE2 618-DDC-ABD either intranasally (IN-pre group, 13ug/g body weight (BW) in 30ul PBS divided equally between both nostrils) or intraperitoneally (IP-pre group, 13ug/g BW in 200ul PBS) (n=10 per group, five males and five females each) (1) (**Figure 3**).

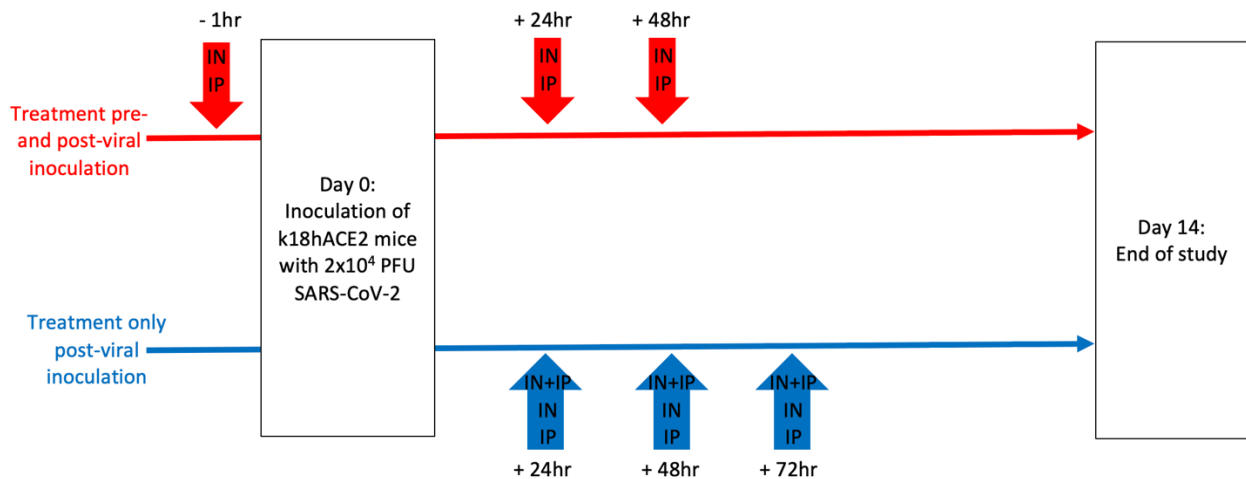


**Figure 3.** Treatment scheme for SARS-CoV-2 inoculated k18hACE2 mice.

In the pre- and post-viral inoculation protocol (red), k18hACE2 mice received ACE2 618-DDC-ABD 1 hour prior to and 24 and 48 hours post viral inoculation. ACE2 618-DDC-ABD was administered either intranasally (IN) or intraperitoneally (IP). In the only-post viral inoculation protocol (blue), k18hACE2 mice received ACE2 618-DDC-ABD 24, 48 and 72 hours post viral inoculation. ACE2 618-DDC-ABD was administered either intranasally (IN), intraperitoneally (IP) or intranasally + intraperitoneally (IN+IP). From: Own Illustration.

### 2.2.2 Post-treatment protocol

ACE2 618-DDC-ABD was administered to k18hACE2 mice 24, 48, and 72 hours post-viral inoculation with  $2 \times 10^4$  PFU SARS-CoV-2 (1). The posttreatment groups received ACE2 618-DDC-ABD either intranasally (IN-post-group, 12ug/g BW in 30ul PBS divided equally between both nostrils, n=10, male), intraperitoneally (IP-post-group, 1ug/g BW in

200ul PBS, n=5, male), or combined intranasally and intraperitoneally at the same doses (IN+IP-post-group; IN: 12ug/g BW in 30ul PBS divided equally between both nostrils and IP: 1ug/g BW in 200ul PBS, n=10, male) (1) (**Figure 3**). Control k18hACE2 mice (n=5, male) were inoculated with the same lethal dose of  $2 \times 10^4$  PFU SARS-CoV-2 and then received bovine serum albumin (BSA) in Phosphate-buffered saline (PBS) combined intranasally and intraperitoneally 24, 48 and 72 hours post-viral inoculation (1).

## 2.3 Sample analysis

### 2.3.1 Hematoxylin and eosin staining

Two lung pathologists evaluated hematoxylin and eosin (H&E)-stained lung sections generated by the Northwestern University Mouse Histology and Phenotyping Laboratory center using a scoring system recently described for k18hACE2 mice infected with SARS-CoV-2 (**Table 2**) (1, 39).

**Table 2.** Scoring system for lung histopathology in k18hACE2 mice infected with SARS-CoV-2 (39). From: Own presentation.

<b>Score</b> <b>Category</b>	<b>0</b>	<b>1</b>	<b>2</b>	<b>3</b>	<b>4</b>
<b>Mononuclear infiltrates</b>	No detection	uncommon detection in <5% lung fields (200x)	detectable in up to 30% of lung fields (200x)	detectable in 33-66% of lung fields (200x)	detectable in >66% of lung fields (200x)
<b>Alveolar hemorrhage</b>	No detection	uncommon detection in <5% lung fields (200x)	detectable in up to 30% of lung fields (200x)	detectable in 33-66% of lung fields (200x)	detectable in >66% of lung fields (200x)
<b>Edema</b>	No detection	uncommon detection in <5% lung fields (200x)	detectable in up to 30% of lung fields (200x)	detectable in 33-66% of lung fields (200x)	detectable in >66% of lung fields (200x)
<b>Cellular necrosis</b>	No detection	uncommon detection in <5% lung fields (200x)	detectable in up to 30% of lung fields (200x)	detectable in 33-66% of lung fields (200x)	detectable in >66% of lung fields (200x)
<b>Hyaline membranes</b>	No detection	uncommon detection in <5% lung fields (200x)	detectable in up to 30% of lung fields (200x)	detectable in 33-66% of lung fields (200x)	detectable in >66% of lung fields (200x)

<b>Thrombosis</b>	No detection	uncommon detection in <5% lung fields (200x)	detectable in up to 30% of lung fields (200x)	detectable in 33-66% of lung fields (200x)	detectable in >66% of lung fields (200x)
<b>Neutrophil infiltration</b>	Within normal range	scattered polymorphonuclear neutrophils (PMNs) sequestered in septa	score 1 + solitary PMNs extravasated in airspaces	score 2 + aggregates in vessel and airspaces	NA

Brain histopathology of H&E-stained brain sections generated by the Northwestern University Mouse Histology and Phenotyping Laboratory center was evaluated by a blinded neuropathologist (1). Additionally, the degree of leukocytosis/lymphocytosis and neuronal pyknosis was scored (**Table 3**) (1).

**Table 3.** Scoring system for brain histopathology in k18hACE2 mice infected with SARS-CoV-2. From: Own presentation.

<b>Score</b>	<b>0</b>	<b>1</b>	<b>2</b>	<b>3</b>
<b>Category</b>				
<b>Leukocytosis/lymphocytosis</b>	None	Mild (focal)	Moderate (multifocal)	Severe (diffuse)
<b>Neuronal pyknosis</b>	None	Mild (focal)	Moderate (multifocal)	Severe (diffuse)

### 2.3.2 Immunofluorescence staining

Immunofluorescence studies were performed on brain slides generated by the Northwestern University Mouse Histology and Phenotyping Laboratory center, using ionized calcium binding adapter molecule 1 (IBA1) (ab178846, Abcam) and glial fibrillary acidic protein (GFAP) (ab4674, Abcam) antibodies (1).

### 2.3.3 Plaque assay for infectious virus

SARS-CoV-2 viral titers in lung and brain samples were measured by the Howard T. Ricketts Regional Biocontainment Laboratory at The University of Chicago. At euthanasia, lungs and brains from k18hACE2 were weighed and then collected in Dulbeccos Modified Eagle Medium (DMEM) with 2% fetal bovine serum (FBS) (1). Lungs and brains from each mouse separately were then homogenized with two 30 s pulses in a tissue homogenizer with 1.4 mm ceramic beads followed by centrifugation (at 1000g, 5 minutes)

(1). The resulting supernatant was serially diluted 10-fold before using it to infect Vero E6 cells (1), susceptible to SARS-CoV-2 infection (42). The inoculum was removed from the cells after 1 hour, and after the addition of 1.25% methylcellulose DMEM the cells were incubated for 3 days (1). After 3 days, plates were fixed for 1 hour in 1:10 formalin and stained with crystal violet for 1 hour (1). They were then counted to determine PFU, the data was expressed as PFU/ml after normalization by organ weight (1).

## **2.4 ACE2 enzymatic activity in the brain**

To examine whether intranasally administered ACE2 618-DDC-ABD can be detected in the brain, non-infected ACE2 deficient mice (ACE2KO mice) were used (total body ACE2/prolylcarboxypeptidase (PRCP) double-knockout mice) (22). ACE2 618-DDC-ABD (10ug/g BW, 35ul total volume in both nostrils) or PBS as control was administered to ACE2KO mice under general ketamine-xylazine anesthesia (1). Four hours after intranasal administration of either ACE2 618-DDC-ABD or PBS, an overdose of Euthasol was used for euthanasia (1). Before collection of the brains, PBS was used to flush out blood from the organs (1). Radioimmunoprecipitation assay (RIPA) buffer was used for the homogenization of brains, followed by centrifugation at 6000g for 10 minutes at 4°C (1). A Bicinchoninic acid (BCA) assay kit (Thermo Fisher Scientific) was used to measure protein concentration in the cleared lysates (1). After dilution with 1x Tris-buffered saline (TBS) pH 7.4 (cat#BP2471-1; Thermo Fisher Scientific), a fluorogenic substrate (Mca-APK-Dnp, from Bachem) was used to measure ACE2 activity at room temperature in microtiter plates (1). The total volume was 100ul per sample (1). The plates were read by fluorescence plate reader (FLX800, BioTek Instruments) (excitation wavelength: 320 nm, emission wavelength: 400nm) (1). Samples were tested in duplicate wells with one of the two wells used as “blank” in which a specific inhibitor of ACE2 (MLN-4760, Millennium Pharmaceuticals) was used at a  $10^{-5}$  end concentration (45, 46) to account for background fluorescence (1). To calculate ACE2 activity, the blank values were subtracted from the values of wells without ACE2 inhibitor and divided by the total protein concentration of the tissue lysates and expressed as RFU (1).

## **2.5 Statistics**

Statistics were calculated using GraphPad Prism v8.4.3 software. Shapiro-Wilk test was applied to test normality (1). For normally distributed data, the unpaired t-test was used

to analyze differences between two groups (1). If comparing more than two groups, an ANOVA followed by post hoc Dunnett's multiple comparisons test was used (1). For non-normally distributed data, the Mann-Whitney test was used to analyze differences between two groups (1). If comparing more than two groups, the Kruskal-Wallis test followed by post-hoc Dunn's multiple comparisons test was used (1). The Log-rank (Mantel-Cox) test was used to compare differences in survival (1).

### 3 Results

#### 3.1 ACE2 618-DDC-ABD neutralizes SARS-CoV-2 infection in A549 and Vero E6 cells

In previous work we showed that ACE2 618-DDC-ABD neutralizes the wild-type, gamma, and delta SARS-CoV-2 variants in cells susceptible to SARS-CoV-2 infection (32). To expand these findings, the effect of ACE2 618-DDC-ABD on the SARS-CoV-2 omicron BA.1 variant was examined in two different cell lines susceptible to SARS-CoV-2 infection, A549 and Vero E6 cells, using cell viability as readout. The efficacy of ACE2 618-DDC-ABD to neutralize infection with the omicron BA.1 variant was compared to its effect on infection with wildtype SARS-CoV-2.

In the human A549 cells, ACE2 618-DDC-ABD neutralized wild-type SARS-CoV-2 infection in a concentration-dependent manner (1). Full protection (eg high cell viability) was provided by high ACE2 618-DDC-ABD concentrations only (**figure 4A**) (1). Compared to neutralization of wild-type SARS-CoV-2, ACE2 618-DDC-ABD was effective to neutralize omicron BA.1 infection of A549 cells at much lower concentrations (**figure 4B**) (1). This difference in the effectivity of ACE2 618-DDC-ABD for neutralization of wild-type against omicron BA.1 SARS-CoV-2 variant was statistically significant (**figure 4C**) (1).

The neutralization of the omicron BA.1 SARS-CoV-2 variant by ACE2 618-DDC-ABD was also tested in Vero E6 cells with different protein concentrations, that all neutralized omicron BA.1 infection (**figure 4D**) (1). Additionally, a soluble mouse ACE2 protein (mACE2 740), which normally has no effect on wild-type SARS-CoV-2 infection (33, 34), was found to neutralize omicron BA.1 at high concentrations (**figure 4E**) (1).

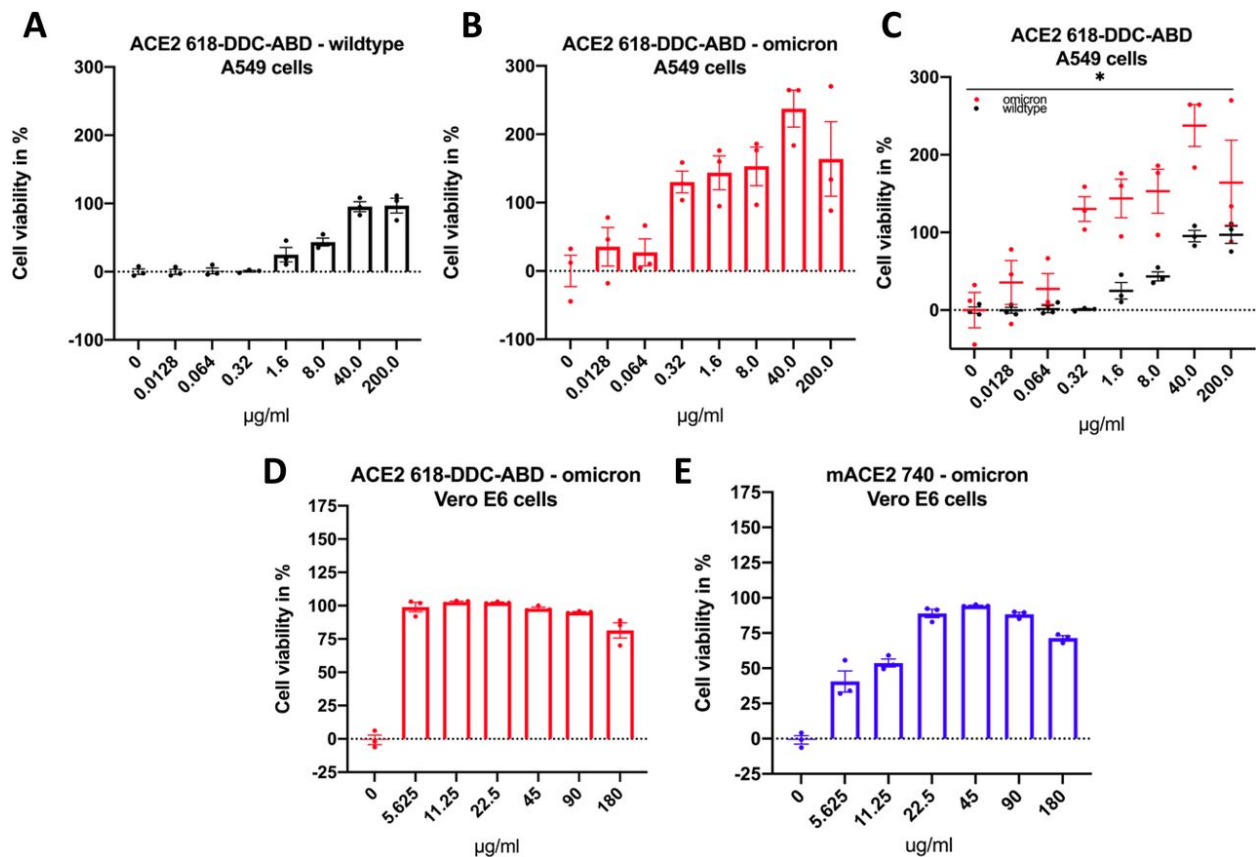


**Figure 4.** ACE2 618-DDC-ABD neutralizes wild-type and omicron SARS-CoV-2 infection *in vitro*. **Panel A.** ACE2 618-DDC-ABD neutralizes wild-type SARS-CoV-2 infection of A549 cells at high concentrations (40 and 200µg/ml), whereas intermediate (1.6 and 8µg/ml) or low concentrations (0.0128-0.32µg/ml) have a decreased or no effect on infectivity. **Panel B.** ACE2 618-DDC-ABD neutralizes omicron SARS-CoV-2 infection of A549 cells at high and intermediate concentrations (0.32-200µg/ml), whereas low concentrations (0.0128 and 0.064 µg/ml) only have a partially protective effect on infectivity. **Panel C.** The differences in neutralization of omicron (red) or wild-type (black) SARS-CoV-2 infection by ACE2 618-DDC-ABD are significant ( $p=0.0144$ ). **Panel D.** ACE2 618-DDC-ABD neutralizes omicron SARS-CoV-2 infection of Vero E6 cells at all concentrations tested (5.626-180µg/ml). **Panel E.** A soluble mouse ACE2 protein, mACE2 740, that normally has no effect on infectivity of wild-type SARS-CoV-2 infection, neutralizes omicron SARS-CoV-2 infection of Vero E6 cells at high concentrations (22.5-180µg/ml) and lower concentrations (5.625 and 11.25µg/ml) provide partial protection.

The results are shown as Mean  $\pm$  standard error of the mean (SEM) and were normalized to the 0 µg/ml control wells and then expressed as a percentage of mock-infected (no SARS-CoV-2) control wells (1). Significance was calculated by two-way ANOVA.

From: Hassler et al (1), Intranasal soluble ACE2 improves survival and prevents brain SARS-CoV-2 infection. Life Science Alliance, Volume 6, No. 7, page 8, figure 5 (not modified) <https://doi.org/10.26508/lsa.202301969> licensed under CC BY 4.0 <https://creativecommons.org/licenses/by/4.0/>

## 3.2 SARS-CoV-2 infection in k18hACE2 mice

Infection of k18hACE2 mice with the omicron BA.1 SARS-CoV-2 variant produces mild, non-lethal infection (47-49). Therefore, wild-type SARS-CoV-2 (Washington isolate) that causes lethal disease in k18hACE2 mice was used for the *in vivo* studies (36, 37, 39).

Control k18hACE2 mice were also inoculated with SARS-CoV-2 and received BSA in PBS, administered both intranasally and intraperitoneally, instead of ACE2 618-DDC-ABD (1). All mice in this control group had to be euthanized on day 5 post-inoculation (**figure 5A**) due to either severe body weight loss and/or a high clinical score, as per protocol (**figure 5B, C**) (1).

### 3.2.1 ACE2 618-DDC-ABD administration pre- and post-viral inoculation

In the pre-treatment groups, ACE2 618-DDC-ABD was administered to k18hACE2 mice 1 hour before and 24 and 48 hours after inoculation with SARS-CoV-2, with either intranasal (IN-pre) or intraperitoneal (IP-pre) protein administration (1).

Survival on day 5 was 90% in the IN-pre group and 40% in the IP-pre group (**figure 5D**). The difference between the two groups was significant ( $p=0.0024$ ) (1). As compared to the infected control group that received BSA in PBS, moreover, survival in the IN-pre group was significantly higher ( $p=0.0084$ ) (1). Survival was not significantly different when comparing the IP-pre group to the control group ( $p=0.1106$ ) (1). Because four of the nine remaining mice from the IN-pre group were euthanized on day 5 to obtain organs for comparison to the other groups, only five mice remained in this group thereafter. These five mice were monitored until day 14, the end of the study, and had essentially normal clinical scores and stable body weight by day 14 (**figure 5D-F**) (1).

The remaining four mice in the IP-pre group had to be euthanized by day 7 (**figure 5D**) as their clinical score and weight loss worsened (**figure 5E, F**) and they reached the endpoint criteria according to the study protocol (see methods) (1).

### 3.2.2 ACE2 618-DDC-ABD administration only post-viral inoculation

In the post-treatment-groups, ACE2 618-DDC-ABD was administered to k18hACE2 mice 24, 48 and 72 hours after inoculation with SARS-CoV-2, with either intranasal (IN-post), intraperitoneal (IP-post), or combined intranasal-intraperitoneal (IN+IP-post) protein administration (1).

Survival on day 5 was 30% in the IN+IP-post group, 20% in the IN-post group, and 20% in the IP-post group (**figure 5G**) (1). On day 14, survival was 20% in the IN+IP-post group, 10% in the IN-post group, and 0% in the IP-post group (**figure 5G**) (1). A common feature in the post-treatment groups was rapid body weight loss (**figure 5H**) and poor clinical scores (**figure 5I**) that worsened overall faster than in the pre-treated groups (1). When comparing the IN-post, IN+IP-post or IP-post-groups to each other or the control group or IP-pre-group, the differences in survival did not reach significance (1). When comparing the post-treated groups (IN+IP-post, IN-post, IP-post) to the IN-pre group, however, survival was significantly improved in the IN-pre group as compared to each of the three different post-treated groups ( $p=0.0181$ ,  $p=0.0046$ ,  $p=0.0064$ , respectively) (1).

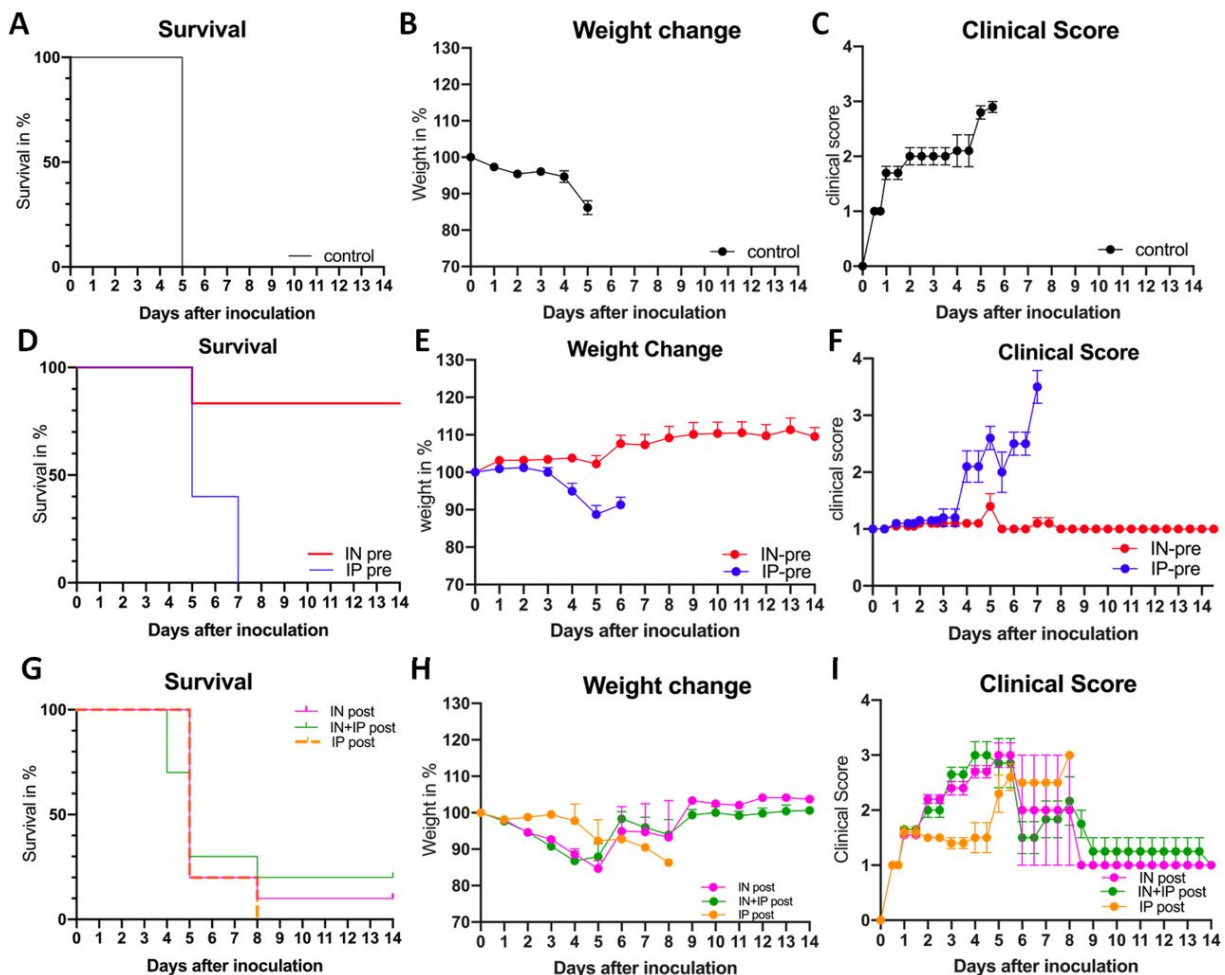


**Figure 5.** Survival, body weight change and clinical score in k18hACE2 mice infected with SARS-CoV-2.

**Panels A-C.** Survival by day 5 was 0% in the infected control group that received BSA in PBS (black), mice rapidly lost weight and had poor clinical scores. **Panels D-F.** Survival by day 5 was 9 out of 10 (90%) in the IN-pre group (red) and 4 out of 10 (40%) in the IP-pre group (blue). The

remaining 4 mice in the IP-pre group (blue) all had to be euthanized by day 7 because of worsening clinical scores, as per protocol. Mice in the IN-pre group had stable body weights and low clinical scores, compared to the IP-pre group in which body weight loss occurred and clinical scores were high. **Panels G-I.** Survival by day 5 was 3 out of 10 (30%) in the IN+IP-post group (green), 2 out of 10 (20%) in the IN-post group (pink) and 1 out of 5 (20%) in the IP-post group (orange). Survival by day 14 was 2 out of 10 (20%) in the IN+IP-post group (green), 1 out of 10 (10%) in the IN-post group, and 0 out of 5 (0%) in the IP-post group. Body weight loss occurred in most mice from the post-treated groups, and clinical scores were high. Mean  $\pm$  SEM are shown (for weight change and clinical score). From: Hassler et al (1), Intranasal soluble ACE2 improves survival and prevents brain SARS-CoV-2 infection. Life Science Alliance, Volume 6, No. 7, page 2, figure 1 (not modified) <https://doi.org/10.26508/lsa.202301969> licensed under CC BY 4.0, <https://creativecommons.org/licenses/by/4.0/>

### 3.2.3 SARS-CoV-2 titers in brains and lungs

SARS-CoV-2 infected control mice that received BSA in PBS had high brain and lung viral titers (**figure 6A, B**), with brain titers being significantly higher than lung titers ( $p=0.0295$ ) (1).

The IN-pre group was the only group in which brain SARS-CoV-2 titers were completely undetectable in all mice (**figure 6A**) (1). In all remaining ACE2 618-DDC-ABD treated groups, by contrast, brain viral titers were high and not significantly different as compared to the control group (**figure 6A**) (1). Only a few mice in each post-treated group had undetectable brain viral titers, however, in the mice that survived until day 14 from the IN-post ( $n=1$ ) and IN+IP-post group ( $n=2$ ), brain titers were undetectable (1).

Lung titers were decreased in all ACE2 618-DDC-ABD treated groups as compared to infected controls, but the differences were significant only for the IN-pre, IN-post, and IN+IP-post groups as compared to controls (**figure 6B**) (1).

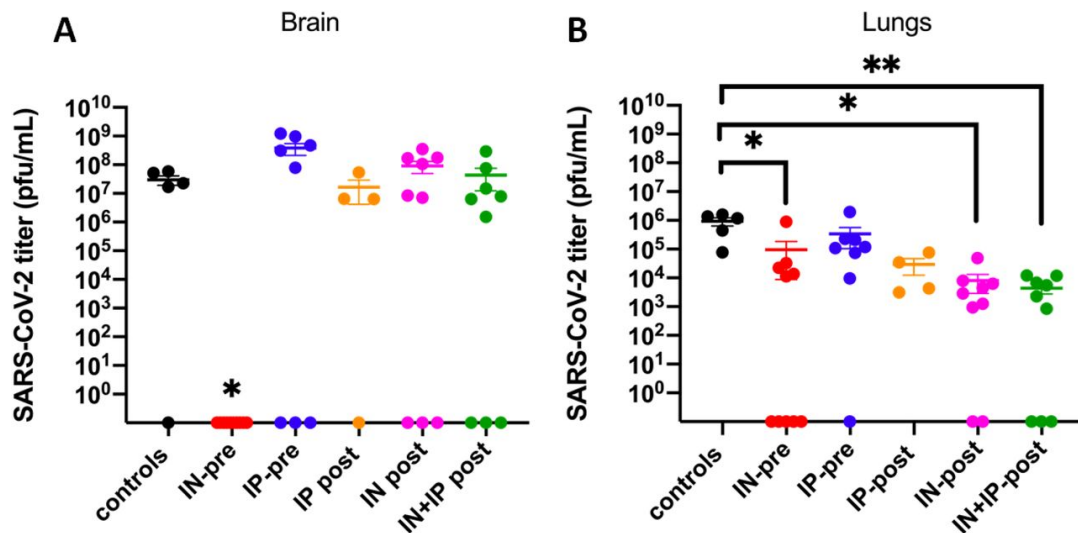


**Figure 6.** Brain and lung SARS-CoV-2 titers in k18hACE2 mice infected with SARS-CoV-2.

**Panel A.** Brain SARS-CoV-2 titers were high in the infected control group (black) that received BSA in PBS. In the IN-pre group (red), brain viral titers were undetectable in all mice, whereas they were high in most mice from the IP-pre group (blue) ( $p=0.0167$ ). In the post-treated groups (orange, pink, green), brain titers were high in most mice. **Panel B.** Lung SARS-CoV-2 titers were highest in the infected control group that received BSA in PBS (black). All ACE2 618-DDC-ABD treated groups had decreased lung titers, which reached significance as compared to controls in the IN-pre group ( $p=0.0244$ ), IN-post group ( $p=0.0136$ ), and IN+IP-post group ( $p=0.0078$ ). PFU = Plaque forming units. Mean  $\pm$  SEM is shown, ANOVA followed by Dunn's multiple comparisons test was used to calculate significance (1). If not indicated by asterisks, the differences did not reach significance. From: Hassler et al (1), Intranasal soluble ACE2 improves survival and prevents brain SARS-CoV-2 infection. Life Science Alliance, Volume 6, No. 7, page 4, figure 1 (not modified) <https://doi.org/10.26508/lsa.202301969> licensed under CC BY 4.0 <https://creativecommons.org/licenses/by/4.0/>

### 3.2.4 ACE2 618-DDC-ABD can be detected in the brain after intranasal administration

Because the BSL-3 facility can only release organs in formalin to ensure that SARS-CoV-2 has been deactivated, brains from infected k18hACE2 mice were not used for this experiment. Human ACE2 expression in k18hACE2 mice driven by the k18 promoter, moreover, also occurs in the brain, although at relatively low levels (36). When measuring ACE2 enzymatic activity in brains from k18hACE2 mice, therefore, a differentiation between ACE2 enzymatic activity from administered ACE2 618-DDC-ABD, the human ACE2 expressed via the k18 promoter and the natural mouse ACE2 present in the brain would not be possible. Therefore, healthy, non-infected ACE2KO mice deficient for ACE2

(22) were used to measure ACE2 enzymatic activity in brain lysates 4 hours after intranasal administration of ACE2 618-DDC-ABD. ACE2 enzymatic activity was detected at low levels in brain lysates from ACE2KO mice that received ACE2 618-DDC-ABD but not brain lysates from ACE2KO mice that received PBS ( $0.14 \pm 0.098$  RFU/ug protein/h and  $0.004 \pm 0.0002$  RFU/ug/protein/hr,  $p=0.015$ ) (1).

### **3.2.5 Brain histopathology in SARS-CoV-2 infected k18hACE2 mice that received ACE2 618-DDC-ABD pre- and post-viral inoculation**

The main histopathological changes found in H&E-stained brains from the SARS-CoV-2 infected control group were generally mild, including variable degrees of leukocytosis and endothelial hypertrophy in the striatum, cerebral cortex, and hypothalamus (1). In some mice, moreover, perivascular and parenchymal inflammation in the hypothalamus and basal ganglia were seen occasionally (**figure 7A-C**) (1). The degree of leukocytosis/lymphocytosis was scored on a scale of 0-3 (**figure 7J**) (1).

All mice from the IN-pre group, by contrast, presented with normal-appearing brain histopathology (**figure 7D-F**) (1). In the IP-pre group, histopathology resembled that of untreated controls (**figure 7G-I**) (1). Leukocytosis/lymphocytosis was found to be partially decreased in the IP-pre group and was undetectable in the IN-pre group, as compared to controls (**figure 7J**) (1). Neuronal pyknosis, scored on a scale of 0–3, was found to be significantly reduced in both the IP-pre ( $0.875 \pm 0.125$ ) and IN-pre group ( $1 \pm 0$ ) as compared with the infected control group that received BSA in PBS ( $2 \pm 0$ ,  $p=0.0001$  and  $p=0.0003$ , respectively) (1).

The presence of reactive astrocytosis and microgliosis was examined by immunofluorescence using the astrocyte marker GFAP and microglial marker IBA1 (50, 51). Both GFAP and IBA1 staining was strongly present in brains from infected controls that received BSA in PBS, and the microglial cells displayed showed a strong degree of ramifications (**figure 7K, N and figure 8A, D**) (1). In the IP-pre group, GFAP and IBA1 staining were reduced but still detectable (**figure 7L, O and figure 8B, E**) (1). In the IN-pre group, by contrast, both GFAP and IBA1 staining was very weak and microglia ramifications were almost completely absent (**figure 7M, P and figure 8C, F**) (1). Because of the high sample volume, the post-treated groups were not examined by immunofluorescence.

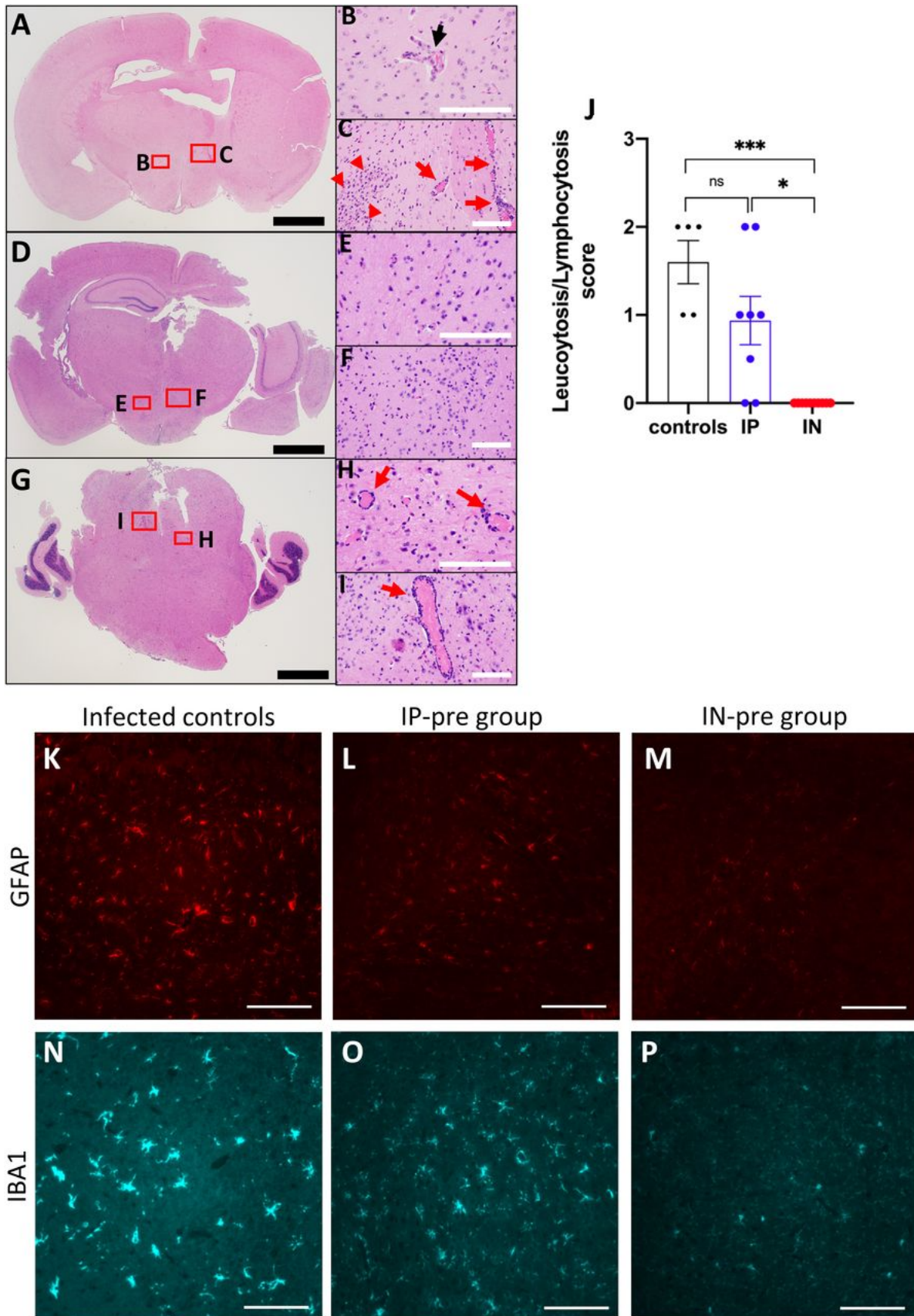


**Figure 7.** Brain histopathology and immunofluorescence staining for GFAP and IBA1 in k18hACE2 mice infected with SARS-CoV-2 that received ACE2 618-DDC-ABD pre- and post-viral inoculation.

**Panels A-C.** An example of a brain from an infected mouse that received BSA in PBS displaying perivascular (red arrows) and parenchymal leukocytosis (red arrowheads) and endothelial hypertrophy (black arrows) in the hypothalamus. **Panels D-E.** An example of a brain from a mouse from the IN-pre group displaying the absence of histopathological changes in the hypothalamus. **Panels G-I.** Example of brain from a mouse from the IP-pre group displaying perivascular lymphocytosis (red arrows) in the brain stem. Black scale bars = 1mm, white scale bars = 100um. **Panel J.** The leukocytosis/lymphocytosis score based on data from all mice was highest in the infected untreated control group (black) and decreased in the IP-pre group (blue). Leukocytosis was completely absent in brains in the IN-pre group (red), these differences were significant compared to both the control group ( $p=0.0007$ ) and the IP-pre group ( $p=0.01$ ). **Panel K-M.** Examples of immunofluorescence staining for GFAP, an astrocyte marker, displaying strong staining in the control group, with decreased staining in the IP-pre group and almost complete absence of staining in the IN-pre group. **Panel N-P.** Examples of immunofluorescence staining for IBA 1, a microglia marker, displaying strong staining in the control group, with decreased staining in the IP-group and almost complete absence of staining in the IN-pre group. All Immunofluorescence photomicrographs were taken at 40x magnification, scale bar = 100um.

Mean  $\pm$  SEM is shown, one-way ANOVA followed by Dunn's multiple comparisons test was used to calculate significance (1).

From Hassler et al (1), Intranasal soluble ACE2 improves survival and prevents brain SARS-CoV-2 infection. Life Science Alliance, Volume 6, No. 7, page 5, figure 3 (not modified) <https://doi.org/10.26508/lsa.202301969> licensed under CC BY 4.0 <https://creativecommons.org/licenses/by/4.0/>

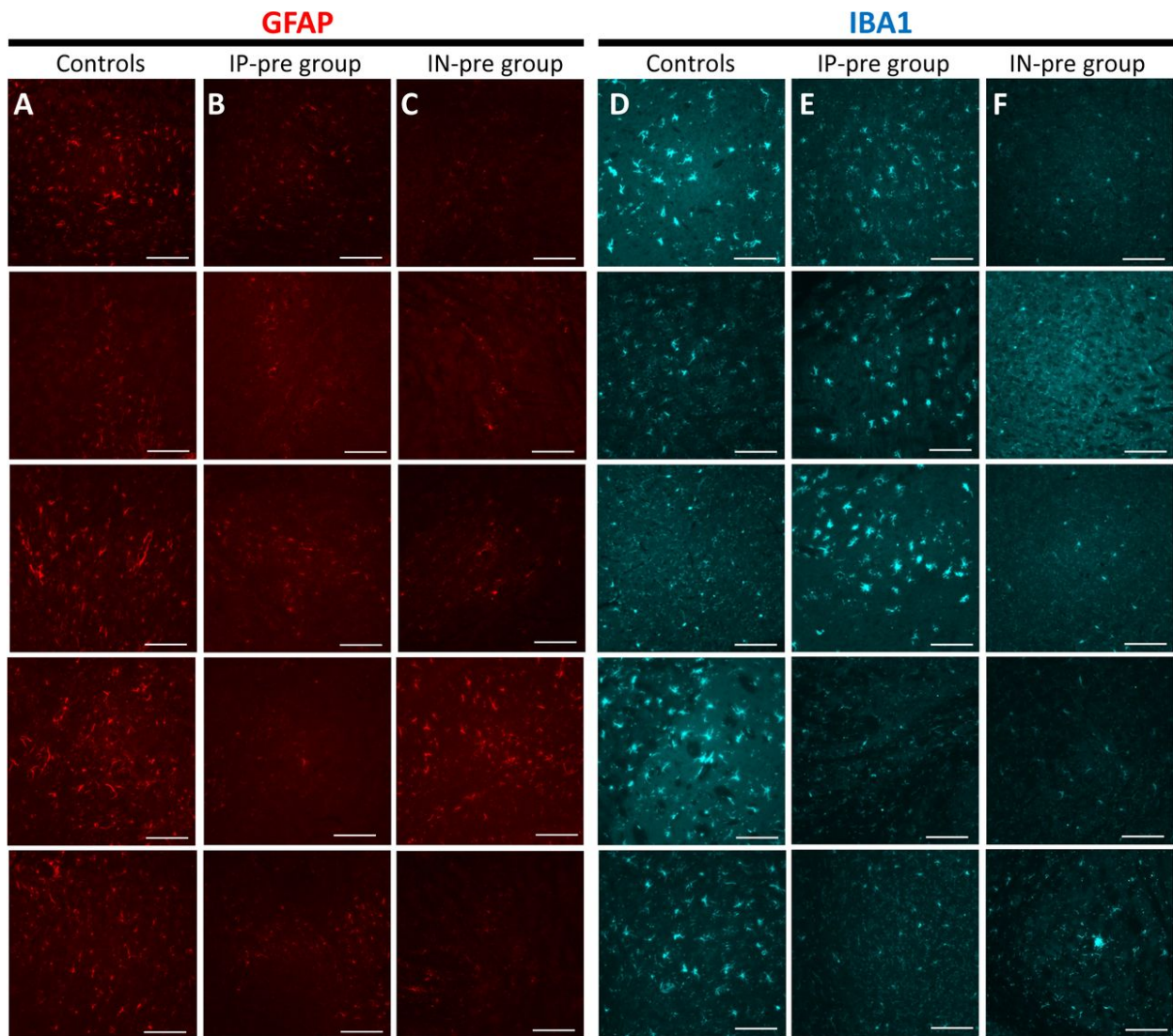


**Figure 8.** GFAP and IBA1 immunofluorescence staining in k18hACE2 mice infected with SARS-CoV-2 that received ACE2 618-DDC-ABD pre- and post-viral inoculation.

**Panels A-C.** Representative examples (n=5 per group) of immunofluorescence staining for GFAP (red), an astrocyte marker, showing strong staining in the infected control group that received BSA in PBS (**A**). GFAP staining is decreased in the IP-pre group (**B**) and the IN-pre group (**C**).

**Panels D-F.** Representative examples (n=5 per group) of immunofluorescence staining for IBA1 (blue), a microglia marker, showing strong staining in the infected control group that received BSA in PBS (**D**). IBA1 staining is partially reduced in the IP-pre group (**E**), and markedly reduced in the IN-pre group (**F**). Scale bar=100 $\mu$ m, 40x magnification. The photomicrographs from the upper row are also displayed in Figure 5K–P.

From: Hassler et al (1), Intranasal soluble ACE2 improves survival and prevents brain SARS-CoV-2 infection. Life Science Alliance, Volume 6, No. 7, supplement, figure S2 (not modified) <https://doi.org/10.26508/lsa.202301969> licensed under CC BY 4.0 <https://creativecommons.org/licenses/by/4.0/>

### 3.2.6 Brain histopathology in SARS-CoV-2 infected k18hACE2 mice that received ACE2 618-DDC-ABD only post-viral inoculation

Brain histopathology in H&E-stained brains from mice that received ACE2 618-DDC-ABD intraperitoneally only post-viral inoculation (IP-post) (**figure 9A-D**) was similar to that of the infected control group that received BSA in PBS (**figure 7A-C**) (1). Hypothalamus and lateral cortex in some mice from the IN-post (**figure 9E-H**) and IN+IP-post group (**figure 9I-L**), moreover, showed leptomenigeal and perivascular lymphocytosis (1). The leukocytosis/lymphocytosis and neuronal pyknosis scores were lower in all post-treated groups than in controls, but this difference was significant only for neuronal pyknosis in the IN+IP-post group (**figure 9M, N**) (1).

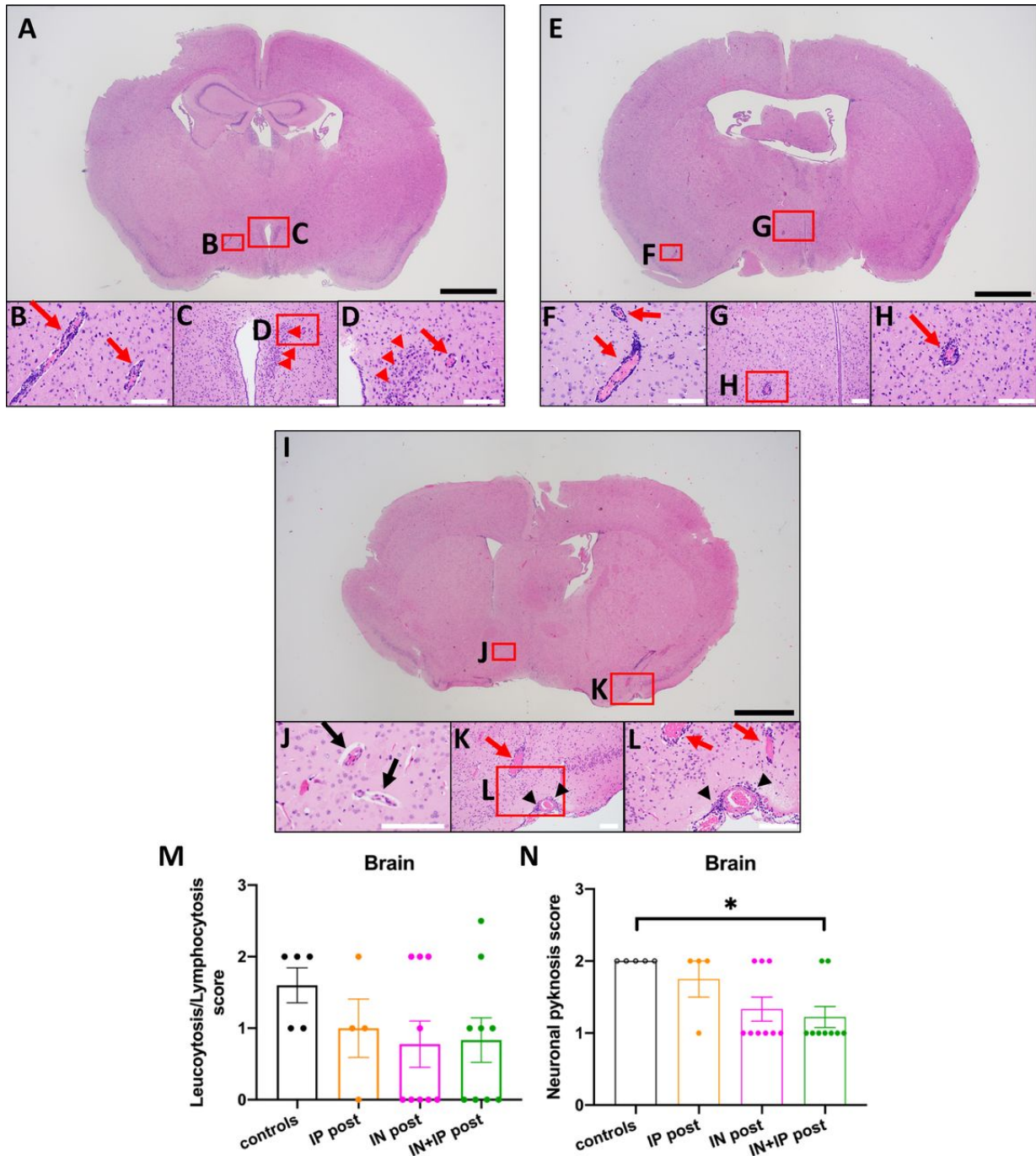


**Figure 9.** Brain histopathology in k18hACE2 mice infected with SARS-CoV-2 that received ACE2 618-DDC-ABD only post-viral inoculation.

**Panels A-D.** An example of a brain from a mouse from the IP-post group displaying perivascular lymphocytosis (red arrows) and parenchymal inflammation (red arrowheads) in the hypothalamus. **Panels E-H.** Examples of a brain from a mouse from the IN-post group displaying perivascular lymphocytosis (red arrows) in the lateral cortex (F) and hypothalamus (G, H). **Panels I-L.** Examples of a brain from a mouse from the IN+IP-post group displaying endothelial hypertrophy (black arrows, hypothalamus), perivascular lymphocytosis (red arrows, lateral cortex), and leptomeningeal inflammation (black arrowheads, lateral cortex). Black scale bars = 1mm, white scale

bars = 100um. **Panels M, N.** The leukocytosis/lymphocytosis and neuronal pyknosis scores based on data from each post-treated group (orange, pink, green) were lower than in infected untreated controls (black). The differences were significant only for neuronal pyknosis (**N**) when comparing the control to the IN+IP-post group ( $p=0.0370$ ).

Mean  $\pm$  SEM is shown, one-way ANOVA followed by Dunn's multiple comparisons test was used to calculate significance (1).

From: Hassler et al (1), Intranasal soluble ACE2 improves survival and prevents brain SARS-CoV-2 infection. Life Science Alliance, Volume 6, No. 7, supplement, figure S1 (not modified) <https://doi.org/10.26508/lsa.202301969> licensed under CC BY 4.0 <https://creativecommons.org/licenses/by/4.0/>

### **3.2.7 Lung histopathology in SARS-CoV-2 infected k18hACE2 mice that received ACE2 618-DDC-ABD pre- and post-viral inoculation**

H&E-stained lung sections were evaluated by two lung pathologists (see **Table 2**, methods). The main features found in lungs from the infected control mice that received BSA in PBS included dense perivascular mononuclear infiltrates and collections of intra-alveolar neutrophils, and more rarely foci of necrotic debris and alveolar hemorrhage (**figure 10A-E**) (1). These histopathological findings were almost completely absent in mice from the IN-pre group that received ACE2 618-DDC-ABD, except for minimal perivascular mononuclear infiltrates in some cases (**figure 10F-J**) (1). In the IP-pre group, lung histopathology was improved as compared to the infected control group that received BSA in PBS, but to a lesser degree than in the IN-pre group as there were also areas that displayed injury (**figure 10K-O**) (1). Based on the scoring system used for lung histopathology (see **Table 2**, methods) (39), scores were highest in the infected control group that received BSA in PBS, and lowest in the IN-pre group (**figure 10P**) (1). The differences were significant for the categories mononuclear infiltrates and hemorrhage when comparing the IN-pre or IP-pre group to the control group (**figure 10P**) (1).

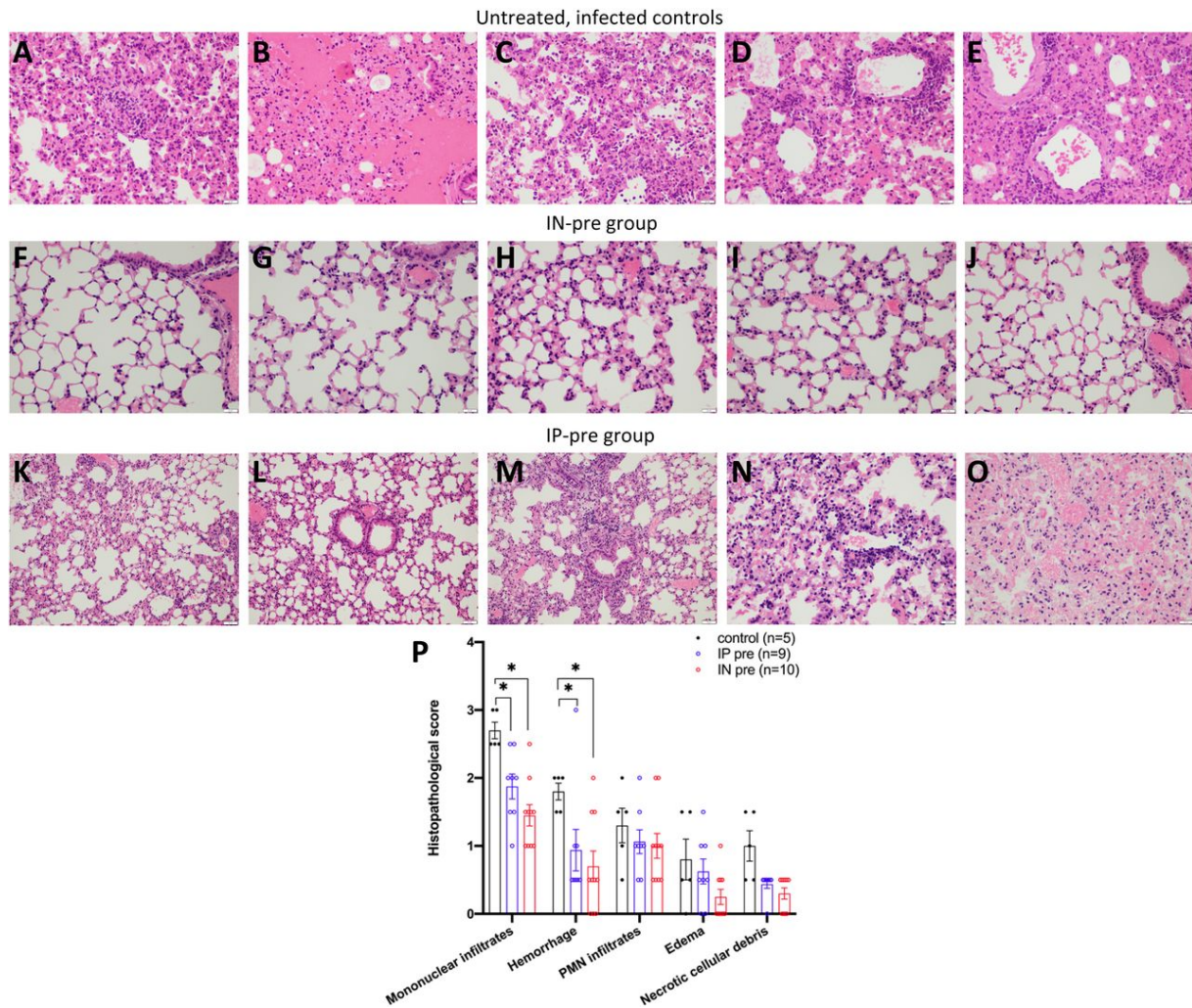


**Figure 10.** Lung histopathology in k18hACE2 mice infected with SARS-CoV-2 that received ACE2 618-DDC-ABD pre- and post-viral inoculation.

**Panels A-E.** Representative examples of lung histopathology from 5 mice from the infected control group that received BSA in PBS show rare foci of necrotic debris (A), alveolar hemorrhage (B), collections of interalveolar neutrophils (C), and dense perivascular mononuclear infiltrates (D, E). **Panels F-J.** Representative examples of lung histopathology from 5 mice from the IN-pre group show almost complete absence of lung injury. **Panels K-O.** Representative examples of lung histopathology from 5 mice from the IP-pre group show some areas of near-normal lung histopathology (K, L). In some mice there were mild perivascular mononuclear infiltrates (M, N), focal alveolar hemorrhage (O) and intra-alveolar neutrophils, although at a lesser degree than in infected controls that received BSA in PBS. **Panel P.** Lung histopathology scores were highest in the infected untreated control group (black), and lower in the IP-pre (blue) and IN-pre group (red). Significance is denoted by \* =  $p < 0.05$ , and was determined by mixed-effects analysis followed by Tukey's multiple comparisons test (1). Mean  $\pm$  SEM is shown. Scale bar = 500  $\mu$ m. The magnification of lung photomicrographs, taken from H&E-stained sections, was 40x. From: Hassler et al (1), Intranasal soluble ACE2 improves survival and prevents brain SARS-CoV-2 infection. Life

---

Science Alliance, Volume 6, No. 7, page 7, figure 4 (not modified)  
<https://doi.org/10.26508/lsa.202301969> licensed under CC BY 4.0 <https://creativecommons.org/licenses/by/4.0/>

### **3.2.8 Lung histopathology in SARS-CoV-2 infected k18hACE2 mice that received ACE2 618-DDC-ABD only post-viral inoculation**

In the groups that received ACE2 618-DDC-ABD only post-viral inoculation, lung histopathological findings were similar to that of the infected control group that received BSA in PBS (**figure 11A**) (1). Mild improvement of histopathology was seen in few mice from the IN-post (**figure 11B**) and IN+IP-post groups (**figure 11C**) (1). Based on the scoring system for lung histopathology (see **Table 2**, methods) (39), alveolar hemorrhage and necrotic cellular debris were decreased the most as compared to the infected untreated controls, the differences were not statistically significant (**figure 11D**) (1).

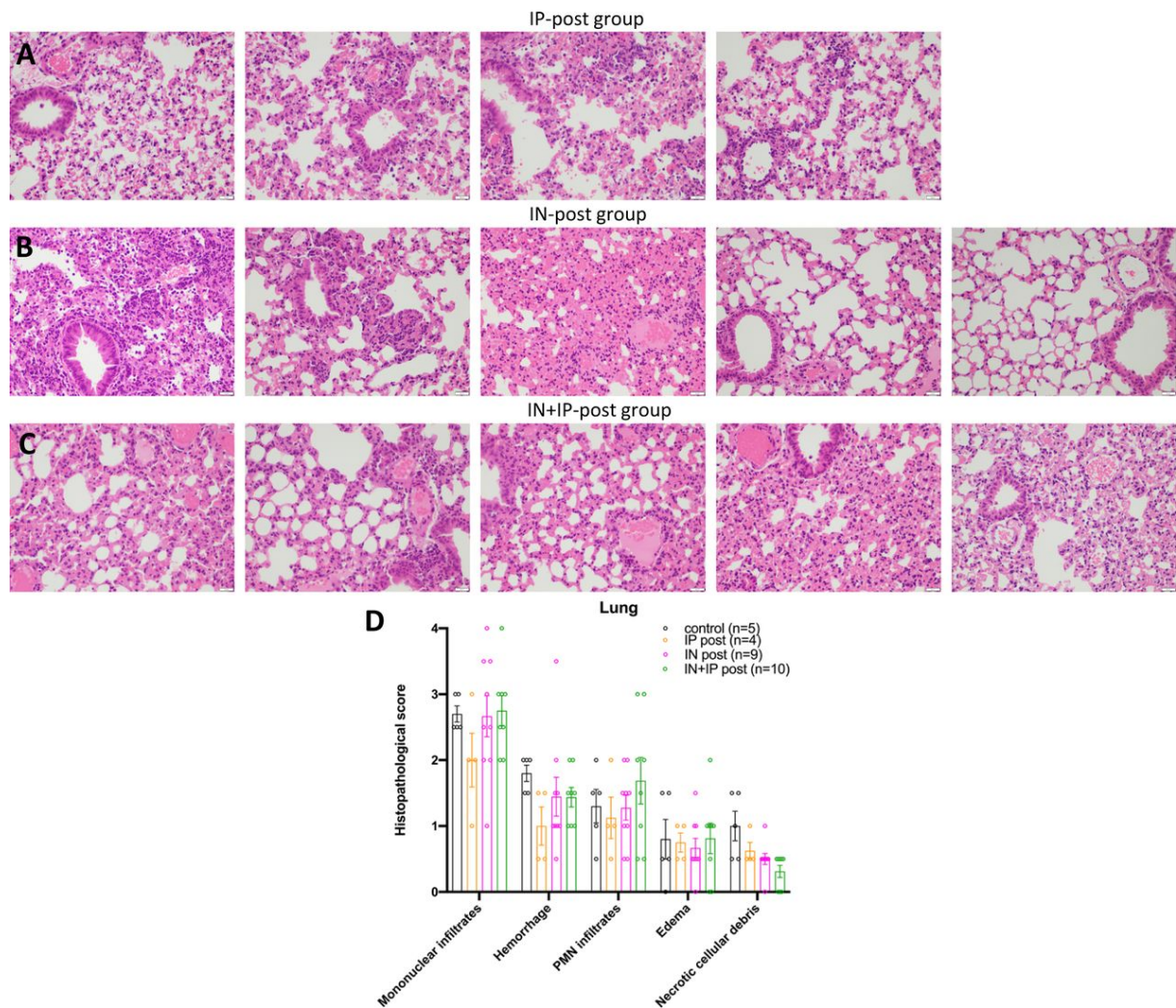


**Figure 11.** Lung histopathology in k18hACE2 mice infected with SARS-CoV-2 that received ACE2 618-DDC-ABD post-viral inoculation only.

**Panel A.** Examples of representative lung histopathology from 4 different mice from the IP-post group show perivascular mononuclear infiltrations and intra-alveolar neutrophils. **Panel B, C.** Examples of representative lung histopathology from 5 different mice from the IN-post group (**B**) and IN+IP-post group (**C**) show mild improvement of lung histopathology. **Panel D.** Lung histopathology scores were decreased slightly in some post-treated groups (orange, pink, green) as compared to infected controls that received BSA in PBS (black). Mean  $\pm$  SEM is shown, mixed-effects analysis followed by Tukey's multiple comparisons test was used to calculate significance (1). Scale bar = 500  $\mu$ m. The magnification of lung photomicrographs, taken from H&E-stained sections, was 40x. From: Hassler et al (1), Intranasal soluble ACE2 improves survival and prevents brain SARS-CoV-2 infection. Life Science Alliance, Volume 6, No. 7, supplement, figure S3 (not modified) <https://doi.org/10.26508/lsa.202301969> licensed under CC BY 4.0 <https://creativecommons.org/licenses/by/4.0/>

## 4 Discussion

### 4.1 Main findings

This study showed that ACE2 618-DDC-ABD, a bioengineered soluble ACE2 protein with prolonged *in vivo* duration of action and improved binding affinity for the S1 spike protein of SARS-CoV-2, is more effective in protecting k18hACE2 mice from lethal SARS-CoV-2 infection when administered intranasally than intraperitoneally, and provided near complete protection in terms of survival and lung and brain histopathology (1). Lung titers were reduced, but importantly brain viral titers were undetectable in the IN-pre group suggesting that protection from brain SARS-CoV-2 invasion is an important factor for survival of SARS-CoV-2 infected k18hACE2 mice (1). Administration of ACE2 618-DDC-ABD both before and after viral inoculation, moreover, was found to be superior to administration only after viral inoculation (1). Administration of ACE2 618-DDC-ABD intraperitoneally or only post-viral inoculation provided only partial protection (1). These findings extend a previous proof of concept study, of which I was also the first author (32). In this previous study, ACE2 618-DDC-ABD was administered combined intranasally and intraperitoneally both before and after inoculation with SARS-CoV-2 (32). Thus, in the aggregate, these studies show that intranasal ACE2 618-DDC-ABD delivery before viral inoculation is clearly superior to systemic or post-inoculation administration and that brain protection is essential to protect from lethality.

The k18hACE2 mouse model is a commonly used mouse model of lethal SARS-CoV-2 infection, and intranasal inoculation with a high dose of SARS-CoV-2 is followed by up to 100% lethality by day 5 to 7 post-inoculation (32, 37, 39, 41, 52). The initial descriptions of the k18hACE2 mouse model infected with SARS-CoV hypothesized that infection of vital brain areas may be responsible for the high lethality (36, 53). Intracranial inoculation of k18hACE2 mice with low doses of SARS-CoV, moreover, caused high lethality despite only mild lung injury (53). A different study showed that exposure of k18hACE2 mice to aerosolized SARS-CoV-2 particles resulted in absence of brain SARS-CoV-2 titers that was associated with a very low fatality rate despite severe lung injury (54). Our findings demonstrate the importance of protecting from brain SARS-CoV-2 invasion to confer survival in k18hACE2 mice and possibly prevent long term complications of COVID-19 (1). Indeed, the present study found that brain viral titers were undetectable in all mice that survived until day 14, supporting the association of high SARS-CoV-2 brain viral titers

with lethality in k18hACE2 mice infected with SARS-CoV-2 (1). Moreover, brain titers were not markedly reduced in the other ACE2 618-DDC-ABD treated groups, except for three mice that survived until day 14 in which brain titers were undetectable (1).

The levels of brain ACE2 enzymatic activity 4 hours after intranasal ACE2 618-DDC-ABD administration to uninfected ACE2KO mice, although detectable, were very low (1). It is likely that interception of SARS-CoV-2 cell entry by ACE2 618-DDC-ABD already in the nasal turbinates is most important to protect from infection and brain SARS-CoV-2 invasion (1).

Brain histopathology findings that have been reported in k18hACE2 mice include encephalitis, neuronal pyknosis, spongiosis and cell death, (micro-) hemorrhage, thrombosis, vasculitis and leukocyte infiltration (37, 39, 55-58). IBA1 and GFAP staining, indicative of an underlying state of inflammation of the CNS, has also been described in brains of SARS-CoV-2 infected k18hACE2 mice (57, 58). Some studies, however, only found minimal brain injury or injury limited to only a few k18hACE2 mice (37, 39). The brain histopathology findings described here consisted mainly of lymphocytosis, endothelial hypertrophy, and parenchymal inflammation, and were subtle even in the infected control mice that received BSA in PBS (1). GFAP and IBA1 immunofluorescence staining was strong in the brains of the infected k18hACE2 mice that received only BSA in PBS (1). In the IN-pre group that received ACE2 618-DDC-ABD before viral inoculation, however, these findings were absent and brain histopathology appeared mostly normal (1). Importantly, astrocyte and microglia activation have also been reported by two studies examining the brains of deceased COVID-19 patients by immunohistochemistry and imaging mass cytometry (59, 60). It is therefore important to highlight that both GFAP and IBA1 staining were markedly reduced in the IN-pre group that received ACE2 618-DDC-ABD, suggesting brain protection by this route and timing of administration (1).

Lung histopathology in infected control mice that received BSA in PBS consisted mainly of dense perivascular mononuclear infiltrates, collections of intra-alveolar neutrophils, and more rarely foci of necrotic cellular debris and hemorrhage (1), and is consistent with previously described findings by us and others (32, 37, 39, 41). Marked improvements in lung histopathology upon administration of ACE2 618-DDC-ABD were seen in the IN-pre group which displayed near-normal lung histopathology (1). Lung histopathology in the IP-pre group was also improved but to a lesser extent (1). Of note, lung viral titers were completely absent in half of the mice from the IN-pre group, but only one mouse from the

IP-pre group (1). The groups that received ACE2 618-DDC-ABD only after viral inoculation displayed partial improvements in lung histopathology, but lung viral titers were undetectable in only few mice per group (1). A reduction in SARS-CoV-2 lung titers, therefore, may improve lung injury, but if incomplete may only provide partial protection (1). In our previous work with SARS-CoV-2 infected k18hACE2 mice, kidney histopathology showed variable degrees of mild proximal tubular injury, that was improved in mice that received ACE2 618-DDC-ABD (32). Consistent with mild kidney injury in this model, kidney SARS-CoV-2 titers were completely absent in all SARS-CoV-2 infected k18hACE2 mice (32). Kidney SARS-CoV-2 invasion in patients with COVID-19 has been reported mainly in kidney tissue obtained at autopsy, whereas detection of SARS-CoV-2 in kidney biopsies has been more difficult (61-67). Therefore, there is still some controversy as to how commonly kidney SARS-CoV-2 invasion occurs in patients with COVID-19 and kidney involvement, as previously discussed in two of my publications (68, 69).

In summary, the IN-pre group was the group in which brain SARS-CoV-2 titers were completely absent and also displayed markedly improved lung and brain histopathology and almost complete absent brain IBA1 and GFAP immunofluorescence staining. This suggests that prevention of brain SARS-CoV-2 invasion by administration of intranasal ACE2 618-DDC-ABD already before viral inoculation is key to protect from lethality in this model. None of the mice that received ACE2 618-DDC-ABD only via intraperitoneal administration survived until the end of the study independent of whether the protein was administered only after or both before and after viral inoculation.

As recently shown in a follow-up paper published in January 2024, ACE2 618-DDC-ABD also protects from lethality in k18hACE2 mice inoculated with the delta SARS-CoV-2 variant (70). The first dose of ACE2 618-DDC-ABD was given 6 hours prior to viral inoculation with the delta SARS-CoV-2 variant followed by two additional doses at 24 and 48 hours post viral inoculation (70). Prophylactic use of ACE2 618-DDC-ABD may be extended even further, given its prolonged *in vivo* duration of action (32). Future studies, therefore, may include an even more extended pre-treatment inoculation time frame, as well as using lower doses of ACE2 618-DDC-ABD to establish dose-dependency effects.

## 4.2 State of research of soluble ACE2 proteins for SARS-CoV-2

The rationale for the use of soluble ACE2 proteins for neutralization of SARS-CoV-2 infection is based mainly on the so-called “decoy” effect (30, 31). By administering a large enough amount of soluble ACE2 proteins, the binding of the S1 spike protein of SARS-CoV-2 to membrane-bound ACE2 can be intercepted, preventing cell entry and subsequent replication of SARS-CoV-2 (30). Additional therapeutic benefit, moreover, may stem from administration of soluble ACE2 proteins that retain their enzymatic activity, like ACE2 618-DDC-ABD. According with this concept, Zhang et al found that using a catalytically active soluble ACE2 protein provided better protection from SARS-CoV-2 infection than a catalytically inactive ACE2 protein (71).

Native soluble ACE2 and membrane-bound ACE2 are enzymatically active and convert excess Ang II to Ang-(1-7) and are also responsible for the dissipation of other pro-inflammatory peptides like des-Arg<sup>9</sup> Bradykinin (2-4). Des-Arg<sup>9</sup> Bradykinin and Ang II have been shown to be pro-inflammatory and exacerbate lung injury in mouse models (72-75). In both SARS-CoV and SARS-CoV-2 infection, moreover, there is internalization of the SARS-CoV-2-ACE2 complex, causing ACE2 depletion in the lung with accumulation of Ang II and des-Arg<sup>9</sup> bradykinin (73, 74, 76, 77). Exogenously administered enzymatically active soluble ACE2 proteins like ACE2 618-DDC-ABD, therefore, not only exert their effect by neutralizing SARS-CoV-2 infection via the decoy effect but also provide ACE2 enzymatic activity (78). Because the BSL-3 facility can only release organ tissues in formalin to ensure the deactivation of infectious viruses we were not able to measure tissue ACE2 activity or peptide levels in the infected k18hACE2 mice in this study.

ACE2 618-DDC-ABD has been optimized in terms of both binding affinity for SARS-CoV-2 and *in vivo* duration of action (32). This has been achieved by introducing a dodecapeptide motif (DDC), that mediates dimerization via disulfide bonds (35). Compared to its monomeric counterpart ACE2 618-ABD, the dimeric ACE2 618-DDC-ABD has an about 30-fold increased binding affinity for the S1 spike of SARS-CoV-2 (32). Extended duration of action is conferred by the Albumin binding domain (ABD) (34). This is shown by high levels of plasma ACE2 enzymatic activity still detectable 48 hours after injection of ACE2 618-DDC-ABD (32). An alternative approach to achieve an extended duration of action of soluble ACE2 proteins is the fusion with a fragment crystallizable (Fc) domain (79-83). This approach, however, may cause Fc-receptor activation with subsequent antibody-

dependent enhancement or cytotoxicity (84, 85). Chen et al, by contrast, reported that an ACE2-Fc decoy with Fc-mutations known to enhance Fc-binding better protected k18hACE2 mice from lethality as compared to a ACE2-Fc protein with mutationally abrogated Fc-binding (83).

To enhance binding affinity for the S1 spike protein of SARS-CoV-2, several groups have used a variety of bioengineered ACE2 proteins with different mutations within the ACE2 sequence (71, 79, 81-83, 86-91). Some proposed ACE2 decoys including ACE2 618-DDC-ABD, by contrast, consist of the natural ACE2 amino acid sequence (32, 33, 92). Others have proposed ACE2 tetrameric proteins (79, 93) as this may confer ideal binding to the SARS-CoV-2 spike protein that also functions as a trimer (94). While most groups have used either systemic, intranasal or inhaler administration of ACE2 decoys (82, 83, 88, 89, 91, 92, 95), intranasal gene therapy using an adeno associated virus for sustained delivery of ACE2 decoys to the nasal epithelium has also been used (90).

The soluble ACE2 proteins described in the above section were tested in cell systems or SARS-CoV-2 animal models. There has been one case report of a patient with severe COVID-19 that was treated with a clinical grade recombinant human soluble ACE2 (1-740) protein, termed APN01 (96). Systemic administration of APN01 was tested in healthy human volunteers and was shown to be well tolerated (97). Two clinical studies in patients hospitalized with COVID-19 have been conducted administering APN01 either intravenously or by inhaler (98, 99). In the former study, conducted in a randomized and double-blind manner, APN01 or PBS were administered intravenously twice daily (98). The primary endpoint, a composite of all-cause death or invasive mechanical ventilation, was improved in APN01-treated patients, but this did not reach significance (98). Results from the latter study using an inhaler approach for administration of APN01 are not available (99). Intranasal or inhaler administration of soluble ACE2 proteins should provide more direct protection from SARS-CoV-2 infection than systemic administration as demonstrated here (1).

### **4.3 Universality of ACE2 proteins for SARS-CoV-2 infection**

It was also examined whether ACE2-618-DDC-ABD neutralizes the omicron BA.1 variant. In cells susceptible to SARS-CoV-2 infection, omicron BA.1 was neutralized by significantly lower concentrations of ACE2 618-DDC-ABD than needed for the wild-type SARS-

CoV-2 (1). Studies in omicron infected k18hACE2 mice are needed to confirm this effect *in vivo*. Monoclonal antibodies, by contrast, are often markedly less effective for newly emerging SARS-CoV-2 variants (100-105). Omicron, moreover, was also reported to partially evade neutralization by antibodies found in patient serum from prior infection or vaccination (101, 105, 106). The omicron variant first appeared in fall 2021 and since then has evolved, with several omicron subvariants circulating concurrently (107-109). As of January 2024, it was estimated by the CDC that the omicron variant JN.1 accounted for more than 60% of new SARS-CoV-2 infections (109). The omicron JN.1 variant was reported to more effectively escape neutralization by antibodies found in patient serum than its predecessor BA.2.86, explaining its rapid spread despite decreased affinity for ACE2 (110, 111). Further studies are needed to test ACE2 618-DDC-ABD neutralization of current (JN.1) and emerging SARS-CoV-2 variants.

The efficacy of ACE2 618-DDC-ABD to neutralize *in vitro* infectivity of the omicron BA.1, gamma, and delta SARS-CoV-2 variants (1, 32) supports the concept of soluble ACE2 proteins being universally effective for current and future variants of SARS-CoV-2 that use membrane-bound ACE2 as their main cell entry receptor (28, 112). Mutations of SARS-CoV-2 that would cause specificity of the RBD for membrane-bound ACE2 and simultaneously decreased affinity for a mutated soluble ACE2 variant have been reported to be rare (113). This may also be true for ACE2 618-DDC-ABD, which has been shortened to 618 amino acids but otherwise has not been altered in its amino acid sequence (32). It was found, moreover, that there is no mutational escape after 15 passages of SARS-CoV-2 in the presence of a soluble ACE2 protein (89). By contrast, in the presence of a monoclonal antibody, mutational escape was found after only 4 passages of SARS-CoV-2 (89). Future mutated SARS-CoV-2 variants or other newly emerging coronaviruses that use ACE2 as their main cell entry receptor are therefore expected to be sensitive to neutralization by soluble ACE2 protein-based approaches (112).

#### **4.4 Conclusion**

Intranasal administration of ACE2 618-DDC-ABD prior to viral inoculation conferred protection from brain SARS-CoV-2 invasion, whereas with systemic administration and/or post-viral inoculation administration of ACE2 618-DDC-ABD brain SARS-CoV-2 titers were high in most animals (1). The best outcome in terms of survival and organ protection

in the k18hACE2 mouse model of lethal SARS-CoV-2 infection is achieved by the intranasal administration of ACE2 618-DDC-ABD before SARS-CoV-2 inoculation followed by two additional doses after (1). These results support the development of soluble ACE2-based therapies for current and future variants of SARS-CoV-2 and other emerging coronaviruses that use ACE2 as their main cell entry receptor. Future studies that examine how far administration of ACE2 618-DDC-ABD prior to viral inoculation can be extended, as well as dose-dependency and *in vivo* efficacy of ACE2 618-DDC-ABD against other SARS-CoV-2 variants are needed.

## References

1. Hassler L, Wysocki J, Ahrendsen JT, Ye M, Gelarden I, Nicolaescu V, Tomatsidou A, Gula H, Cianfarini C, Forster P, Khurram N, Singer BD, Randall G, Missiakas D, Henkin J, Batlle D. Intranasal soluble ACE2 improves survival and prevents brain SARS-CoV-2 infection. *Life science alliance*. 2023;6(7).
2. Tipnis SR, Hooper NM, Hyde R, Karran E, Christie G, Turner AJ. A human homolog of angiotensin-converting enzyme: cloning and functional expression as a captopril-insensitive carboxypeptidase. *Journal of Biological Chemistry*. 2000;275(43):33238-43.
3. Donoghue M, Hsieh F, Baronas E, Godbout K, Gosselin M, Stagliano N, Donovan M, Woolf B, Robison K, Jeyaseelan R, Breitbart R, Acton S. A novel angiotensin-converting enzyme-related carboxypeptidase (ACE2) converts angiotensin I to angiotensin 1-9. *Circulation research*. 2000;87(5):e1-e9.
4. Vickers C, Hales P, Kaushik V, Dick L, Gavin J, Tang J, Godbout K, Parsons T, Baronas E, Hsieh F, Acton S, Patane M, Nichols A, Tummino P. Hydrolysis of biological peptides by human angiotensin-converting enzyme-related carboxypeptidase. *Journal of Biological Chemistry*. 2002;277(17):14838-43.
5. Bader M. ACE2, angiotensin-(1-7), and Mas: the other side of the coin. *Pflügers Archiv-European Journal of Physiology*. 2013;465:79-85.
6. Marquez A, Wysocki J, Pandit J, Batlle D. An update on ACE2 amplification and its therapeutic potential. *Acta Physiologica*. 2021;231(1):e13513.
7. Ferrario CM. ACE 2: More of Ang 1-7 or less Ang II? *Current opinion in nephrology and hypertension*. 2011;20(1):1.
8. Lores E, Wysocki J, Batlle D. ACE2, the kidney and the emergence of COVID-19 two decades after ACE2 discovery. *Clinical Science*. 2020;134(21):2791-805.
9. Li W, Moore MJ, Vasilieva N, Sui J, Wong SK, Berne MA, Somasundaran M, Sullivan JL, Luzuriaga K, Greenough TC, Choe H, Farzan M. Angiotensin-converting enzyme 2 is a functional receptor for the SARS coronavirus. *Nature*. 2003;426(6965):450-4.
10. Rota PA, Oberste MS, Monroe SS, Nix WA, Campagnoli R, Icenogle JP, Penaranda S, Bankamp B, Maher K, Chen MH, Tong S, Tamin A, Lowe L, Frace M, DeRisi JL, Chen Q, Wang D, Erdman DD, Peret TC, Burns C, Ksiazek TG, Rollin PE, Sanchez A, Liffick S, Holloway B, Limor J, McCaustland K, Olsen-Rasmussen M, Fouchier R, Gunther S, Osterhaus AD, Drosten C, Pallansch MA, Anderson LJ, Bellini WJ. Characterization of a novel coronavirus associated with severe acute respiratory syndrome. *Science*. 2003;300(5624):1394-9.
11. Hoffmann M, Kleine-Weber H, Schroeder S, Krüger N, Herrler T, Erichsen S, Schiergens TS, Herrler G, Wu N-H, Nitsche A, Müller M, Drosten C, Pöhlmann S. SARS-CoV-2 cell entry depends on ACE2 and TMPRSS2 and is blocked by a clinically proven protease inhibitor. *cell*. 2020;181(2):271-80. e8.
12. Wan Y, Shang J, Graham R, Baric RS, Li F. Receptor recognition by the novel coronavirus from Wuhan: an analysis based on decade-long structural studies of SARS coronavirus. *Journal of virology*. 2020;94(7):10.1128/jvi.00127-20.
13. Shang J, Ye G, Shi K, Wan Y, Luo C, Aihara H, Geng Q, Auerbach A, Li F. Structural basis of receptor recognition by SARS-CoV-2. *Nature*. 2020;581(7807):221-4.
14. Jackson CB, Farzan M, Chen B, Choe H. Mechanisms of SARS-CoV-2 entry into cells. *Nature reviews Molecular cell biology*. 2022;23(1):3-20.
15. Xu C, Wang Y, Liu C, Zhang C, Han W, Hong X, Wang Y, Hong Q, Wang S, Zhao Q, Wang Y, Yang Y, Chen K, Zheng W, Kong L, Wang F, Zuo Q, Huang Z, Cong Y.

- Conformational dynamics of SARS-CoV-2 trimeric spike glycoprotein in complex with receptor ACE2 revealed by cryo-EM. *Sci Adv.* 2021;7(1).
16. Yu S, Zheng X, Zhou B, Li J, Chen M, Deng R, Wong G, Lavillette D, Meng G. SARS-CoV-2 spike engagement of ACE2 primes S2' site cleavage and fusion initiation. *Proceedings of the National Academy of Sciences.* 2022;119(1):e2111199119.
  17. Walls AC, Tortorici MA, Snijder J, Xiong X, Bosch B-J, Rey FA, Velesler D. Tectonic conformational changes of a coronavirus spike glycoprotein promote membrane fusion. *Proceedings of the National Academy of Sciences.* 2017;114(42):11157-62.
  18. Fan X, Cao D, Kong L, Zhang X. Cryo-EM analysis of the post-fusion structure of the SARS-CoV spike glycoprotein. *Nature communications.* 2020;11(1):3618.
  19. Bayati A, Kumar R, Francis V, McPherson PS. SARS-CoV-2 infects cells after viral entry via clathrin-mediated endocytosis. *Journal of Biological Chemistry.* 2021;296.
  20. Ou T, Mou H, Zhang L, Ojha A, Choe H, Farzan M. Hydroxychloroquine-mediated inhibition of SARS-CoV-2 entry is attenuated by TMPRSS2. *PLoS pathogens.* 2021;17(1):e1009212.
  21. Bader M, Turner AJ, Alenina N. ACE2, a multifunctional protein—from cardiovascular regulation to COVID-19. Portland Press Ltd.; 2020. p. 3229-32.
  22. Serfozo P, Wysocki J, Gulua G, Schulze A, Ye M, Liu P, Jin J, Bader M, Myöhänen T, García-Horsman JA, Batlle D. Ang II (angiotensin II) conversion to angiotensin-(1-7) in the circulation is POP (prolyl oligopeptidase)-dependent and ACE2 (angiotensin-converting enzyme 2)-independent. *Hypertension.* 2020;75(1):173-82.
  23. Wysocki J, Batlle D. ACE2 in the Urine: Where Does It Come From? *Kidney360.* 2022;3(12):2001.
  24. Yan R, Zhang Y, Li Y, Xia L, Guo Y, Zhou Q. Structural basis for the recognition of SARS-CoV-2 by full-length human ACE2. *Science.* 2020;367(6485):1444-8.
  25. Zhang H, Wada J, Hida K, Tsuchiyama Y, Hiragushi K, Shikata K, Wang H, Lin S, Kanwar YS, Makino H. Collectrin, a collecting duct-specific transmembrane glycoprotein, is a novel homolog of ACE2 and is developmentally regulated in embryonic kidneys. *Journal of Biological Chemistry.* 2001;276(20):17132-9.
  26. Poglitsch M, Domenig O, Schwager C, Stranner S, Peball B, Janzek E, Wagner B, Jungwirth H, Loibner H, Schuster M. Recombinant expression and characterization of human and murine ACE2: species-specific activation of the alternative renin-angiotensin-system. *International journal of hypertension.* 2012;2012.
  27. Garreta E, Prado P, Stanifer ML, Monteil V, Marco A, Ullate-Agote A, Moya-Rull D, Vilas-Zornoza A, Tarantino C, Romero JP, Jonsson G, Oria R, Leopoldi A, Hagelkruys A, Gallo M, Gonzalez F, Domingo-Pedrol P, Gavalda A, Del Pozo CH, Hasan Ali O, Ventura-Aguiar P, Campistol JM, Prosper F, Mirazimi A, Boulant S, Penninger JM, Montserrat N. A diabetic milieu increases ACE2 expression and cellular susceptibility to SARS-CoV-2 infections in human kidney organoids and patient cells. *Cell Metab.* 2022;34(6):857-73 e9.
  28. Batlle D, Monteil V, Garreta E, Hassler L, Wysocki J, Chandar V, Schwartz RE, Mirazimi A, Montserrat N, Bader M, Penninger J. Evidence in favor of the essentiality of human cell membrane-bound ACE2 and against soluble ACE2 for SARS-CoV-2 infectivity. *Cell.* 2022;185(11):1837-9.
  29. Hofmann H, Geier M, Marzi A, Krumbiegel M, Peipp M, Fey GH, Gramberg T, Pöhlmann S. Susceptibility to SARS coronavirus S protein-driven infection correlates with expression of angiotensin converting enzyme 2 and infection can be blocked by soluble receptor. *Biochemical and biophysical research communications.* 2004;319(4):1216-21.

30. Batlle D, Wysocki J, Satchell K. Soluble angiotensin-converting enzyme 2: a potential approach for coronavirus infection therapy? *Clinical science*. 2020;134(5):543-5.
31. Zhang H, Penninger JM, Li Y, Zhong N, Slutsky AS. Angiotensin-converting enzyme 2 (ACE2) as a SARS-CoV-2 receptor: molecular mechanisms and potential therapeutic target. *Intensive care medicine*. 2020;46:586-90.
32. Hassler L, Wysocki J, Gelarden I, Sharma I, Tomatsidou A, Ye M, Gula H, Nicoleascu V, Randall G, Pshenychnyi S, Khurram N, Kanwar YS, Missiakas D, Henkin J, Yeldandi A, Batlle D. A novel soluble ACE2 protein provides lung and kidney protection in mice susceptible to lethal SARS-CoV-2 infection. *Journal of the American Society of Nephrology*. 2022;33(7):1293-307.
33. Monteil V, Kwon H, Prado P, Hagelkruys A, Wimmer RA, Stahl M, Leopoldi A, Garreta E, Hurtado Del Pozo C, Prosper F, Romero JP, Wirnsberger G, Zhang H, Slutsky AS, Conder R, Montserrat N, Mirazimi A, Penninger JM. Inhibition of SARS-CoV-2 Infections in Engineered Human Tissues Using Clinical-Grade Soluble Human ACE2. *Cell*. 2020;181(4):905-13 e7.
34. Wysocki J, Ye M, Hassler L, Gupta AK, Wang Y, Nicoleascu V, Randall G, Wertheim JA, Batlle D. A novel soluble ACE2 variant with prolonged duration of action neutralizes SARS-CoV-2 infection in human kidney organoids. *Journal of the American Society of Nephrology: JASN*. 2021;32(4):795.
35. Schimpf A, Hempel F, Li A, Linne U, Maier UG, Reetz MT, Geyer A. Hinge-type dimerization of proteins by a tetracysteine peptide of high pairing specificity. *Biochemistry*. 2018;57(26):3658-64.
36. McCray Jr PB, Pewe L, Wohlford-Lenane C, Hickey M, Manzel L, Shi L, Netland J, Jia HP, Halabi C, Sigmund CD, Meyerholz DK, Kirby P, Look D, Perlman S. Lethal infection of K18-hACE2 mice infected with severe acute respiratory syndrome coronavirus. *Journal of virology*. 2007;81(2):813-21.
37. Winkler ES, Bailey AL, Kafai NM, Nair S, McCune BT, Yu J, Fox JM, Chen RE, Earnest JT, Keeler SP, Ritter J, Kang L-I, Dort S, Robichaud A, Head R, Holtzman M, Diamond MS. SARS-CoV-2 infection of human ACE2-transgenic mice causes severe lung inflammation and impaired function. *Nature immunology*. 2020;21(11):1327-35.
38. Zhou P, Yang XL, Wang XG, Hu B, Zhang L, Zhang W, Si HR, Zhu Y, Li B, Huang CL, Chen HD, Chen J, Luo Y, Guo H, Jiang RD, Liu MQ, Chen Y, Shen XR, Wang X, Zheng XS, Zhao K, Chen QJ, Deng F, Liu LL, Yan B, Zhan FX, Wang YY, Xiao GF, Shi ZL. A pneumonia outbreak associated with a new coronavirus of probable bat origin. *Nature*. 2020;579(7798):270-3.
39. Zheng J, Wong L-YR, Li K, Verma AK, Ortiz ME, Wohlford-Lenane C, Leidinger MR, Knudson CM, Meyerholz DK, McCray Jr PB, Perlman S. COVID-19 treatments and pathogenesis including anosmia in K18-hACE2 mice. *Nature*. 2021;589(7843):603-7.
40. Golden JW, Cline CR, Zeng X, Garrison AR, Carey BD, Mucker EM, White LE, Shamblin JD, Brocato RL, Liu J, Babka A, Rauch H, Smith J, Hollidge B, Fitzpatrick C, Badger C, Hooper J. Human angiotensin-converting enzyme 2 transgenic mice infected with SARS-CoV-2 develop severe and fatal respiratory disease. *JCI insight*. 2020;5(19).
41. Oladunni FS, Park JG, Pino PA, Gonzalez O, Akhter A, Allue-Guardia A, Olmo-Fontanez A, Gautam S, Garcia-Vilanova A, Ye C, Chiem K, Headley C, Dwivedi V, Parodi LM, Alfson KJ, Staples HM, Schami A, Garcia JI, Whigham A, Platt RN, 2nd, Gazi M, Martinez J, Chuba C, Earley S, Rodriguez OH, Mdaki SD, Kavelish KN, Escalona R, Hallam CRA, Christie C, Patterson JL, Anderson TJC, Carrion R, Jr., Dick EJ, Jr., Hall-Ursone S, Schlesinger LS, Alvarez X, Kaushal D, Giavedoni LD, Turner J, Martinez-

- Sobrido L, Torrelles JB. Lethality of SARS-CoV-2 infection in K18 human angiotensin-converting enzyme 2 transgenic mice. *Nat Commun.* 2020;11(1):6122.
42. Chu H, Chan JF, Yuen TT, Shuai H, Yuan S, Wang Y, Hu B, Yip CC, Tsang JO, Huang X, Chai Y, Yang D, Hou Y, Chik KK, Zhang X, Fung AY, Tsoi HW, Cai JP, Chan WM, Ip JD, Chu AW, Zhou J, Lung DC, Kok KH, To KK, Tsang OT, Chan KH, Yuen KY. Comparative tropism, replication kinetics, and cell damage profiling of SARS-CoV-2 and SARS-CoV with implications for clinical manifestations, transmissibility, and laboratory studies of COVID-19: an observational study. *Lancet Microbe.* 2020;1(1):e14-e23.
43. Meng B, Abdullahi A, Ferreira I, Goonawardane N, Saito A, Kimura I, Yamasoba D, Gerber PP, Fatihi S, Rathore S, Zepeda SK, Papa G, Kemp SA, Ikeda T, Toyoda M, Tan TS, Kuramochi J, Mitsunaga S, Ueno T, Shirakawa K, Takaori-Kondo A, Brevini T, Mallery DL, Charles OJ, Collaboration C-NBC-, Genotype to Phenotype Japan C, Ecuador CC, Bowen JE, Joshi A, Walls AC, Jackson L, Martin D, Smith KGC, Bradley J, Briggs JAG, Choi J, Madissoon E, Meyer KB, Mlcochova P, Ceron-Gutierrez L, Doffinger R, Teichmann SA, Fisher AJ, Pizzuto MS, de Marco A, Corti D, Hosmillo M, Lee JH, James LC, Thukral L, Veessler D, Sigal A, Sampaziotis F, Goodfellow IG, Matheson NJ, Sato K, Gupta RK. Altered TMPRSS2 usage by SARS-CoV-2 Omicron impacts infectivity and fusogenicity. *Nature.* 2022;603(7902):706-14.
44. Suzuki R, Yamasoba D, Kimura I, Wang L, Kishimoto M, Ito J, Morioka Y, Nao N, Nasser H, Uriu K, Kosugi Y, Tsuda M, Orba Y, Sasaki M, Shimizu R, Kawabata R, Yoshimatsu K, Asakura H, Nagashima M, Sadamasu K, Yoshimura K, Genotype to Phenotype Japan C, Sawa H, Ikeda T, Irie T, Matsuno K, Tanaka S, Fukuhara T, Sato K. Attenuated fusogenicity and pathogenicity of SARS-CoV-2 Omicron variant. *Nature.* 2022;603(7902):700-5.
45. Ye M, Wysocki J, Gonzalez-Pacheco FR, Salem M, Evora K, Garcia-Halpin L, Poglitsch M, Schuster M, Battle D. Murine Recombinant Angiotensin-Converting Enzyme 2: Effect on Angiotensin II-Dependent Hypertension and Distinctive Angiotensin-Converting Enzyme 2 Inhibitor Characteristics on Rodent and Human Angiotensin-Converting Enzyme 2. *Hypertension.* 2012;60(3):730-40.
46. Wysocki J, Lores E, Ye M, Soler MJ, Battle D. Kidney and lung ACE2 expression after an ACE inhibitor or an Ang II receptor blocker: implications for COVID-19. *Journal of the American Society of Nephrology: JASN.* 2020;31(9):1941.
47. He Y, Henley J, Sell P, Comai L. Differential outcomes of infection by wild-type SARS-CoV-2 and the B. 1.617. 2 and B. 1.1. 529 variants of concern in K18-hACE2 transgenic mice. *Viruses.* 2023;16(1):60.
48. Halfmann PJ, Iida S, Iwatsuki-Horimoto K, Maemura T, Kiso M, Scheaffer SM, Darling TL, Joshi A, Loeber S, Singh G, Foster SL, Ying B, Case JB, Chong Z, Whitener B, Moliva J, Floyd K, Ujie M, Nakajima N, Ito M, Wright R, Uraki R, Warang P, Gagne M, Li R, Sakai-Tagawa Y, Liu Y, Larson D, Osorio JE, Hernandez-Ortiz JP, Henry AR, Ciuderis K, Florek KR, Patel M, Odle A, Wong LR, Bateman AC, Wang Z, Edara VV, Chong Z, Franks J, Jeevan T, Fabrizio T, DeBeauchamp J, Kercher L, Seiler P, Gonzalez-Reiche AS, Sordillo EM, Chang LA, van Bakel H, Simon V, Consortium Mount Sinai Pathogen Surveillance study g, Douek DC, Sullivan NJ, Thackray LB, Ueki H, Yamayoshi S, Imai M, Perlman S, Webby RJ, Seder RA, Suthar MS, Garcia-Sastre A, Schotsaert M, Suzuki T, Boon ACM, Diamond MS, Kawaoka Y. SARS-CoV-2 Omicron virus causes attenuated disease in mice and hamsters. *Nature.* 2022;603(7902):687-92.
49. Tarres-Freixas F, Trinite B, Pons-Grifols A, Romero-Durana M, Riveira-Munoz E, Avila-Nieto C, Perez M, Garcia-Vidal E, Perez-Zsolt D, Munoz-Basagoiti J, Raich-Regue D, Izquierdo-Useros N, Andres C, Anton A, Pumarola T, Blanco I, Noguera-Julian M, Guallar V, Lepore R, Valencia A, Urrea V, Vergara-Alert J, Clotet B, Ballana E, Carrillo J,

- Segales J, Blanco J. Heterogeneous Infectivity and Pathogenesis of SARS-CoV-2 Variants Beta, Delta and Omicron in Transgenic K18-hACE2 and Wildtype Mice. *Front Microbiol.* 2022;13:840757.
50. Ito D, Imai Y, Ohsawa K, Nakajima K, Fukuuchi Y, Kohsaka S. Microglia-specific localisation of a novel calcium binding protein, Iba1. *Molecular brain research.* 1998;57(1):1-9.
51. Tykhomyrov A, Pavlova A, Nedzvetsky V. Glial fibrillary acidic protein (GFAP): on the 45th anniversary of its discovery. *Neurophysiology.* 2016;48:54-71.
52. Dong W, Mead H, Tian L, Park JG, Garcia JI, Jaramillo S, Barr T, Kollath DS, Coyne VK, Stone NE, Jones A, Zhang J, Li A, Wang LS, Milanes-Yearsley M, Torrelles JB, Martinez-Sobrido L, Keim PS, Barker BM, Caligiuri MA, Yu J. The K18-Human ACE2 Transgenic Mouse Model Recapitulates Non-severe and Severe COVID-19 in Response to an Infectious Dose of the SARS-CoV-2 Virus. *J Virol.* 2022;96(1):e0096421.
53. Netland J, Meyerholz DK, Moore S, Cassell M, Perlman S. Severe acute respiratory syndrome coronavirus infection causes neuronal death in the absence of encephalitis in mice transgenic for human ACE2. *Journal of virology.* 2008;82(15):7264-75.
54. Fumagalli V, Rava M, Marotta D, Di Lucia P, Laura C, Sala E, Grillo M, Bono E, Giustini L, Perucchini C, Mainetti M, Sessa A, Garcia-Manteiga JM, Donnici L, Manganaro L, Delbue S, Broccoli V, De Francesco R, D'Adamo P, Kuka M, Guidotti LG, Iannacone M. Administration of aerosolized SARS-CoV-2 to K18-hACE2 mice uncouples respiratory infection from fatal neuroinvasion. *Sci Immunol.* 2022;7(67):eabl9929.
55. Kumari P, Rothan HA, Natekar JP, Stone S, Pathak H, Strate PG, Arora K, Brinton MA, Kumar M. Neuroinvasion and encephalitis following intranasal inoculation of SARS-CoV-2 in K18-hACE2 mice. *Viruses.* 2021;13(1):132.
56. Vidal E, López-Figueroa C, Rodon J, Pérez M, Brustolin M, Cantero G, Guallar V, Izquierdo-Useros N, Carrillo J, Blanco J, Clotet B, Vergara-Alert J, Segales J. Chronological brain lesions after SARS-CoV-2 infection in hACE2-transgenic mice. *Veterinary pathology.* 2022;59(4):613-26.
57. Seehusen F, Clark JJ, Sharma P, Bentley EG, Kirby A, Subramaniam K, Wunderlin-Giuliani S, Hughes GL, Patterson EI, Michael BD, Owen A, Hiscox J, Stewart J, Kipar A. Neuroinvasion and neurotropism by SARS-CoV-2 variants in the K18-hACE2 mouse. *Viruses.* 2022;14(5):1020.
58. Carossino M, Kenney D, O'Connell AK, Montanaro P, Tseng AE, Gertje HP, Grosz KA, Ericsson M, Huber BR, Kurnick SA, Subramaniam S, Kirkland TA, Walker JR, Francis KP, Klose AD, Paragas N, Bosmann M, Saeed M, Balasuriya UBR, Douam F, Crossland NA. Fatal Neurodissemination and SARS-CoV-2 Tropism in K18-hACE2 Mice Is Only Partially Dependent on hACE2 Expression. *Viruses.* 2022;14(3).
59. Schwabenland M, Salie H, Tanevski J, Killmer S, Lago MS, Schlaak AE, Mayer L, Matschke J, Puschel K, Fitzek A, Ondruschka B, Mei HE, Boettler T, Neumann-Haefelin C, Hofmann M, Breithaupt A, Genc N, Stadelmann C, Saez-Rodriguez J, Bronsert P, Knobloch KP, Blank T, Thimme R, Glatzel M, Prinz M, Bengsch B. Deep spatial profiling of human COVID-19 brains reveals neuroinflammation with distinct microanatomical microglia-T-cell interactions. *Immunity.* 2021;54(7):1594-610 e11.
60. Matschke J, Lutgehetmann M, Hagel C, Sperhake JP, Schroder AS, Edler C, Mushumba H, Fitzek A, Allweiss L, Dandri M, Dottermusch M, Heinemann A, Pfefferle S, Schwabenland M, Sumner Magruder D, Bonn S, Prinz M, Gerloff C, Puschel K, Krasemann S, Aepfelbacher M, Glatzel M. Neuropathology of patients with COVID-19 in Germany: a post-mortem case series. *Lancet Neurol.* 2020;19(11):919-29.

61. Braun F, Lutgehetmann M, Pfefferle S, Wong MN, Carsten A, Lindenmeyer MT, Norz D, Heinrich F, Meissner K, Wichmann D, Kluge S, Gross O, Puelles K, Schroder AS, Edler C, Aepfelbacher M, Puelles VG, Huber TB. SARS-CoV-2 renal tropism associates with acute kidney injury. *Lancet*. 2020;396(10251):597-8.
62. Puelles VG, Lutgehetmann M, Lindenmeyer MT, Sperhake JP, Wong MN, Allweiss L, Chilla S, Heinemann A, Wanner N, Liu S, Braun F, Lu S, Pfefferle S, Schroder AS, Edler C, Gross O, Glatzel M, Wichmann D, Wiech T, Kluge S, Puelles K, Aepfelbacher M, Huber TB. Multiorgan and Renal Tropism of SARS-CoV-2. *N Engl J Med*. 2020;383(6):590-2.
63. Remmelink M, De Mendonca R, D'Haene N, De Clercq S, Verocq C, Lebrun L, Lavis P, Racu ML, Trepant AL, Maris C, Rorive S, Goffard JC, De Witte O, Peluso L, Vincent JL, Decaestecker C, Taccone FS, Salmon I. Unspecific post-mortem findings despite multiorgan viral spread in COVID-19 patients. *Crit Care*. 2020;24(1):495.
64. Jansen J, Reimer KC, Nagai JS, Varghese FS, Overheul GJ, de Beer M, Rovers R, Daviran D, Fermin LAS, Willemsen B, Beukenboom M, Djurdjaj S, von Stillfried S, van Eijk LE, Mastik M, Bulthuis M, Dunnen WD, van Goor H, Hillebrands JL, Triana SH, Alexandrov T, Timm MC, van den Berge BT, van den Broek M, Nlandu Q, Heijnert J, Bindels EMJ, Hoogenboezem RM, Mooren F, Kuppe C, Miesen P, Grunberg K, Ijzermans T, Steenbergen EJ, Czogalla J, Schreuder MF, Sommerdijk N, Akiva A, Boor P, Puelles VG, Floege J, Huber TB, consortium CM, van Rij RP, Costa IG, Schneider RK, Smeets B, Kramann R. SARS-CoV-2 infects the human kidney and drives fibrosis in kidney organoids. *Cell Stem Cell*. 2022;29(2):217-31 e8.
65. May RM, Cassol C, Hannoudi A, Larsen CP, Lerma EV, Haun RS, Braga JR, Hassen SI, Wilson J, VanBeek C, Vankalakunti M, Barnum L, Walker PD, Bourne TD, Messias NC, Ambruzs JM, Boils CL, Sharma SS, Cossey LN, Baxi PV, Palmer M, Zuckerman JE, Walavalkar V, Urisman A, Gallan AJ, Al-Rabadi LF, Rodby R, Luyckx V, Espino G, Santhana-Krishnan S, Alper B, Lam SG, Hannoudi GN, Matthew D, Belz M, Singer G, Kunaparaju S, Price D, Chawla S, Rondla C, Abdalla MA, Britton ML, Paul S, Ranjit U, Bichu P, Williamson SR, Sharma Y, Gaspert A, Grosse P, Meyer I, Vasudev B, El Kassem M, Velez JCQ, Caza TN. A multi-center retrospective cohort study defines the spectrum of kidney pathology in Coronavirus 2019 Disease (COVID-19). *Kidney Int*. 2021;100(6):1303-15.
66. Isnard P, Vergnaud P, Garbay S, Jamme M, Eloudzeri M, Karras A, Anglicheau D, Galantine V, Jalal Eddine A, Gosset C, Pourcine F, Zarhrate M, Gibier JB, Rensen E, Pietropaoli S, Barba-Spaeth G, Duong-Van-Huyen JP, Molina TJ, Mueller F, Zimmer C, Pontoglio M, Terzi F, Rabant M. A specific molecular signature in SARS-CoV-2-infected kidney biopsies. *JCI Insight*. 2023;8(5).
67. Sharma P, Uppal NN, Wanchoo R, Shah HH, Yang Y, Parikh R, Khanin Y, Madireddy V, Larsen CP, Jhaveri KD, Bijol V, Northwell Nephrology C-RC. COVID-19-Associated Kidney Injury: A Case Series of Kidney Biopsy Findings. *J Am Soc Nephrol*. 2020;31(9):1948-58.
68. Hassler L, Batlle D. Potential SARS-CoV-2 kidney infection and paths to injury. *Nature Reviews Nephrology*. 2022;18(5):275-6.
69. Hassler L, Reyes F, Sparks MA, Welling P, Batlle D. Evidence for and against direct kidney infection by SARS-CoV-2 in patients with COVID-19. *Clinical Journal of the American Society of Nephrology*. 2021;16(11):1755-65.
70. Cianfarini C, Hassler L, Wysocki J, Hassan A, Nicolaescu V, Elli D, Gula H, Ibrahim AM, Randall G, Henkin J, Batlle D. Soluble Angiotensin-Converting Enzyme 2 Protein Improves Survival and Lowers Viral Titers in Lethal Mouse Model of Severe Acute

Respiratory Syndrome Coronavirus Type 2 Infection with the Delta Variant. *Cells*. 2024;13(3):203.

71. Zhang L, Narayanan KK, Cooper L, Chan KK, Skeeters SS, Devlin CA, Aguhob A, Shirley K, Rong L, Rehman J, Malik A, Procko E. An ACE2 decoy can be administered by inhalation and potentially targets omicron variants of SARS-CoV-2. *EMBO Molecular Medicine*. 2022;14(11):e16109.

72. Imai Y, Kuba K, Penninger JM. Angiotensin-converting enzyme 2 in acute respiratory distress syndrome. *Cellular and molecular life sciences*. 2007;64:2006-12.

73. Sodhi CP, Wohlford-Lenane C, Yamaguchi Y, Prindle T, Fulton WB, Wang S, McCray Jr PB, Chappell M, Hackam DJ, Jia H. Attenuation of pulmonary ACE2 activity impairs inactivation of des-Arg9 bradykinin/BKB1R axis and facilitates LPS-induced neutrophil infiltration. *American Journal of Physiology-Lung Cellular and Molecular Physiology*. 2018;314(1):L17-L31.

74. Bekassy Z, Lopatko Fagerström I, Bader M, Karpman D. Crosstalk between the renin-angiotensin, complement and kallikrein-kinin systems in inflammation. *Nature Reviews Immunology*. 2022;22(7):411-28.

75. Imai Y, Kuba K, Rao S, Huan Y, Guo F, Guan B, Yang P, Sarao R, Wada T, Leong-Poi H, Crackower MA, Fukamizu A, Hui CC, Hein L, Uhlig S, Slutsky AS, Jiang C, Penninger JM. Angiotensin-converting enzyme 2 protects from severe acute lung failure. *Nature*. 2005;436(7047):112-6.

76. Kuba K, Imai Y, Rao S, Gao H, Guo F, Guan B, Huan Y, Yang P, Zhang Y, Deng W, Bao L, Zhang B, Liu G, Wang Z, Chappell M, Liu Y, Zheng D, Leibbrandt A, Wada T, Slutsky AS, Liu D, Qin C, Jiang C, Penninger JM. A crucial role of angiotensin converting enzyme 2 (ACE2) in SARS coronavirus-induced lung injury. *Nat Med*. 2005;11(8):875-9.

77. Yamaguchi T, Hoshizaki M, Minato T, Nirasawa S, Asaka MN, Niiyama M, Imai M, Uda A, Chan JF, Takahashi S, An J, Saku A, Nukiwa R, Utsumi D, Kiso M, Yasuhara A, Poon VK, Chan CC, Fujino Y, Motoyama S, Nagata S, Penninger JM, Kamada H, Yuen KY, Kamitani W, Maeda K, Kawaoka Y, Yasutomi Y, Imai Y, Kuba K. ACE2-like carboxypeptidase B38-CAP protects from SARS-CoV-2-induced lung injury. *Nat Commun*. 2021;12(1):6791.

78. Davidson AM, Wysocki J, Battle D. Interaction of SARS-CoV-2 and other coronavirus with ACE (angiotensin-converting enzyme)-2 as their main receptor: therapeutic implications. *Hypertension*. 2020;76(5):1339-49.

79. Li Y, Wang H, Tang X, Fang S, Ma D, Du C, Wang Y, Pan H, Yao W, Zhang R, Zou X, Zheng J, Xu L, Farzan M, Zhong G. SARS-CoV-2 and three related coronaviruses utilize multiple ACE2 orthologs and are potentially blocked by an improved ACE2-Ig. *Journal of virology*. 2020;94(22):10.1128/jvi.01283-20.

80. Liu P, Wysocki J, Souma T, Ye M, Ramirez V, Zhou B, Wilsbacher LD, Quaggin SE, Battle D, Jin J. Novel ACE2-Fc chimeric fusion provides long-lasting hypertension control and organ protection in mouse models of systemic renin angiotensin system activation. *Kidney international*. 2018;94(1):114-25.

81. Glasgow A, Glasgow J, Limonta D, Solomon P, Lui I, Zhang Y, Nix MA, Rettko NJ, Zha S, Yamin R, Kao K, Rosenberg OS, Ravetch JV, Wiita AP, Leung KK, Lim SA, Zhou XX, Hobman TC, Kortemme T, Wells JA. Engineered ACE2 receptor traps potentially neutralize SARS-CoV-2. *Proc Natl Acad Sci U S A*. 2020;117(45):28046-55.

82. Urano E, Itoh Y, Suzuki T, Sasaki T, Kishikawa JI, Akamatsu K, Higuchi Y, Sakai Y, Okamura T, Mitoma S, Sugihara F, Takada A, Kimura M, Nakao S, Hirose M, Sasaki T, Koketsu R, Tsuji S, Yanagida S, Shioda T, Hara E, Matoba S, Matsuura Y, Kanda Y, Arase H, Okada M, Takagi J, Kato T, Hoshino A, Yasutomi Y, Saito A, Okamoto T. An

inhaled ACE2 decoy confers protection against SARS-CoV-2 infection in preclinical models. *Sci Transl Med.* 2023;15(711):eadi2623.

83. Chen Y, Sun L, Ullah I, Beaudoin-Bussieres G, Anand SP, Hederman AP, Tolbert WD, Sherburn R, Nguyen DN, Marchitto L, Ding S, Wu D, Luo Y, Gottumukkala S, Moran S, Kumar P, Piszczek G, Mothes W, Ackerman ME, Finzi A, Uchil PD, Gonzalez FJ, Pazgier M. Engineered ACE2-Fc counters murine lethal SARS-CoV-2 infection through direct neutralization and Fc-effector activities. *Sci Adv.* 2022;8(28):eabn4188.

84. De Taeye SW, Bentlage AE, Mebius MM, Meesters JI, Lissenberg-Thunnissen S, Falck D, Sénard T, Salehi N, Wuhrer M, Schuurman J, Labrijn A, Rispens T, Vidarsson G. FcγR binding and ADCC activity of human IgG allotypes. *Frontiers in immunology.* 2020;11:740.

85. Lee WS, Wheatley AK, Kent SJ, DeKosky BJ. Antibody-dependent enhancement and SARS-CoV-2 vaccines and therapies. *Nature microbiology.* 2020;5(10):1185-91.

86. Chan KK, Dorosky D, Sharma P, Abbasi SA, Dye JM, Kranz DM, Herbert AS, Procko E. Engineering human ACE2 to optimize binding to the spike protein of SARS coronavirus 2. *Science.* 2020;369(6508):1261-5.

87. Jing W, Procko E. ACE2-based decoy receptors for SARS coronavirus 2. *Proteins: Structure, Function, and Bioinformatics.* 2021;89(9):1065-78.

88. Zhang L, Dutta S, Xiong S, Chan M, Chan KK, Fan TM, Bailey KL, Lindeblad M, Cooper LM, Rong L. Engineered ACE2 decoy mitigates lung injury and death induced by SARS-CoV-2 variants. *Nature chemical biology.* 2022;18(3):342-51.

89. Higuchi Y, Suzuki T, Arimori T, Ikemura N, Mihara E, Kirita Y, Ohgitani E, Mazda O, Motooka D, Nakamura S, Sakai Y, Itoh Y, Sugihara F, Matsuura Y, Matoba S, Okamoto T, Takagi J, Hoshino A. Engineered ACE2 receptor therapy overcomes mutational escape of SARS-CoV-2. *Nat Commun.* 2021;12(1):3802.

90. Sims JJ, Greig JA, Michalson KT, Lian S, Martino RA, Meggersee R, Turner KB, Nambiar K, Dyer C, Hinderer C, Horiuchi M, Yan H, Huang X, Chen SJ, Wilson JM. Intranasal gene therapy to prevent infection by SARS-CoV-2 variants. *PLoS Pathog.* 2021;17(7):e1009544.

91. Liu J, Mao F, Chen J, Lu S, Qi Y, Sun Y, Fang L, Yeung ML, Liu C, Yu G, Li G, Liu X, Yao Y, Huang P, Hao D, Liu Z, Ding Y, Liu H, Yang F, Chen P, Sa R, Sheng Y, Tian X, Peng R, Li X, Luo J, Cheng Y, Zheng Y, Lin Y, Song R, Jin R, Huang B, Choe H, Farzan M, Yuen KY, Tan W, Peng X, Sui J, Li W. An IgM-like inhalable ACE2 fusion protein broadly neutralizes SARS-CoV-2 variants. *Nat Commun.* 2023;14(1):5191.

92. Benjakul S, Anthi AK, Kolderup A, Vaysburd M, Lode HE, Mallery D, Fossum E, Vikse EL, Albecka A, Ianevski A, Kainov D, Karlsen KF, Sakya SA, Nyquist-Andersen M, Gjolberg TT, Moe MC, Bjoras M, Sandlie I, James LC, Andersen JT. A pan-SARS-CoV-2-specific soluble angiotensin-converting enzyme 2-albumin fusion engineered for enhanced plasma half-life and needle-free mucosal delivery. *PNAS Nexus.* 2023;2(12):pgad403.

93. Guo L, Bi W, Wang X, Xu W, Yan R, Zhang Y, Zhao K, Li Y, Zhang M, Cai X, Jiang S, Xie Y, Zhou Q, Lu L, Dang B. Engineered trimeric ACE2 binds viral spike protein and locks it in "Three-up" conformation to potently inhibit SARS-CoV-2 infection. *Cell Res.* 2021;31(1):98-100.

94. Wrapp D, Wang N, Corbett KS, Goldsmith JA, Hsieh C-L, Abiona O, Graham BS, McLellan JS. Cryo-EM structure of the 2019-nCoV spike in the prefusion conformation. *Science.* 2020;367(6483):1260-3.

95. Shoemaker RH, Panettieri RA, Jr., Libutti SK, Hochster HS, Watts NR, Wingfield PT, Starkl P, Pimenov L, Gawish R, Hladik A, Knapp S, Boring D, White JM, Lawrence Q, Boone J, Marshall JD, Matthews RL, Cholewa BD, Richig JW, Chen BT, McCormick

- DL, Guginsberger R, Holler S, Penninger JM, Wirnsberger G. Development of an aerosol intervention for COVID-19 disease: Tolerability of soluble ACE2 (APN01) administered via nebulizer. *PLoS One*. 2022;17(7):e0271066.
96. Zoufaly A, Poglitsch M, Aberle JH, Hoepfer W, Seitz T, Traugott M, Grieb A, Pawelka E, Laferl H, Wenisch C, Neuhold S, Haider D, Stiasny K, Bergthaler A, Puchhammer-Stoeckl E, Mirazimi A, Montserrat N, Zhang H, Slutsky AS, Penninger JM. Human recombinant soluble ACE2 in severe COVID-19. *Lancet Respir Med*. 2020;8(11):1154-8.
97. Haschke M, Schuster M, Poglitsch M, Loibner H, Salzberg M, Bruggisser M, Penninger J, Krähenbühl S. Pharmacokinetics and pharmacodynamics of recombinant human angiotensin-converting enzyme 2 in healthy human subjects. *Clinical pharmacokinetics*. 2013;52:783-92.
98. NCT04335136: Recombinant Human Angiotensin-converting Enzyme 2 (rhACE2) as a Treatment for Patients With COVID-19 (APN01-COVID-19) [Available from: <https://clinicaltrials.gov/study/NCT04335136> , last accessed 02/17/2024, 10:53 AM.
99. NCT05065645: Study to Assess the Safety, Tolerability, Pharmacokinetics and Pharmacodynamics of Inhaled APN01 Developed as Treatment for COVID-19 [Available from: <https://clinicaltrials.gov/study/NCT05065645?term=NCT05065645&rank=1> , last accessed 02/17/2024 10:54 AM.
100. VanBlargan LA, Errico JM, Halfmann PJ, Zost SJ, Crowe Jr JE, Purcell LA, Kawaoka Y, Corti D, Fremont DH, Diamond MS. An infectious SARS-CoV-2 B. 1.1. 529 Omicron virus escapes neutralization by therapeutic monoclonal antibodies. *Nature medicine*. 2022;28(3):490-5.
101. Mannar D, Saville JW, Zhu X, Srivastava SS, Berezuk AM, Tuttle KS, Marquez AC, Sekirov I, Subramaniam S. SARS-CoV-2 Omicron variant: Antibody evasion and cryo-EM structure of spike protein–ACE2 complex. *Science*. 2022;375(6582):760-4.
102. Wang P, Nair MS, Liu L, Iketani S, Luo Y, Guo Y, Wang M, Yu J, Zhang B, Kwong PD, Graham BS, Mascola JR, Chang JY, Yin MT, Sobieszczyk M, Kyratsous CA, Shapiro L, Sheng Z, Huang Y, Ho DD. Antibody resistance of SARS-CoV-2 variants B.1.351 and B.1.1.7. *Nature*. 2021;593(7857):130-5.
103. Weisblum Y, Schmidt F, Zhang F, DaSilva J, Poston D, Lorenzi JC, Muecksch F, Rutkowska M, Hoffmann HH, Michailidis E, Gaebler C, Agudelo M, Cho A, Wang Z, Gazumyan A, Cipolla M, Luchsinger L, Hillyer CD, Caskey M, Robbiani DF, Rice CM, Nussenzweig MC, Hatzioannou T, Bieniasz PD. Escape from neutralizing antibodies by SARS-CoV-2 spike protein variants. *Elife*. 2020;9.
104. Planas D, Veyer D, Baidaliuk A, Staropoli I, Guivel-Benhassine F, Rajah MM, Planchais C, Porrot F, Robillard N, Puech J, Prot M, Gallais F, Gantner P, Velay A, Le Guen J, Kassis-Chikhani N, Edriss D, Belec L, Seve A, Courtellemont L, Pere H, Hocqueloux L, Fafi-Kremer S, Prazuck T, Mouquet H, Bruel T, Simon-Loriere E, Rey FA, Schwartz O. Reduced sensitivity of SARS-CoV-2 variant Delta to antibody neutralization. *Nature*. 2021;596(7871):276-80.
105. Hoffmann M, Kruger N, Schulz S, Cossmann A, Rocha C, Kempf A, Nehlmeier I, Graichen L, Moldenhauer AS, Winkler MS, Lier M, Dopfer-Jablonka A, Jack HM, Behrens GMN, Pohlmann S. The Omicron variant is highly resistant against antibody-mediated neutralization: Implications for control of the COVID-19 pandemic. *Cell*. 2022;185(3):447-56 e11.
106. Rössler A, Riepler L, Bante D, von Laer D, Kimpel J. SARS-CoV-2 Omicron variant neutralization in serum from vaccinated and convalescent persons. *New England Journal of Medicine*. 2022;386(7):698-700.

107. Saxena SK, Kumar S, Ansari S, Paweska JT, Maurya VK, Tripathi AK, Abdel-Moneim AS. Characterization of the novel SARS-CoV-2 Omicron (B. 1.1. 529) variant of concern and its global perspective. *Journal of medical virology*. 2022;94(4):1738-44.
108. Zhang W, Shi K, Geng Q, Herbst M, Wang M, Huang L, Bu F, Liu B, Aihara H, Li F. Structural evolution of SARS-CoV-2 omicron in human receptor recognition. *Journal of virology*. 2023;97(8):e00822-23.
109. CDC Variant proportions [Available from: <https://covid.cdc.gov/covid-data-tracker/#variant-proportions>], last accessed 02/17/2024 10:56 AM.
110. Kaku Y, Okumura K, Padilla-Blanco M, Kosugi Y, Uriu K, Hinay AA, Jr., Chen L, Plianchaisuk A, Kobiyama K, Ishii KJ, Genotype to Phenotype Japan C, Zahradnik J, Ito J, Sato K. Virological characteristics of the SARS-CoV-2 JN.1 variant. *Lancet Infect Dis*. 2024;24(2):e82.
111. Yang S, Yu Y, Xu Y, Jian F, Song W, Yisimayi A, Wang P, Wang J, Liu J, Yu L, Niu X, Wang J, Wang Y, Shao F, Jin R, Wang Y, Cao Y. Fast evolution of SARS-CoV-2 BA.2.86 to JN.1 under heavy immune pressure. *Lancet Infect Dis*. 2024;24(2):e70-e2.
112. Hassler L, Penninger J, Batlle D. On the essentiality of the angiotensin converting enzyme 2 receptor for SARS-CoV-2 infection and the potential of soluble angiotensin converting enzyme 2 proteins as universal approach for variants causing COVID-19. *Clinical and Translational Medicine*. 2022;12(10):e1080.
113. Chan KK, Tan TJ, Narayanan KK, Procko E. An engineered decoy receptor for SARS-CoV-2 broadly binds protein S sequence variants. *Science Advances*. 2021;7(8):eabf1738.

## Eidesstattliche Versicherung

„Ich, Luise Hassler, versichere an Eides statt durch meine eigenhändige Unterschrift, dass ich die vorgelegte Dissertation mit dem Thema: „Intranasal soluble ACE2 improves organ histopathology and survival in k18hACE2 mice infected with SARS-CoV-2“ / „Intranasales lösliches ACE2 Protein verbessert Überleben und Organhistopathologie in SARS-CoV-2 infizierten k18hACE2 Mäusen“ selbstständig und ohne nicht offengelegte Hilfe Dritter verfasst und keine anderen als die angegebenen Quellen und Hilfsmittel genutzt habe.

Alle Stellen, die wörtlich oder dem Sinne nach auf Publikationen oder Vorträgen anderer Autoren/innen beruhen, sind als solche in korrekter Zitierung kenntlich gemacht. Die Abschnitte zu Methodik (insbesondere praktische Arbeiten, Laborbestimmungen, statistische Aufarbeitung) und Resultaten (insbesondere Abbildungen, Graphiken und Tabellen) werden von mir verantwortet.

Ich versichere ferner, dass ich die in Zusammenarbeit mit anderen Personen generierten Daten, Datenauswertungen und Schlussfolgerungen korrekt gekennzeichnet und meinen eigenen Beitrag sowie die Beiträge anderer Personen korrekt kenntlich gemacht habe (siehe Anteilserklärung). Texte oder Textteile, die gemeinsam mit anderen erstellt oder verwendet wurden, habe ich korrekt kenntlich gemacht.

Meine Anteile an etwaigen Publikationen zu dieser Dissertation entsprechen denen, die in der untenstehenden gemeinsamen Erklärung mit dem/der Erstbetreuer/in, angegeben sind. Für sämtliche im Rahmen der Dissertation entstandenen Publikationen wurden die Richtlinien des ICMJE (International Committee of Medical Journal Editors; [www.icmje.org](http://www.icmje.org)) zur Autorenschaft eingehalten. Ich erkläre ferner, dass ich mich zur Einhaltung der Satzung der Charité – Universitätsmedizin Berlin zur Sicherung Guter Wissenschaftlicher Praxis verpflichte.

Weiterhin versichere ich, dass ich diese Dissertation weder in gleicher noch in ähnlicher Form bereits an einer anderen Fakultät eingereicht habe.

Die Bedeutung dieser eidesstattlichen Versicherung und die strafrechtlichen Folgen einer unwahren eidesstattlichen Versicherung (§§156, 161 des Strafgesetzbuches) sind mir bekannt und bewusst.“

Datum

Unterschrift

## Declaration of contribution

Luise Hassler contributed the following to the publication listed below: Hassler, L., Wysocki, J., Ahrendsen, J. T., Ye, M., Gelarden, I., Nicolaescu, V., Tomatsidou, A., Gula, H., Cianfarini, C., Forster, P., Khurram, N., Singer, B.D., Randall, G., Missiakas, D., Henkin, J. & Batlle, D., Intranasal soluble ACE2 improves survival and prevents brain SARS-CoV-2 infection, Life Science Alliance, 6(7), 2023.

### Contribution:

- The publication and its revisions were primarily written and edited by Luise Hassler and Daniel Batlle, with additional editing by Jared T. Ahrendsen, Jack Henkin, Jan Wysocki, Ian Gelarden and Benjamin D. Singer. The remaining co-authors read the manuscript prior to publication and provided input. Prof. Michael Bader also read the manuscript.
- The experiments with live SARS-CoV-2 in k18hACE2 mice, Vero E6, and A549 cells were planned by Daniel Batlle, Jan Wysocki and Luise Hassler, and were carried out in the BSL-3 facility of the Howard T. Ricketts Regional Biocontainment Laboratory at The University of Chicago by Vlad Nicolaescu, Anastasia Tomatsidou and Haley Gula who were supervised by Glenn Randall and Dominique Missiakas.
- The primary data of all experiments with live SARS-CoV-2 in k18hACE2 mice and Vero E6 and A549 cells was sent to the Batlle lab from the BSL-3 facility. Interpretation and analysis of the data was performed by Luise Hassler, Daniel Batlle and Jan Wysocki. From this data, figures 1, 2 and 5 were created by Luise Hassler under the supervision of Daniel Batlle and Jan Wysocki. Figure legends for these figures were written by Luise Hassler and edited by Daniel Batlle and Jan Wysocki. Vlad Nicolaescu helped with the interpretation of the data in figure 5.
- Minghao Ye, with the help of Luise Hassler, prepared the lungs and brains from SARS-CoV-2 infected k18hACE2 mice delivered from the BSL-3 facility for paraffin embedding and generation of slides for staining studies by the Mouse Histology and Phenotyping Laboratory center at Northwestern University. The Mouse Histology and Phenotyping Laboratory center at Northwestern University also created H&E-stained slides of lungs and brain.
- Brain histopathology was evaluated by Jared T. Ahrendsen, who took the photographs and created figures 3A-I and S1A-L, which were then edited by Luise Hassler before publication. Figures 3J and S1M, N were created by Luise Hassler based on the analysis of brain histopathology from Jared T. Ahrendsen.
- Brain immunofluorescence stainings for GFAP and IBA1 were performed and photographed by Minghao Ye and the photographs were then analyzed by Jared T. Ahrendsen, Daniel Batlle and Luise Hassler. Figures 3K-P and S2 were created by Luise Hassler.
- The legends for figures 3 and S1 were written by Jared T. Ahrendsen and edited by Luise Hassler and Daniel Batlle. The legend for figure S2 was written by Luise Hassler and edited by Daniel Batlle and Jared T. Ahrendsen.
- Lung histopathology was evaluated by Ian Gelarden and Nigar Khurram. Ian Gelarden took photographs which Luise Hassler used to create figures 4A-O and S3A-C. Figures 4P and S3D were created by Luise Hassler based on the analysis of lung histopathology from Ian Gelarden and Nigar

Khurram. The legend for figures 4 and S3 was written by Ian Gelarden and edited by Luise Hassler and Daniel Batlle.

- Cosimo Cianfarini and Peter Forster performed the experiments to measure ACE2 enzymatic activity in the brain under the supervision of Jan Wysocki.
- Statistical analysis was performed by Luise Hassler under the supervision of Jan Wysocki and Daniel Batlle.

---

Unterschrift, Datum und Stempel des/der erstbetreuenden Hochschullehrers/in

---

Unterschrift des Doktoranden/der Doktorandin

## Printed copy of the publication

Published Online: 11 April, 2023 | Supp Info: <http://doi.org/10.26508/lsa.202301969>  
Downloaded from [life-science-alliance.org](http://life-science-alliance.org) on 12 January, 2024

### Research Article



# Intranasal soluble ACE2 improves survival and prevents brain SARS-CoV-2 infection

Luise Hassler<sup>1,2</sup>, Jan Wysocki<sup>1</sup>, Jared T Ahrendsen<sup>3</sup>, Minghao Ye<sup>1</sup>, Ian Gelarden<sup>3</sup>, Vlad Nicolaescu<sup>4,5</sup>, Anastasia Tomatsidou<sup>4,5</sup>, Haley Gula<sup>4,5</sup>, Cosimo Cianfarini<sup>1</sup>, Peter Forster<sup>1</sup>, Nigar Khurram<sup>3</sup>, Benjamin D Singer<sup>6</sup>, Glenn Randall<sup>4,5</sup>, Dominique Missiakas<sup>4,5</sup>, Jack Henkin<sup>7</sup>, Daniel Battle<sup>1</sup>

**A soluble ACE2 protein bioengineered for long duration of action and high affinity to SARS-CoV-2 was administered either intranasally (IN) or intraperitoneally (IP) to SARS-CoV-2-inoculated k18hACE2 mice. This decoy protein (ACE2 618-DDC-ABD) was given either IN or IP, pre- and post-inoculation, or IN, IP, or IN + IP but only post-inoculation. Survival by day 5 was 0% in untreated mice, 40% in the IP-pre, and 90% in the IN-pre group. In the IN-pre group, brain histopathology was essentially normal and lung histopathology significantly improved. Consistent with this, brain SARS-CoV-2 titers were undetectable and lung titers reduced in the IN-pre group. When ACE2 618-DDC-ABD was administered only post-inoculation, survival was 30% in the IN + IP, 20% in the IN, and 20% in the IP group. We conclude that ACE2 618-DDC-ABD results in markedly improved survival and provides organ protection when given intranasally as compared with when given either systemically or after viral inoculation, and that lowering brain titers is a critical determinant of survival and organ protection.**

DOI [10.26508/lsa.202301969](https://doi.org/10.26508/lsa.202301969) | Received 3 February 2023 | Revised 1 April 2023 | Accepted 4 April 2023 | Published online 11 April 2023

## Introduction

Early in 2020, shortly after ACE2 was reported to be the main cell entry receptor for SARS-CoV-2 (1, 2), our laboratory proposed the use of soluble ACE2 proteins to neutralize SARS-CoV-2 via a decoy effect (3). The potential of soluble ACE2 proteins to neutralize SARS-CoV-2 was soon after shown using human organoids (4). This cellular model expresses human ACE2, the essential cell entry receptor for SARS-CoV-2 and TMPRSS2, a protease critical for internalization of the ACE2-SARS-CoV-2 complex (2, 4, 5, 6). Because mice and rats are resistant to SARS-CoV-2, the human transgenic k18hACE2 mouse has been used widely to test the efficacy of new

interventions geared to prevent and treat SARS-CoV-2 infection (7, 8, 9, 10, 11, 12, 13, 14, 15). The k18hACE2 model is lethal when infected with a high dose of WT SARS-CoV-2 and replicates severe lung disease in humans (10, 11, 14, 16, 17). There is also some evidence of brain injury (9, 10, 14, 18, 19, 20), but the precise cause of the universal lethality is not known. Expression of ACE2 in brain neurons has been demonstrated by immunocytochemistry and enzymatic assays suggesting that neuroinvasion of SARS-CoV-2 may occur (21, 22).

Soluble ACE2 proteins for SARS-CoV-2 offer theoretical advantages over antibody-based approaches which are increasingly resistant to emerging SARS-CoV-2 variants (23, 24, 25, 26, 27, 28, 29, 30, 31, 32, 33). For instance, multiple passaging in the presence of soluble ACE2 proteins does not lead to mutational escape of SARS-CoV-2, whereas mutational escape of the virus is seen rapidly after passaging in the presence of monoclonal antibodies (34). ACE2 decoys have a unique advantage over monoclonal antibodies because viral mutants are unlikely to decrease decoy affinity without simultaneous loss of ACE2 affinity, making decoys less susceptible to resistance by viral mutation (35, 36, 37).

We bioengineered a soluble ACE2 protein, based on a truncate of human ACE2 with 618 amino acids that was fused with an albumin-binding domain (ABD) to confer prolonged in vivo duration of action via albumin binding (5). Later, we used a dodecapeptide (DDC) motif (38) to form a dimer and were able to enhance the binding affinity for SARS-CoV-2 markedly (8). In the k18hACE2 model infected with SARS-CoV-2, administration of this protein (termed ACE2 618-DDC-ABD) resulted in markedly improved survival and greatly reduced lung injury (8). ACE2 618-DDC-ABD in this previous study was administered combined intranasally (IN) and intraperitoneally (IP) to ensure proof-of-concept efficacy but the brain histopathology was not studied (8). Here, we investigated the intranasal as compared with the intraperitoneal administration of ACE2 618-DDC-ABD and in addition examined the impact of treatment when initiated before or only after viral inoculation on survival, organ protection, and viral titers.

<sup>1</sup>Division of Nephrology/Hypertension, Department of Medicine, Northwestern University, Feinberg School of Medicine, Chicago, IL, USA <sup>2</sup>Charité Universitätsmedizin Berlin, Berlin, Germany <sup>3</sup>Department of Pathology, Northwestern University, Feinberg School of Medicine, Chicago, IL, USA <sup>4</sup>Department of Microbiology, University of Chicago, Chicago, IL, USA <sup>5</sup>Ricketts Regional Biocontainment Laboratory, University of Chicago, Lemont, IL, USA <sup>6</sup>Division of Pulmonary and Critical Care Medicine, Northwestern University, Feinberg School of Medicine, Chicago, IL, USA <sup>7</sup>Center for Developmental Therapeutics, Northwestern University, Evanston, IL, USA

Correspondence: [d-battle@northwestern.edu](mailto:d-battle@northwestern.edu)

© 2023 Hassler et al.

<https://doi.org/10.26508/lsa.202301969> vol 6 | no 7 | e202301969 1 of 13

From: Hassler et al (1), Intranasal soluble ACE2 improves survival and prevents brain SARS-CoV-2 infection. Life Science Alliance, Volume 6, No. 7, page 1, (not modified) <https://doi.org/10.26508/lsa.202301969> licensed under CC BY 4.0 <https://creativecommons.org/licenses/by/4.0/>

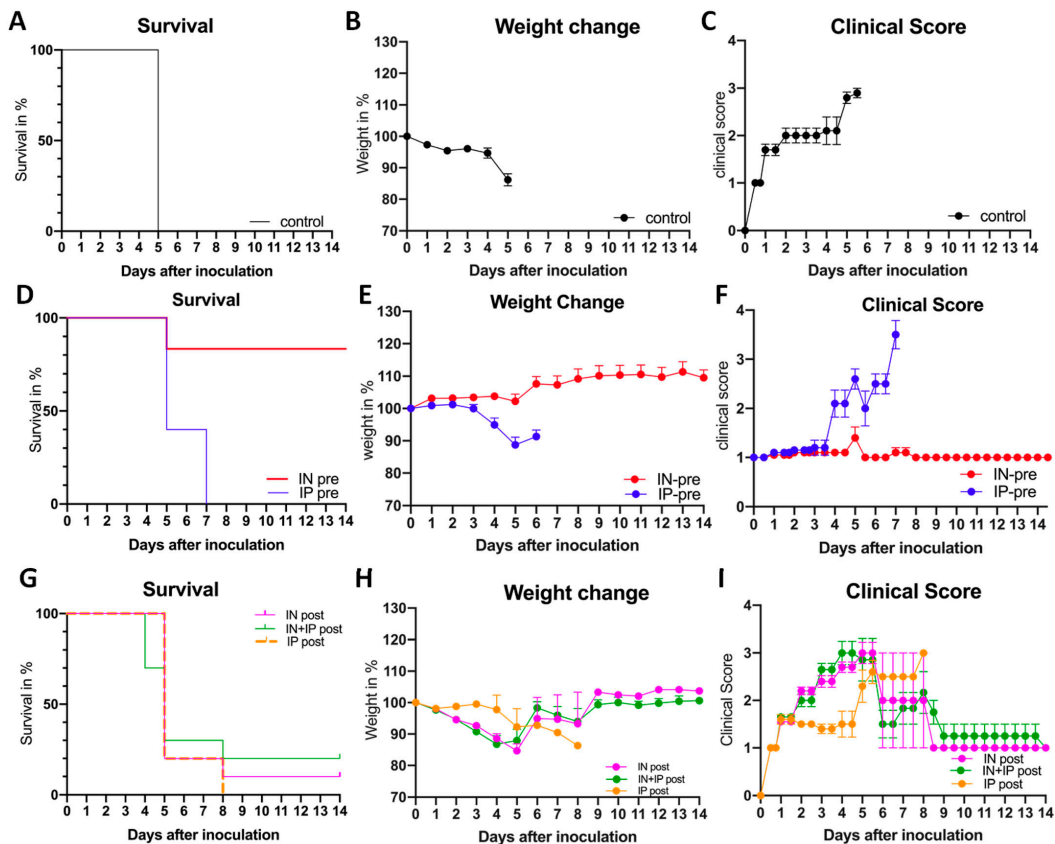


**Figure 1.** Survival, body weight, and clinical score after viral inoculation with  $2 \times 10^6$  PFU SARS-CoV-2 comparing intranasal (IN) versus intraperitoneal (IP) versus IN + IP administration of ACE2 618-DDC-ABD to k18hACE2 mice 1 h before and 24 and 48 h post (pre group, D, E, F) or only 24, 48, and 72 h post (post group, G, H, I). (A, B, C) Vehicle-treated group. Infected mice that received vehicle (BSA in PBS, black) had 0% survival on day 5 (A), lost up to 20% of their body weight (B), and developed high clinical scores (C). (D, E, F) Administration before and post-viral inoculation. In the IN-pre group (red), nine out of 10 mice survived until day 5 (90%), whereas in the IP-pre group (blue) only four out of 10 mice survived until day 5 (40%). Four of the nine surviving mice from the IN-pre group that were healthy by clinical score were then euthanized to obtain organs for comparison, and the remaining five mice all survived until day 14. By contrast, none of the four remaining mice in the IP-pre group survived until day 14 (D). The IN-pre group (red) had no body weight loss (E), and clinical score was normal (F), whereas the IP-pre group (blue) experienced body weight loss and worsening clinical score. (G, H, I) Administration post-viral inoculation. In the IN + IP-post group (green), 3 out of 10 mice survived until 5 (30%) and 2 out of 10 (20%) until day 14. In the IN-post group (pink), survival was 2 out of 10 (20%) on day 5 and 1 out of 10 (10%) on day 14 (G). In the IP-post group (orange), survival was 1 out of 5 (20%) on day 5 and 0 out of 5 (0%) on day 14 (G). In most mice that received ACE2 618-DDC-ABD post-viral inoculation weight loss was severe, and clinical scores were high although a few mice had stable weight and normal clinical score (H, I).

## Results

### Survival, clinical score, and weight loss in SARS-CoV-2-infected k18hACE2 mice

The effects of intranasal (IN) versus intraperitoneal (IP) administration of ACE2 618-DDC-ABD were examined in the k18hACE2 mouse, a lethal model of SARS-CoV-2 infection. According to study protocol, animals that lost more than 20% of their body weight or had a clinical score of three or higher were humanely euthanized,

and this was considered a mortality event (7, 8). Survival was 0% in the infected untreated control mice, all of which had to be humanely euthanized on day 5 (Fig 1A). They all had severe body weight loss (Fig 1B) and/or a high clinical score (Fig 1C).

### Administration of ACE2 618-DDC-ABD pre- and post-viral inoculation

In mice that received ACE2 618-DDC-ABD combined pre- and post-viral inoculation, survival on day 5 was 90% in the IN-pre group (9

out of 10), and only 40% in the IP-pre group (4 out of 10) ( $P = 0.0024$ ) (Fig 1D). As compared with the infected untreated group with 0% survival, the IN-pre group survival was also highly significant ( $P = 0.0084$ ). In the IP-pre group, survival was improved but it did not reach statistical significance as compared with the infected untreated group ( $P = 0.1106$ , all by log-rank [Mantel-Cox] test).

To obtain organs for comparison, four of the nine mice from the IN-pre group that were not affected by SARS-CoV-2 inoculation (by body weight and clinical score) were euthanized on day 5; the remaining five all survived until the end of the study (day 14) with near normal clinical scores and no weight loss (Fig 1E and F). The mice in the IP-pre group, by contrast, all had to be euthanized by day 7 because of worsening clinical scores and weight loss, according to the study protocol approved by the Institutional Animal Care and Use Committees (IACUC) (see the Materials and Methods Section) (Fig 1D–F).

#### Administration of ACE2 618-DDC-ABD only post-viral inoculation

In mice that received ACE2 618-DDC-ABD only post-viral inoculation, survival in the IN + IP-post group was 30% on day 5 (3 out of 10 mice) and 20% on day 14 (2 out of 10 mice) (Fig 1G). In the IN-post group, survival was 20% on day 5 (2 out of 10) and 10% on day 14 (1 out of 10). In the IP-post group, survival was 20% on day 5 (1 out of 5 mice) but 0% on day 14 (0 out of 5 mice) (Fig 1G). For comparison, infected untreated mice had 0% survival on day 5 (Fig 1A). Most of the animals that received ACE2 618-DDC-ABD post-viral inoculation had rapid body weight loss and a worsening clinical score, but some ( $n = 2$  IN + IP-post,  $n = 1$  IN-post) recovered over the course of the study and survived until day 14 with stable body weight and relatively good clinical scores (Fig 1H and I).

As compared with untreated infected controls, in the post-inoculation groups (IN + IP-post, IN-post, and IP-post), survival was improved, but the differences did not reach statistical significance ( $P = 0.8171$ ,  $P = 0.2994$ , and  $P = 0.3173$ , respectively). These three posttreatment groups (IN + IP-post, IN-post, and IP-post) had significantly worse survival than the IN-pretreatment group ( $P = 0.0181$ ,  $P = 0.0046$ , and  $P = 0.0064$ , respectively). When compared with the IP-pretreatment group, there were no statistically significant differences in survival for any of these three posttreatment groups ( $P = 0.8237$ ,  $P = 0.7827$ , and  $P = 0.8914$ , respectively).

#### SARS-CoV-2 brain and lung titers

Brain (Fig 2A) and lung viral titers (Fig 2B) were very high in infected untreated mice ( $3.0 \times 10^7 \pm 1.1 \times 10^7$  PFU/ml and  $9.33 \times 10^5 \pm 2.87 \times 10^5$  PFU/ml, respectively). When comparing the two organs, the titers were significantly higher in the brain than lung tissue ( $P = 0.0295$ ). Brain titers in the IN-pre-treated group were undetectable ( $0 \pm 0$  PFU/ml), whereas titers in the IP group were very high ( $3.82 \times 10^8 \pm 1.69 \times 10^8$  PFU/ml,  $P = 0.0167$ ) and similar to the infected untreated group (Fig 2A).

In all post-treated groups, brain viral titers were high or decreased only marginally as compared with the untreated infected mice (IP-post:  $1.66 \times 10^7 \pm 1.25 \times 10^7$ ; IN-post:  $9.06 \times 10^7 \pm 4.08 \times 10^7$ ; and IN + IP-post:  $4.4 \times 10^7 \pm 3.17 \times 10^7$ ) (Fig 2A). In the few survivors from the IN + IP-post and IN-post groups ( $n = 2$  and  $n = 1$ ,

respectively), however, brain titers were undetectable on day 14 (Fig 2A).

Lung titers were lower in all pre- and post-treated groups as compared with the infected untreated mice and reached statistical significance for the IN-pre, IN-post, and IN + IP-post groups (Fig 2B). The IN-pre group had lower titers than the IP-pre group, but the difference did not reach statistical significance ( $9.67 \times 10^4 \pm 8.79 \times 10^4$  and  $3.37 \times 10^5 \pm 2.32 \times 10^5$  PFU/ml, respectively,  $P = 0.3615$ ) (Fig 2B).

In the post-treated groups, the lung titers were as follows: IP-post:  $2.94 \times 10^4 \pm 1.71 \times 10^4$  PFU/ml; IN-post:  $8.06 \times 10^3 \pm 5.17 \times 10^3$ ; and IN + IP-post:  $4.4 \times 10^3 \pm 1.66 \times 10^3$  (Fig 2B). The IN-pre, IN-post, and IN + IP-post groups had significantly lower viral titers than the infected untreated group ( $P = 0.0244$ ,  $P = 0.0136$ , and  $P = 0.0078$ , respectively), whereas the differences between each other did not reach statistical significance. When ACE2 618-DDC-ABD was given only intraperitoneally (either pre- or post-viral inoculation), lung titers were not significantly reduced.

#### Brain histopathology

In brains of the infected untreated mice, leukocytosis and/or endothelial hypertrophy were features consistently seen, although of variable degrees. These findings were mainly observed in the striatum, cerebral cortex, and hypothalamus (Fig 3A–C). In addition, both perivascular and parenchymal inflammation were occasionally seen in the hypothalamus and basal ganglia. In the IN-pre group, by contrast, these histopathologic features in hypothalamus and cortex were absent in all mice (Fig 3D–F). In the IP-pre group, there was also perivascular leukocytosis in areas of the brainstem in some (Fig 3G–I) but not all mice. The leukocytosis score was improved significantly for the IN-pre group compared with both infected untreated mice and the IP-pre group ( $P = 0.0007$  and  $P = 0.0199$ , respectively) (Fig 3J).

Another histopathologic abnormality found in untreated infected brains was neuronal pyknosis. This was scored on a scale of 0–3 and was significantly reduced in both the IP-pre ( $0.875 \pm 0.125$ ) and IN-pre group ( $1 \pm 0$ ) as compared with untreated infected mice ( $2 \pm 0$ ,  $P = 0.0001$  and  $P = 0.0003$ , respectively).

In the IP-post group, perivascular/parenchymal inflammation and endothelial hypertrophy in the hypothalamus was also seen (Fig 3I–D). Likewise, in the IN-post and IN + IP-post groups, leptomeningeal and perivascular lymphocytosis and endothelial hypertrophy in the hypothalamus and lateral cortex were seen in some animals (Fig 3I–L) similar to the infected untreated mice (Fig 3A–C). The score for perivascular leukocytosis was lower in the IP-post, IN-post, and IN + IP-post group than in the infected untreated mice but did not reach statistical significance (Fig 3I–M). The score for neuronal pyknosis was decreased in all post-treated groups, but the difference was significant only for the IN + IP-post group as compared with infected untreated mice ( $P = 0.037$ ) (Fig 3I–N).

#### Immunofluorescence for markers of astrocytes and microglia

Immunofluorescence for the astrocyte marker GFAP and the microglial marker IBA1 revealed high expression of both markers in infected untreated mice in patterns consistent with reactive astrocytosis and microgliosis, respectively (Fig 3K and N). GFAP staining was partially decreased in the IP-pre group (Fig 3L) and markedly reduced in the IN-pre group (Fig 3M). IBA1 staining

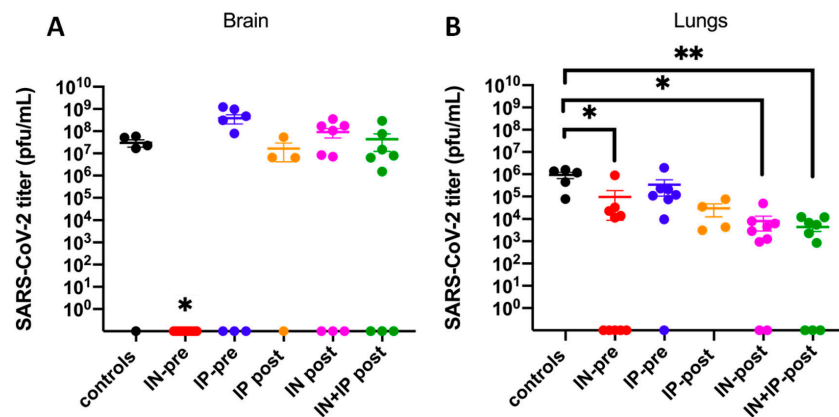


**Figure 2.** Brain (A) and lung (B) viral titers in k18hACE2 mice inoculated with  $2 \times 10^6$  PFU SARS-CoV-2 that received ACE2 618-DDC-ABD 1 h pre- and 24 and 48 h post-viral inoculation.

(A) Brain titers were high in all but one infected untreated control mice (black), most mice from the IP-pre group (blue) and the post-treated groups (orange, pink, green). In the IN-pre group (red), by contrast, titers were undetectable in all mice, and significantly lower than that in the IP-pre group ( $P = 0.0167$ ). (B) Lung titers were highest in the untreated infected control mice (black). In the other groups, lung titers were lower and non-detectable in some mice. As indicated by the asterisks, significant differences were found between controls (black) and the IN-pre group (red,  $P = 0.0244$ ), the IN-post group (pink,  $P = 0.0136$ ), and the IN + IP-post group (green,  $P = 0.0078$ ). Note that in two mice from the IP-pre group and one mouse per post-treated group organs could not be obtained. Significance was calculated using ANOVA followed by Dunn's multiple comparisons test. If not indicated by the asterisk, the differences did not reach statistical significance. Viral titers were normalized by organ weight. Mean  $\pm$  SEM are shown.

showed partially reduced microglia cells with ramifications in mice in the IP-pre group (Fig 3O), whereas the ramifications were markedly reduced in the IN-pre group (Fig 3P). Several other examples of these differences are shown in the supplement (Fig S2).

#### Lung histopathology

Lungs from untreated infected mice showed dense perivascular mononuclear infiltrates and collections of intra-alveolar neutrophils. There were also rare foci of necrotic debris and alveolar hemorrhage (Fig 4A–E). The lungs of mice from the IN-pre group show near normal lung histopathology with only minimal perivascular mononuclear infiltrates (Fig 4F–J). The lungs of mice from the IP-pre group showed few perivascular mononuclear infiltrates, focal minimal alveolar hemorrhage, and occasional intra-alveolar neutrophils, whereas some areas also show near-normal lung histopathology (Fig 4K–O). The lung histopathology scores for mononuclear infiltrates, hemorrhage, PMN infiltrates, edema, and necrotic cellular debris were worse in the untreated infected group than in both the IP-pre and IN-pre-treated groups (Fig 4P). The differences in both pre-treated groups (IP-pre and IN-pre) as compared with infected untreated mice were highly significant for the main histopathologic findings: mononuclear infiltrates ( $P = 0.0297$  and  $P = 0.0107$ , respectively) and alveolar hemorrhage ( $P = 0.0219$  and  $P = 0.0165$ , respectively) (Fig 4P). The scores were better in the IN-pre group than the IP-pre group, but the difference did not reach statistical significance (Fig 4P).

The lungs from the post-treated groups also showed perivascular mononuclear infiltrations and intra-alveolar neutrophils and resembled the infected untreated group (Fig S3A–C). In some

mice from the IN-post and IN + IP-post group (Fig S3B and C), lung histopathology was improved but to a lesser extent than in the pre-treated groups (see Fig 4). The histopathological scores were not significantly different in infected untreated controls as compared with the post-treated groups (Fig S3D). Alveolar hemorrhage was reduced in the post-treated groups, but the difference was not statistically significant (Fig S3D).

#### ACE2 618-DDC-ABD neutralizes WT and Omicron SARS-CoV-2 in two cell types

In human A549 cells, ACE2 618-DDC-ABD neutralized WT SARS-CoV-2 (as shown by cell viability) at high concentrations (40 and 200  $\mu\text{g}/\text{ml}$ ). Lower concentrations (1.6 and 8  $\mu\text{g}/\text{ml}$ ) neutralized infection only partially, and very low concentrations (0.0128–0.32  $\mu\text{g}/\text{ml}$ ) had no effect on viral neutralization (Fig 5A).

By contrast, the Omicron BA.1 variant was neutralized by much lower concentrations of ACE2 618-DDC-ABD than WT SARS-CoV-2 (Fig 5B). When comparing the two sets of data (Omicron and WT variants), the difference was highly significant ( $P = 0.01$ ) (Fig 5C).

This enhanced effect of ACE2 618-DDC-ABD on the neutralization of the Omicron variant in A549 cells was also found when we used Vero E6 cells, a nonhuman primate cell line that has been widely used for infectivity studies with SARS-CoV-2 (4, 8). In Vero E6 cells, ACE2 618-DDC-ABD neutralized the Omicron BA.1 variant at all concentrations tested (5.625–180  $\mu\text{g}/\text{ml}$ ) (Fig 5D).

The high sensitivity of this Omicron variant to ACE2 618-DDC-ABD prompted us to test a mouse soluble ACE2 protein that normally has no effect on WT SARS-CoV-2 infectivity (5). The mouse ACE2 740

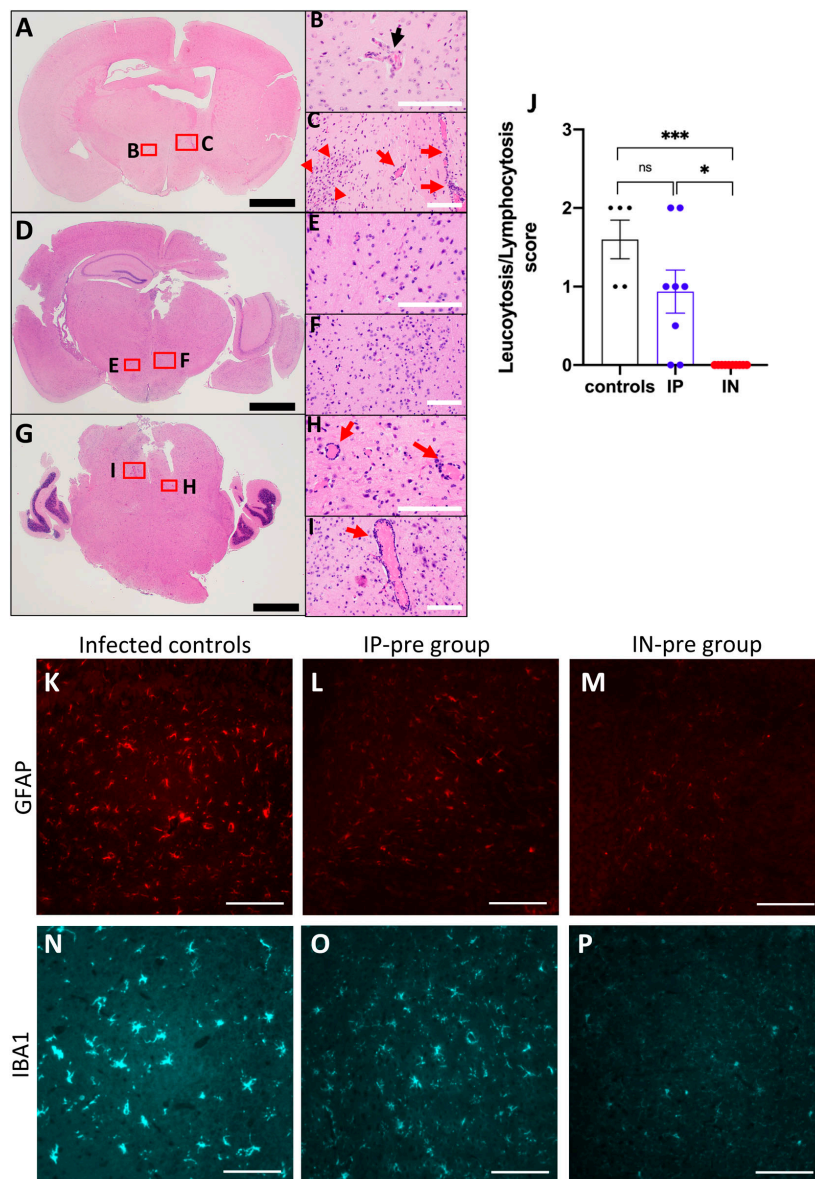


**Figure 3. Representative neuropathology of k18hACE2 mice inoculated with  $2 \times 10^4$  PFU SARS-CoV-2.** (A, B, C) Example of an infected untreated mouse with endothelial hypertrophy (black arrow, (B)), perivascular (red arrows, (C)), and parenchymal lymphocytosis (red arrowheads, (C)) in the hypothalamus. (D, E, F) Example of a mouse from the IP-pre group that received ACE2 618-DDC-ABD showing normal appearing hypothalamus, including vasculature. Black scale bars = 1 mm, white scale bars = 100  $\mu$ m. (G, H, I) Example of a mouse from the IP-pre group that received ACE2 618-DDC-ABD also showing perivascular lymphocytosis (red arrows, (H, I)) in areas of the brainstem. (J) When data from all animals ( $n = 5$  controls,  $n = 8$  IP-pre,  $n = 10$  IN-pre) were scored for leukocytosis/lymphocytosis, there were significant differences between the groups ( $P = 0.0007$  and  $P = 0.01$ , respectively). Data shown as mean  $\pm$  SEM. Significance was indicated by \*\*\*, ns, and \*.



protein neutralized Omicron BA.1 infection fully at high concentrations, whereas lower concentrations were only partially effective (Fig 5E).

## Discussion

The main finding of this study was that a soluble ACE2 protein, bioengineered to have extended duration of action and increased binding affinity for SARS-CoV-2, showed clear superiority of intranasal over systemic (intraperitoneal) administration in the k18hACE2 mouse model of SARS-CoV-2 infection. This superiority was shown by improvements in survival, clinical scores, and reduced lung viral titers. In the brains, moreover, the titers were undetectable in all animals in the group that received the treatment intranasally before viral inoculation. The soluble ACE2 protein, termed ACE2 618-DDC-ABD, was bioengineered to have increased duration of action by fusing a 618 amino acid truncate with an ABD and designed to have increased binding affinity to the S1 spike of SARS-CoV-2 by using a dodecapeptide (DDC) dimerization motif (8). Administration of this soluble ACE2 protein before viral inoculation, moreover, was far more effective regarding all the outcomes than administration only post-viral inoculation.

The k18hACE2 model in which human ACE2 transgene expression is driven by the k18 promoter is lethal after 5–7 d of inoculation with a high dose of WT SARS-CoV-2 (8, 10, 11, 14, 16, 17). The precise cause of the rapid lethality upon SARS-CoV-2 infection in this model is not fully understood. Brain SARS-CoV-2 titers in the infected untreated control group were one order of magnitude higher than that in the lungs (compare Fig 2A and B). The absence of brain titers in mice pre-treated intranasally explains, in our opinion, the much better survival than in untreated and groups treated with ACE2 618-DDC-ABD intraperitoneally. The group pre-treated by IN administration was indeed the only group in which brain viral titers were not detectable in any of the mice studied (Fig 2A). High brain viral titers, by contrast, were detected in the other groups with the exception of a few mice that survived until day 14 and, of note, these survivors had no brain viral titers detectable. Elevated brain viral titers, therefore, were associated with poor outcomes in terms of survival in both the pre- and post-viral inoculation groups. From these observations, we conclude that improved survival conferred by ACE2 618-DDC-ABD appears to be determined by two main factors: route of administration (IN better than IP) and timing (pre- and post-viral inoculation better than only post-viral inoculation).

Consistent with our data, previous studies had suggested that brain invasion of SARS-CoV-2 in k18hACE2 mice may be associated with more severe disease (18, 19). It should be pointed out, however, that brain injury was limited to only few animals in some studies (10, 14). Some of the findings that have been previously reported include encephalitis with leukocyte infiltration, hemorrhage, neuronal cell death, necrosis, and spongiosis (10, 14, 18, 19,

20, 39). In these previous studies with the k18hACE2 mice (10, 18, 19, 20, 39), however, no therapies were given. Therefore, the brain pathology could not be assessed regarding responses to therapies improving survival and organ protection. Here, we were able to show that survival conferred by the administration of our soluble ACE2 protein was associated with non-detectable brain viral titers. Consistent with the importance of viral brain invasion, in a study where k18hACE2 mice were inoculated intracranially with low doses of SARS-CoV, there was lethality despite little infection in the lungs (40). When SARS-CoV-2 was administered to k18hACE2 mice in aerosolized form for more direct lung delivery, and despite robust viral replication in the respiratory tract with airway obstruction, there was markedly reduced fatality and viral neuroinvasion (41). Our findings with intranasal delivery of soluble ACE2 before viral inoculation clearly demonstrate the importance of obliterating brain SARS-CoV-2 invasion for survival and brain protection.

We wish to point out, however, that the brain histopathologic findings were subtle even in untreated infected mice. The brain findings most frequently seen were perivascular and leptomeningeal lymphocytosis, endothelial hypertrophy, and parenchymal inflammation (Fig 3). These findings were mainly located in the striatum, cerebral cortex, and hypothalamus. Immunofluorescence for markers of microglia (IBA1) and astrocytes (GFAP) (42, 43) in the brain of infected untreated mice revealed high IBA1 and GFAP expression, consistent with reactive microgliosis and astrocytosis suggestive of an underlying neuroinflammatory state (Fig 3). Markers for astrocytes and microglia activation were also found in a study that examined cerebrospinal fluid from patients with severe Neuro-COVID-19 (44). In studies that used immunohistochemistry and imaging mass cytometry to examine brains from deceased COVID-19 patients, astrocyte and microglia activation was found as well (45, 46). In the IN group that received the treatment before viral inoculation, most brains appeared normal and IBA1 and GFAP expression was decreased, suggesting prevention of astrocyte and microglia activation and reduced neuroinflammation. Despite clear improvement in these parameters in mice treated with intranasal ACE2 618-DDC-ABD before viral inoculation, it remains to be determined how in brains from untreated infected mice viral invasion is associated with high mortality without more evident and severe histological damage.

Lung histopathology of the infected untreated mice showed dense perivascular mononuclear infiltrates, rare foci of alveolar hemorrhage and necrotic debris, and collections of intra-alveolar neutrophils. These findings were less pronounced in the IP-pre group and essentially absent in the IN-pre group which showed near-normal lung histopathology. It is very likely that in the IN-pre group the significantly improved lung histopathology was because SARS-CoV-2 lung titers were undetectable in half of the mice from this group (see Fig 2B). In the post-treated groups, lung histopathology was improved but not significantly different from the untreated infected controls; this suggests that a reduction in SARS-CoV-2 lung viral titers, if incomplete, could not fully prevent lung injury.

calculated by one-way ANOVA followed by Dunn's multiple comparisons test. (K, L, M) Examples of GFAP staining (red) which is strongest in an untreated infected brain (K), reduced partially in a brain from the IP-pre group (L), and very weak in a brain from the IN-pre group (M). (N, O, P) Examples of IBA1 staining (blue) which is strongest and showed the most pronounced ramifications in an untreated infected brain (N), reduced partially in a brain from the IP-pre group (O), and almost completely absent in a brain from the IN-pre group (P). All IF-photomicrographs were taken at 40x magnification, scale bar = 100  $\mu$ m.

From: Hassler et al (1), Intranasal soluble ACE2 improves survival and prevents brain SARS-CoV-2 infection. Life Science Alliance, Volume 6, No. 7, page 6, (not modified) <https://doi.org/10.26508/lsa.202301969> licensed under CC BY 4.0 <https://creativecommons.org/licenses/by/4.0/>

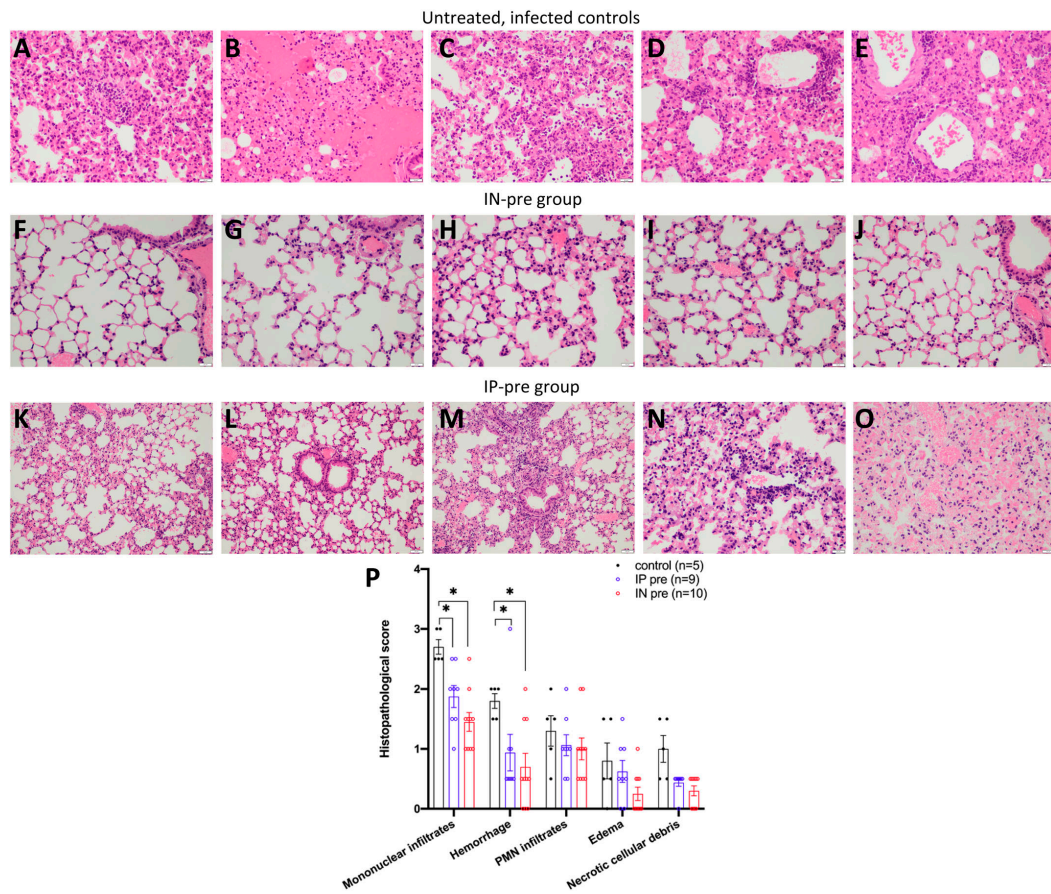


**Figure 4. Representative examples of lung histopathology in H&E-stained lung slides of SARS-CoV-2-infected k18hACE2 mice.** (A, B, C, D, E) Five different mice from the vehicle control group (n = 5) that were infected with SARS-CoV-2 show dense perivascular mononuclear infiltrates (D, E), collections of intra-alveolar neutrophils (C), rare foci of necrotic debris (A), and alveolar hemorrhage (B). (F, G, H, I, J) Five mice from the IN-pre group that received ACE2 618-DDC-ABD (n = 10) show near normal lung histopathology with minimal perivascular mononuclear infiltrates and hemorrhage in some cases. (K, L, M, N, O) Five mice from the IP-pre group that received ACE2 618-DDC-ABD (n = 8) show milder perivascular mononuclear infiltrates (M, N) with other areas of near normal lung histopathology (K, L), focal minimal alveolar hemorrhage (O), and occasional intra-alveolar neutrophils. (P) The lung histopathology scores for mononuclear infiltrates, hemorrhage, PMN infiltrates, edema, and necrotic cellular debris are high in the controls (black) and lower in both the IP-pre (blue) and IN-pre (red) groups. Data shown as mean  $\pm$  SEM are shown. Significance is indicated in the figure with \* =  $P < 0.05$ , calculated by mixed-effects analysis followed by Tukey's multiple comparisons test. All photomicrographs were taken from H&E-stained sections at 40x magnification, scale bar = 500  $\mu$ m.

The mechanisms whereby soluble ACE2 proteins can neutralize SARS-CoV-2 have been previously discussed by us and others (3, 47). ACE2 exists in two forms: a full-length membrane bound form and a shorter soluble form that lacks the transmembrane domain (48, 49) and circulates in the blood in very small amounts (50). Both forms bind the receptor-binding domain of the SARS-CoV-2 S1 spike protein. By administering an abundant amount of soluble ACE2, the spike protein of SARS-CoV-2 can be intercepted from binding to the

membrane bound ACE2 by the so-called decoy effect (3). To increase the binding affinity of ACE2 618-DDC-ABD to the receptor-binding domain of the SARS-CoV-2 S1 spike, a DDC motif was introduced that induces dimerization (8). By fusion with an ABD-tag, moreover, increased duration of action was achieved as demonstrated by its preserved plasma enzymatic activity for several days (5, 8). Membrane bound and soluble ACE2, including ACE2 618-DDC-ABD, metabolize angiotensin II and des-Arg<sup>9</sup> bradykinin,

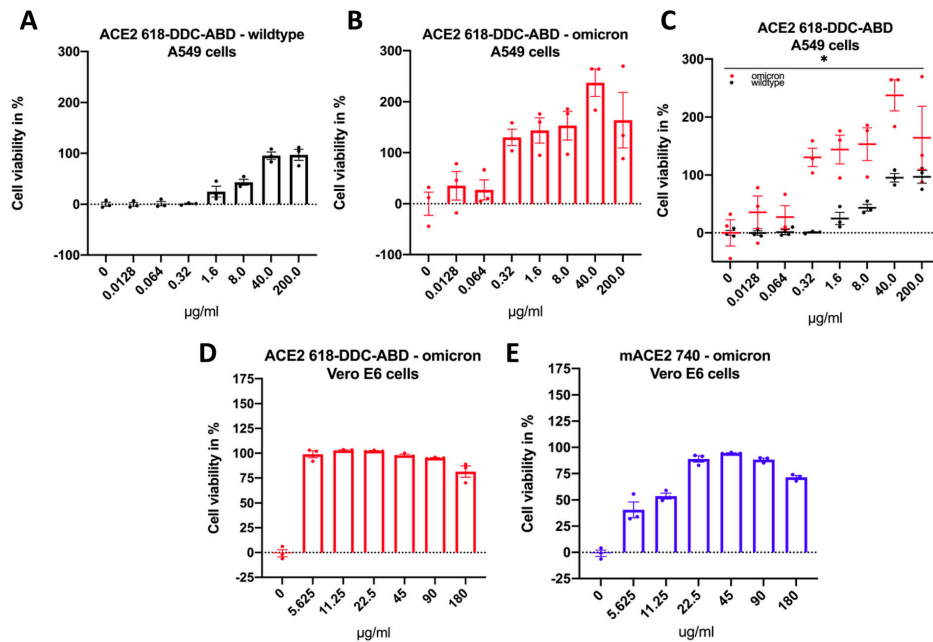


**Figure 5. Neutralization of SARS-CoV-2 variants (500 PFU each) by human and mouse soluble ACE2 proteins after co-incubation for 1 h followed by infection of A549 or Vero E6 cells.**

(A) In A549 cells, human ACE2 618-DDC-ABD neutralizes WT SARS-CoV-2 at high concentrations (40 and 200  $\mu\text{g/ml}$ ), whereas lower concentrations (1.6 and 8  $\mu\text{g/ml}$ ) neutralize infection only partially and very low concentrations (0.0128–0.32  $\mu\text{g/ml}$ ) have no effect on infectivity. (B) In A549 cells, human ACE2 618-DDC-ABD neutralizes of the Omicron BA.1 variant of SARS-CoV-2 at concentrations lower than WT SARS-CoV-2 (0.32–200  $\mu\text{g/ml}$ ), and even very low concentrations have a partial effect. (C) The differences between WT (black) and Omicron BA.1 (red) neutralization by ACE2 618-DDC-ABD are significant ( $P = 0.0144$ , calculated by two-way ANOVA). (D) In Vero E6 cells, ACE2 618-DDC-ABD neutralizes the Omicron BA.1 variant at all concentrations tested (5.625–180  $\mu\text{g/ml}$ ), whereas lower concentrations (5.625–180  $\mu\text{g/ml}$ ), whereas lower concentrations have a partial effect. Values were normalized to the 0  $\mu\text{g/ml}$  control and expressed as a percentage of mock (no virus) control wells. Mean  $\pm$  SEM are shown.

two peptides that may be detrimental when accumulating (47, 51, 52, 53). This action may be especially beneficial in COVID-19 where internalization of ACE2–SARS-CoV-2 complexes causes depletion of cell membrane ACE2 which fosters accumulation of these pro-inflammatory peptides (53, 54, 55). Unfortunately, we were unable to measure these peptides because organ tissues could not be released from the BSL-3 facility. A high dose of soluble, enzymatically active form of ACE2 was well tolerated in the present study and, moreover, studies in normal mice not infected with SARS-CoV-2 showed that the administration of high doses of ACE2 do not lower blood pressure and has no effect on body weight or kidney function when given for months (56). In a safety and tolerability study in healthy human volunteers, systemic administration of a human soluble ACE2 18-740 (APN01) by intravenous injection was similarly well tolerated without causing hypotension or pulse rate disturbances (57). This is consistent with results obtained in preclinical pharmacological and toxicological investigations in rodents (58), piglets (59), and nonhuman primates, in which much higher doses of ACE2 18-740 (APN01) (up to 40 mg/kg) have been tested without any tolerability issues (57).

The membrane bound full-length ACE2 is essential for facilitating SARS-CoV-2 infection (6, 60). As shown by previous work with the soluble human ACE2 740 (6) and here with ACE2 618-DDC-ABD in two different permissive cell types, A549 and Vero E6 cells, high concentrations of soluble ACE2 are needed to neutralize infection of cells with WT SARS-CoV-2. Other variants of SARS-CoV-2, however, may be effectively treated with lower doses of soluble ACE2 proteins. This can be inferred from our findings in two different permissive cell lines, where ACE2 618-DDC-ABD neutralizes the Omicron BA.1 variant at lower protein concentrations (at least 20-fold lower than those required to neutralize WT SARS-CoV-2). It is also important to emphasize that soluble ACE2 protein-based approaches have universal effects against all the variants of SARS-CoV-2 (36). This is contrary to monoclonal antibodies that have the limitation of becoming less efficacious with each mutation of SARS-CoV-2, as consistently shown for the Omicron variants (23, 24, 25, 26, 27, 28, 29, 30, 31, 32, 33). Therefore, soluble ACE2 based therapies are likely to provide universal efficacy against all SARS-CoV-2 variants that evade monoclonal antibodies.



We conclude that ACE2 618-DDC-ABD provides better survival and organ protection when administered intranasally than systemically. Treatment post-viral inoculation, although less effective, still provides partially improved survival and organ protection. Abrogating brain SARS-CoV-2 invasion is a critical determinant of survival and organ protection in the k18hACE2 mouse model of lethal SARS-CoV-2 infection.

## Materials and Methods

### In vivo infectivity studies

All work with live SARS-CoV-2 in k18hACE2 mice was performed in the BSL-3 facility of the Ricketts Regional Biocontainment Laboratory, following a protocol approved by the IACUC of Northwestern University and University of Chicago. We used k18hACE2 mice that express full-length human ACE2 and are susceptible to SARS-CoV-2 infection (10, 14, 16, 17, 61, 62), purchased from Jackson Laboratory (8–13 wk old). Animals were infected intranasally with  $2 \times 10^4$  PFU SARS-CoV-2 in 20  $\mu$ l (novel coronavirus/Washington/1/2020 was provided by N Thornburg [CDC] via the World Reference Center for Emerging Viruses and Arboviruses). Animals infected with this viral load invariably succumb to disease by days 5–9 (10, 14, 16, 17). We used different protocols to examine pretreatment and posttreatment effects of the soluble ACE2 618-DDC-ABD protein and to compare intranasal (IN) versus intraperitoneal (IP) administration effects. In the pretreatment groups, ACE2 618-DDC-ABD was administered to k18hACE2 mice ( $n = 10$ , five male and five female) via IN (30  $\mu$ l,  $-13 \mu$ g/g BW) or via IP (200  $\mu$ l,  $-13 \mu$ g/g BW) 1 h before SARS-CoV-2 followed by the same dose and 24 and 48 h later for a total of three doses. In the posttreatment groups, ACE2 618-DDC-ABD was administered either IN (30  $\mu$ l,  $-12 \mu$ g/g BW,  $n = 10$ , male) or IP (200  $\mu$ l,  $-1 \mu$ g/g BW,  $n = 5$ , male) or combined intranasally and intraperitoneally (IN + IP) ( $n = 10$ , male) 24, 48, and 72 h only post-viral inoculation ( $2 \times 10^4$  PFU SARS-CoV-2). Controls ( $n = 5$ , male) received BSA in PBS both IN and IP at the same doses and time points as the ACE2 618-DDC-ABD post-treated animals.

Animals were weighed once daily and monitored twice daily for health using a clinical scoring system (Table S1). Animals that lost more than 20% of their baseline body weight or had a clinical score of three were euthanized for humane reasons (humanely euthanized) and considered a fatal event as per study protocol. Mice were euthanized by using CO<sub>2</sub>-forced inhalation. After the last breathing movement, cervical dislocation was performed to prevent the mice from recovering from CO<sub>2</sub> exposure. To be able to compare viral titers and organ pathology at the same time point, randomly selected animals from the IN group (which all appeared healthy based on clinical score) were euthanized on day 5 together with the animals from the IP group that were euthanized because the mortality endpoint was reached. Otherwise, animals that did not reach the severity of these criteria were monitored for up to 14 d in the BSL-3 facility and euthanized at day 14.

Portions of lungs and brains were removed from all euthanized animals and were used for viral load measurements by plaque assay (see below), whereas the remaining portions were fixed in

10% formalin and embedded in paraffin for histopathology and immunostaining. The Mouse Histology and Phenotyping Laboratory center at Northwestern University generated slides for staining studies.

Hematoxylin and eosin (H&E)-stained sections were evaluated by expert lung pathologists on a scoring system, recently described for SARS-CoV-2-infected k18hACE2 mice (8, 14). The categories scored were: mononuclear infiltrates, alveolar hemorrhage, edema, cellular necrosis, hyaline membranes, and thrombosis. The scale was as follows: 0 = no detection, 1 = uncommon detection in <5% lung fields (200x), 2 = detectable in up to 30% of lung fields, 3 = detectable in 33–66% of lung fields, and 4 = detectable in >66% of lung fields. Neutrophil infiltration was evaluated on a scale of 0–3 as follows: 0 = within normal range, 1 = scattered PMNs sequestered in septa, 2 = score 1 and solitary PMNs extravasated in airspaces, 3 = score 2 plus and aggregates in vessel and airspaces.

Brain injury was evaluated on H&E-stained sections by a blinded neuropathologist and scored for leukocytosis and lymphocytosis and neuronal pyknosis on a scale of 0–3. The scale was as follows: 0 = none, 1 = mild (focal), 2 = moderate (multifocal), 3 = severe (diffuse).

### ACE2 enzymatic activity in the brain

In pilot studies in non-infected mice, ACE2 618-DDC-ABD was administered intranasally to see if it reaches the brain. For this, ACE2 deficient mice (total body ACE2/PRCP double-knockout mice) (50) were given ACE2 618-DDC-ABD protein intranasally (10  $\mu$ g/g BW, 35  $\mu$ l total volume in both nostrils) under general ketamine-xylazine anesthesia. The animals recovered from anesthesia and 4 h after intranasal instillation were euthanized by overdose of Euthasol. Mice were perfused with PBS to flush out blood from the organs. Brains were then removed and tissue lysates obtained by homogenization in RIPA buffer (63). The lysates were then clarified by centrifugation at 6,000g for 10 min at 4°C. Protein concentration in the cleared lysates was measured using BCA assay kit (Thermo Fisher Scientific). The cleared tissue lysates were diluted in a 1x TBS, pH 7.4 (cat#BP2471-1; Thermo Fisher Scientific). For ACE2 activity, a fluorogenic substrate Mca-APK-Dnp (Bachem) was used, and the plates were read using a fluorescence plate reader FLX800 (BioTek Instruments) at an excitation wavelength of 320 nm and an emission wavelength of 400 nm. All reactions were performed at ambient temperature in microtiter plates with a 100  $\mu$ l total volume. Each sample was tested in duplicate wells with one of the two wells used as a blank. A specific inhibitor of ACE2 (MLN-4760, gift from Millennium Pharmaceuticals) was used at  $10^{-5}$  M end concentration (64, 65) in the blank wells. ACE2 activity (relative fluorescence units) was calculated by subtracting blank values from values of wells without ACE2 inhibitor and divided by total protein concentration of the tissue lysates. ACE2 enzymatic activity in brain lysates was not detectable in ACE2KO mice that received PBS but was detectable in those infused with ACE2 618-DDC-ABD ( $0.004 \pm 0.0002$  RFU/ $\mu$ g protein/hr and  $0.14 \pm 0.098$  RFU/ $\mu$ g protein/h,  $P = 0.015$ ).

### Plaque assay for infectious virus

Tissue samples were collected in DMEM with 2% FBS and were homogenized using 1.4 mm ceramic beads in a tissue homogenizer



using two 30 s pulses. Samples were then centrifuged at 1,000g for 5 min, and the supernatant was serially diluted 10-fold and used to infect Vero E6 cells for 1 h. Inoculum was removed, and 1.25% methylcellulose DMEM was added to the cells and incubated for 3 d. Plates were fixed in 1:10 formalin for 1 h and stained with crystal violet for 1 h and counted to determine PFU and expressed as PFU/ml after the data were normalized by organ weight.

#### Immunofluorescence

For immunofluorescence staining studies of the brain, IBA1 (ab178846; Abcam) and GFAP (ab4674; Abcam) antibodies were used.

#### SARS-CoV-2 infection of A549 and Vero E6 cells

All work with live SARS-CoV-2 was performed in hACE2-A549 or Vero E6 cells in the BSL-3 facility of the Ricketts Regional Biocontainment Laboratory. 500 PFU of each SARS-CoV-2 strain: WT (novel coronavirus/Washington/1/2020) was provided by N. Thornburg [CDC] via the World Reference Center for Emerging Viruses and Arboviruses) or Omicron BA.1 (BEI NR-56481, obtained through BEI Resources, NIAID, NIH: SARS-related coronavirus 2, Isolate hCoV-19/USA/GA-EHC-2811C/2021 [Lineage B.1.1.529; Omicron variant], NR-56481, contributed by Mehul Suthar) of SARS-CoV-2 was incubated with various concentrations (0.0128, 0.064, 0.32, 1.6, 8.0, 40.0, 200 µg/ml for A549 cells or 5.626, 11.25, 22.5, 45, 90, 180 µg/ml for E6 cells) of the different soluble ACE2 proteins (human ACE2 618-DDC-ABD or mouse ACE2 740) for 1 h at 37°C. This mixture was then used to infect the respective cell types. Cells were then incubated for 3–4 d (WT SARS-CoV-2) or 5 d (Omicron BA.1) until a noticeable cytopathic effect was observed in control wells (0 µg/ml of soluble ACE2 proteins). Cell numbers were assessed by staining cells with crystal violet and reading absorbance of each well at 595 nm. Values were then normalized to the 0 µg/ml control and expressed as a percentage of mock (no virus) control wells.

#### Statistics

GraphPad Prism v8.4.3 (GraphPad Software) was used to calculate statistics. Normality was tested using the Shapiro–Wilk test. Differences between more than two groups with normally distributed data were analyzed by ANOVA followed by post hoc Dunnett's multiple comparisons test. Differences between more than two groups with non-normally distributed data were analyzed by the Kruskal–Wallis test followed by the post hoc Dunn's multiple comparisons test. Differences between two groups with normally distributed data were analyzed by unpaired t test. Differences between two groups with non-normally distributed data were analyzed by Mann–Whitney test. Differences in survival were calculated by log-rank (Mantel–Cox) test.

#### Study approval

All work with live SARS-CoV-2 in k18hACE2 mice was performed in the BSL-3 facility of the Ricketts Regional Biocontainment Laboratory, following a protocol approved by the Institutional Animal

Care and Use Committees of both Northwestern University (IS00004795) and University of Chicago (72642).

## Supplementary Information

Supplementary Information is available at <https://doi.org/10.26508/lsa.202301969>.

## Acknowledgements

Grant support to D Battle from NIH (1R21 AI166940-01) and a gift from the Joseph and Bessie Feinberg Foundation. L Hassler and C Cianfarini were supported by the Biomedical Education Program during a part of their stay in Chicago.

#### Author Contributions

L Hassler: data curation, formal analysis, investigation, visualization, methodology, and writing—original draft, review, and editing. J Wysocki: conceptualization, data curation, formal analysis, supervision, investigation, methodology, and writing—review and editing. JT Ahrendsen: formal analysis, investigation, visualization, and writing—review and editing. I Gelarden: investigation and writing—review and editing. V Nicolaescu, A Tomatsidou, H Gula, C Cianfarini, P Forster, N Khurram, and M Ye: investigation. BD Singer: conceptualization and writing—review and editing. G Randall: supervision, investigation, and writing—review and editing. D Missiakas: supervision, investigation, and project administration. J Henkin: conceptualization and writing—review and editing. D Battle: conceptualization, resources, data curation, formal analysis, supervision, funding acquisition, investigation, visualization, project administration, and writing—original draft, review, and editing.

#### Conflict of Interest Statement

D Battle and J Wysocki are coinventors of patents entitled “Active Low Molecular Weight Variants of Angiotensin Converting Enzyme 2 (ACE2),” “Active low molecular weight variants of Angiotensin Converting Enzyme 2 (ACE2) for the treatment of diseases and conditions of the eye” and “Soluble ACE2 Variants and Uses therefor.” D Battle is founder of Angiotensin Therapeutics Inc. D Battle has received consulting fees from Advicenne unrelated to this work and received unrelated research support from a grant from AstraZeneca; G Randall reports consultancy agreements with Optikira. J Wysocki and J Henkin report scientific advisor capacity for Angiotensin Therapeutics Inc. All remaining authors have nothing to disclose related to this publication.

## References

1. Wan Y, Shang J, Graham R, Baric RS, Li F (2020) Receptor recognition by the novel coronavirus from wuhan: An analysis based on decade-long

From: Hassler et al (1), Intranasal soluble ACE2 improves survival and prevents brain SARS-CoV-2 infection. Life Science Alliance, Volume 6, No. 7, page 10, (not modified) <https://doi.org/10.26508/lsa.202301969> licensed under CC BY 4.0 <https://creativecommons.org/licenses/by/4.0/>

- structural studies of SARS coronavirus. *J Virol* 94: e00127-20. doi:10.1128/jvi.00127-20
2. Hoffmann M, Kleine-Weber H, Schroeder S, Kruger N, Herrler T, Erichsen S, Schiergens TS, Herrler G, Wu NH, Nitsche A, et al (2020) SARS-CoV-2 cell entry depends on ACE2 and TMPRSS2 and is blocked by a clinically proven protease inhibitor. *Cell* 181: 271–280.e8. doi:10.1016/j.cell.2020.02.052
  3. Battle D, Wysocki J, Satchell K (2020) Soluble angiotensin-converting enzyme 2: A potential approach for coronavirus infection therapy? *Clin Sci* 134: 543–545. doi:10.1042/cs20200163
  4. Monteil V, Kwon H, Prado P, Hagelkruys A, Wimmer RA, Stahl M, Leopoldi A, Garreta E, Hurtado Del Pozo C, Prosper F, et al (2020) Inhibition of SARS-CoV-2 infections in engineered human tissues using clinical-grade soluble human ACE2. *Cell* 181: 905–913.e7. doi:10.1016/j.cell.2020.04.004
  5. Wysocki J, Ye M, Hassler L, Gupta AK, Wang Y, Nicolescu V, Randall G, Wertheim JA, Battle D (2021) A novel soluble ACE2 variant with prolonged duration of action neutralizes SARS-CoV-2 infection in human kidney organoids. *J Am Soc Nephrol* 32: 795–803. doi:10.1681/asn.2020101537
  6. Battle D, Monteil V, Garreta E, Hassler L, Wysocki J, Chandar V, Schwartz RE, Mirazimi A, Montserrat N, Bader M, et al (2022) Evidence in favor of the essentiality of human cell membrane-bound ACE2 and against soluble ACE2 for SARS-CoV-2 infectivity. *Cell* 185: 1837–1839. doi:10.1016/j.cell.2022.05.004
  7. Teplensky MH, Distler ME, Kusmierz CD, Evangelopoulos M, Gula H, Elli D, Tomatsidou A, Nicolaescu V, Gelarden I, Yeldandi A, et al (2022) Spherical nucleic acids as an infectious disease vaccine platform. *Proc Natl Acad Sci U S A* 119: e2119093119. doi:10.1073/pnas.2119093119
  8. Hassler L, Wysocki J, Gelarden I, Sharma I, Tomatsidou A, Ye M, Gula H, Nicolescu V, Randall G, Pshenychnyi S, et al (2022) A novel soluble ACE2 protein provides lung and kidney protection in mice susceptible to lethal SARS-CoV-2 infection. *J Am Soc Nephrol* 33: 1293–1307. doi:10.1681/asn.2021091209
  9. McCray PB, Jr, Pewe L, Wohlford-Lenane C, Hickey M, Manzel L, Shi L, Nettand J, Jia HP, Halabi C, Sigmund CD, et al (2007) Lethal infection of K18-hACE2 mice infected with severe acute respiratory syndrome coronavirus. *J Virol* 81: 813–821. doi:10.1128/jvi.02012-06
  10. Winkler ES, Bailey AL, Kafai NM, Nair S, McCune BT, Yu J, Fox JM, Chen RE, Earnest JT, Keeler SP, et al (2020) SARS-CoV-2 infection of human ACE2-transgenic mice causes severe lung inflammation and impaired function. *Nat Immunol* 21: 1327–1335. doi:10.1038/s41590-020-0778-2
  11. Dong W, Mead H, Tian L, Park JG, Garcia JJ, Jaramillo S, Barr T, Kollath DS, Coyne VK, Stone NE, et al (2022) The K18-human ACE2 transgenic mouse model recapitulates non-severe and severe COVID-19 in response to an infectious dose of the SARS-CoV-2 virus. *J Virol* 96: e0096421. doi:10.1128/jvi.00964-21
  12. Zhang L, Dutta S, Xiong S, Chan M, Chan KK, Fan TM, Bailey KL, Lindeblad M, Cooper LM, Rong L, et al (2022) Engineered ACE2 decoy mitigates lung injury and death induced by SARS-CoV-2 variants. *Nat Chem Biol* 18: 342–351. doi:10.1038/s41589-021-00965-6
  13. Zhang L, Narayanan KK, Cooper L, Chan KK, Skeeters SS, Devlin CA, Aguhob A, Shirley K, Rong L, Rehman J, et al (2022) An ACE2 decoy can be administered by inhalation and potentially targets omicron variants of SARS-CoV-2. *EMBO Mol Med* 14: e16109. doi:10.15252/emmm.202216109
  14. Zheng J, Wong LYR, Li K, Verma AK, Ortiz ME, Wohlford-Lenane C, Leidinger MR, Knudson CM, Meyerholz DK, McCray PB, Jr, et al (2021) COVID-19 treatments and pathogenesis including anosmia in K18-hACE2 mice. *Nature* 589: 603–607. doi:10.1038/s41586-020-2943-z
  15. Chen Y, Sun L, Ullah I, Beaudoin-Bussieres G, Anand SP, Hederman AP, Tolbert WD, Sherburn R, Nguyen DN, Marchitto L, et al (2022) Engineered ACE2-Fc counters murine lethal SARS-CoV-2 infection through direct neutralization and Fc-effector activities. *Sci Adv* 8: eabn4188. doi:10.1126/sciadv.abn4188
  16. Golden JW, Cline CR, Zeng X, Garrison AR, Carey BD, Mucker EM, White LE, Shamblin JD, Brocato RL, Liu J, et al (2020) Human angiotensin-converting enzyme 2 transgenic mice infected with SARS-CoV-2 develop severe and fatal respiratory disease. *JCI Insight* 5: e142032. doi:10.1172/jci.insight.142032
  17. Oladunni FS, Park JG, Pino PA, Gonzalez O, Akhter A, Allue-Guardia A, Olmo-Fontanez A, Gautam S, Garcia-Vilanova A, Ye C, et al (2020) Lethality of SARS-CoV-2 infection in K18 human angiotensin-converting enzyme 2 transgenic mice. *Nat Commun* 11: 6122. doi:10.1038/s41467-020-19891-7
  18. Kumari P, Rothan HA, Natekar JP, Stone S, Pathak H, Strate PG, Arora K, Brinton MA, Kumar M (2021) Neuroinvasion and encephalitis following intranasal inoculation of SARS-CoV-2 in K18-hACE2 mice. *Viruses* 13: 132. doi:10.3390/v13010132
  19. Carossino M, Kenney D, O'Connell AK, Montanaro P, Tseng AE, Gertje HP, Grosz KA, Ericsson M, Huber BR, Kurnick SA, et al (2022) Fatal neurodissemination and SARS-CoV-2 tropism in K18-hACE2 mice is only partially dependent on hACE2 expression. *Viruses* 14: 535. doi:10.3390/v14030535
  20. Vidal E, Lopez-Figueroa C, Rodon J, Perez M, Brustolin M, Cantero G, Guallar V, Izquierdo-Useros N, Carrillo J, Blanco J, et al (2022) Chronological brain lesions after SARS-CoV-2 infection in hACE2-transgenic mice. *Vet Pathol* 59: 613–626. doi:10.1177/03009858211066841
  21. Xu J, Lazartigues E (2020) Expression of ACE2 in human neurons supports the neuro-invasive potential of COVID-19 virus. *Cell Mol Neurobiol* 42: 305–309. doi:10.1007/s10571-020-00915-1
  22. Xu J, Sriramula S, Xia H, Moreno-Walton L, Culicchia F, Domenig O, Poglitsch M, Lazartigues E (2017) Clinical relevance and role of neuronal AT1 receptors in ADAM17-mediated ACE2 shedding in neurogenic hypertension. *Circ Res* 121: 43–55. doi:10.1161/circresaha.116.310509
  23. Hoffmann M, Kruger N, Schulz S, Cossmann A, Rocha C, Kempf A, Nehlmeier I, Graichen L, Moldenhauer AS, Winkler MS, et al (2022) The Omicron variant is highly resistant against antibody-mediated neutralization: Implications for control of the COVID-19 pandemic. *Cell* 185: 447–456.e11. doi:10.1016/j.cell.2021.12.032
  24. Mannar D, Saville JW, Zhu X, Srivastava SS, Berezuk AM, Tuttle KS, Marquez AC, Sekirov I, Subramaniam S (2022) SARS-CoV-2 Omicron variant: Antibody evasion and cryo-EM structure of spike protein-ACE2 complex. *Science* 375: 760–764. doi:10.1126/science.abn7760
  25. Tada T, Zhou H, Dcosta BM, Samanovic MI, Chivukula V, Herati RS, Hubbard SR, Mulligan MJ, Landau NR (2022) Increased resistance of SARS-CoV-2 Omicron variant to neutralization by vaccine-elicited and therapeutic antibodies. *EBioMedicine* 78: 103944. doi:10.1016/j.ebiom.2022.103944
  26. VanBlargan LA, Errico JM, Halfmann PJ, Zost SJ, Crowe JE, Purcell LA, Kawaoka Y, Corti D, Fremont DH, Diamond MS (2022) An infectious SARS-CoV-2 B. 1.1. 529 Omicron virus escapes neutralization by therapeutic monoclonal antibodies. *Nat Med* 28: 490–495. doi:10.1038/s41591-021-01678-y
  27. Rössler A, Riepler L, Bante D, von Laer D, Kimpel J (2022) SARS-CoV-2 omicron variant neutralization in serum from vaccinated and convalescent persons. *N Engl J Med* 386: 698–700. doi:10.1056/nejmc2119236
  28. Planas D, Saunders N, Maes P, Guivel-Benhassine F, Planchais C, Buchrieser J, Bolland WH, Porrot F, Staropoli I, Lemoine F, et al (2022) Considerable escape of SARS-CoV-2 Omicron to antibody neutralization. *Nature* 602: 671–675. doi:10.1038/s41586-021-04389-z
  29. Cao Y, Wang J, Jian F, Xiao T, Song W, Yisimayi A, Huang W, Li Q, Wang P, An R, et al (2022) Omicron escapes the majority of existing SARS-CoV-2 neutralizing antibodies. *Nature* 602: 657–663. doi:10.1038/s41586-021-04385-3

From: Hassler et al (1), Intranasal soluble ACE2 improves survival and prevents brain SARS-CoV-2 infection. Life Science Alliance, Volume 6, No. 7, page 11, (not modified) <https://doi.org/10.26508/lsa.202301969> licensed under CC BY 4.0 <https://creativecommons.org/licenses/by/4.0/>

30. Liu L, Iketani S, Guo Y, Chan JF, Wang M, Liu L, Luo Y, Chu H, Huang Y, Nair MS, et al (2022) Striking antibody evasion manifested by the Omicron variant of SARS-CoV-2. *Nature* 602: 676–681. doi:10.1038/s41586-021-04388-0
31. He P, Liu B, Gao X, Yan Q, Pei R, Sun J, Chen Q, Hou R, Li Z, Zhang Y, et al (2022) SARS-CoV-2 Delta and Omicron variants evade population antibody response by mutations in a single spike epitope. *Nat Microbiol* 7: 1635–1649. doi:10.1038/s41564-022-01235-4
32. Iketani S, Liu L, Guo Y, Liu L, Chan JF, Huang Y, Wang M, Luo Y, Yu J, Chu H, et al (2022) Antibody evasion properties of SARS-CoV-2 Omicron sublineages. *Nature* 604: 553–556. doi:10.1038/s41586-022-04594-4
33. Takashita E, Kinoshita N, Yamayoshi S, Sakai-Tagawa Y, Fujisaki S, Ito M, Iwatsuki-Horimoto K, Chiba S, Halfmann P, Nagai H, et al (2022) Efficacy of antibodies and antiviral drugs against covid-19 omicron variant. *N Engl J Med* 386: 995–998. doi:10.1056/nejmc2119407
34. Higuchi Y, Suzuki T, Arimori T, Ikemura N, Mihara E, Kiritu Y, Ohgihara E, Mazda O, Motooka D, Nakamura S, et al (2021) Engineered ACE2 receptor therapy overcomes mutational escape of SARS-CoV-2. *Nat Commun* 12: 3802. doi:10.1038/s41467-021-24013-y
35. Havranek B, Chan KK, Wu A, Procko E, Islam SM (2021) Computationally designed ACE2 decoy receptor binds SARS-CoV-2 spike (S) protein with tight nanomolar affinity. *J Chem Inf Model* 61: 4656–4669. doi:10.1021/acs.jcim.1c00783
36. Hassler L, Penninger J, Batlle D (2022) On the essentiality of the angiotensin converting enzyme 2 receptor for SARS-CoV-2 infection and the potential of soluble angiotensin converting enzyme 2 proteins as universal approach for variants causing COVID-19. *Clin Translational Med* 12: e1080. doi:10.1002/ctm2.1080
37. Chan KK, Tan TJ, Narayanan KK, Procko E (2021) An engineered decoy receptor for SARS-CoV-2 broadly binds protein S sequence variants. *Sci Adv* 7: eabf1738. doi:10.1126/sciadv.abf1738
38. Schimpf A, Hempel F, Li A, Linne U, Maier UG, Reetz MT, Geyer A (2018) Hinge-type dimerization of proteins by a tetracysteine peptide of high pairing specificity. *Biochemistry* 57: 3658–3664. doi:10.1021/acs.biochem.8b00475
39. Seehusen F, Clark JJ, Sharma P, Bentley EG, Kirby A, Subramaniam K, Wunderlin-Giuliani S, Hughes GL, Patterson EI, Michael BD, et al (2022) Neuroinvasion and neurotropism by SARS-CoV-2 variants in the K18-hACE2 mouse. *Viruses* 14: 1020. doi:10.3390/v14051020
40. Netland J, Meyerholz DK, Moore S, Cassell M, Perlman S (2008) Severe acute respiratory syndrome coronavirus infection causes neuronal death in the absence of encephalitis in mice transgenic for human ACE2. *J Virol* 82: 7264–7275. doi:10.1128/jvi.00737-08
41. Fumagalli V, Rava M, Marotta D, Di Lucia P, Laura C, Sala E, Grillo M, Bono E, Giustini L, Perucchini C, et al (2022) Administration of aerosolized SARS-CoV-2 to K18-hACE2 mice uncouples respiratory infection from fatal neuroinvasion. *Sci Immunol* 7: eabl9929. doi:10.1126/sciimmunol.abl9929
42. Ito D, Imai Y, Ohsawa K, Nakajima K, Fukuuchi Y, Kohsaka S (1998) Microglia-specific localisation of a novel calcium binding protein, Iba1. *Mol Brain Res* 57: 1–9. doi:10.1016/s0169-328x(98)00040-0
43. Tykhomyrov A, Pavlova A, Nedzvetsky V (2016) Glial fibrillary acidic protein (GFAP): On the 45th anniversary of its discovery. *Neurophysiology* 48: 54–71. doi:10.1007/s11062-016-9568-8
44. Etter MM, Martins TA, Kulsvehagen L, Possneck E, Duchemin W, Hogan S, Sanabria-Diaz G, Muller J, Chiappini A, Rycken J, et al (2022) Severe neuro-COVID is associated with peripheral immune signatures, autoimmunity and neurodegeneration: A prospective cross-sectional study. *Nat Commun* 13: 6777. doi:10.1038/s41467-022-34068-0
45. Schwabenland M, Salie H, Tanevski J, Killmer S, Lago MS, Schlaak AE, Mayer L, Matschke J, Puschel K, Fitzek A, et al (2021) Deep spatial profiling of human COVID-19 brains reveals neuroinflammation with distinct microanatomical microglia-T-cell interactions. *Immunity* 54: 1594–1610.e11. doi:10.1016/j.immuni.2021.06.002
46. Matschke J, Lutgehetmann M, Hagel C, Sperhake JP, Schroder AS, Edler C, Mushumba H, Fitzek A, Allweiss L, Dandri M, et al (2020) Neuropathology of patients with COVID-19 in Germany: A post-mortem case series. *Lancet Neurol* 19: 919–929. doi:10.1016/s1474-4422(20)30308-2
47. Zhang H, Penninger JM, Li Y, Zhong N, Slutsky AS (2020) Angiotensin-converting enzyme 2 (ACE2) as a SARS-CoV-2 receptor: Molecular mechanisms and potential therapeutic target. *Intensive Care Med* 46: 586–590. doi:10.1007/s00134-020-05985-9
48. Tipnis SR, Hooper NM, Hyde R, Karran E, Christie G, Turner AJ (2000) A human homolog of angiotensin-converting enzyme: Cloning and functional expression as a captopril-insensitive carboxypeptidase. *J Biol Chem* 275: 33238–33243. doi:10.1074/jbc.m002615200
49. Donoghue M, Hsieh F, Baronas E, Godbout K, Gosselin M, Stagliano N, Donovan M, Woolf B, Robison K, Jeyaseelan R, et al (2000) A novel angiotensin-converting enzyme-related carboxypeptidase (ACE2) converts angiotensin I to angiotensin 1-9. *Circ Res* 87: E1–E9. doi:10.1161/01.res.87.5.e1
50. Serfozo P, Wysocki J, Gulua G, Schulze A, Ye M, Liu P, Jin J, Bader M, Myöhänen T, Garcia-Horsman JA, et al (2020) Ang II (angiotensin II) conversion to angiotensin-(1-7) in the circulation is POP (Prolyloligopeptidase)-Dependent and ACE2 (Angiotensin-Converting enzyme 2)-independent. *Hypertension* 75: 173–182. doi:10.1161/hypertensionaha.119.14071
51. Imai Y, Kuba K, Penninger JM (2007) Angiotensin-converting enzyme 2 in acute respiratory distress syndrome. *Cell Mol Life Sci* 64: 2006–2012. doi:10.1007/s00018-007-6228-6
52. Sodhi CP, Wohlford-Lenane C, Yamaguchi Y, Prindle T, Fulton WB, Wang S, McCray PB, Jr, Chappell M, Hackam DJ, Jia H (2018) Attenuation of pulmonary ACE2 activity impairs inactivation of des-Arg9 bradykinin/BKB1R axis and facilitates LPS-induced neutrophil infiltration. *Am J Physiol Lung Cell Mol Physiol* 314: L17–L31. doi:10.1152/ajplung.00498.2016
53. Kuba K, Imai Y, Rao S, Gao H, Guo F, Guan B, Huan Y, Yang P, Zhang Y, Deng W, et al (2005) A crucial role of angiotensin converting enzyme 2 (ACE2) in SARS coronavirus-induced lung injury. *Nat Med* 11: 875–879. doi:10.1038/nm1267
54. Davidson AM, Wysocki J, Batlle D (2020) Interaction of SARS-CoV-2 and other coronavirus with ACE (angiotensin-converting enzyme)-2 as their main receptor: Therapeutic implications. *Hypertension* 76: 1339–1349. doi:10.1161/hypertensionaha.120.15256
55. Yamaguchi T, Hoshizaki M, Minato T, Nirasawa S, Asaka MN, Niyama M, Imai M, Uda A, Chan JF, Takahashi S, et al (2021) ACE2-like carboxypeptidase B38-CAP protects from SARS-CoV-2-induced lung injury. *Nat Commun* 12: 6791. doi:10.1038/s41467-021-27097-8
56. Wysocki J, Ye M, Khattab AM, Fogo A, Martin A, David NV, Kanwar Y, Osborn M, Batlle D (2017) Angiotensin-converting enzyme 2 amplification limited to the circulation does not protect mice from development of diabetic nephropathy. *Kidney Int* 91: 1336–1346. doi:10.1016/j.kint.2016.09.032
57. Haschke M, Schuster M, Poglitsch M, Loibner H, Salzberg M, Bruggisser M, Penninger J, Krähenbühl S (2013) Pharmacokinetics and pharmacodynamics of recombinant human angiotensin-converting enzyme 2 in healthy human subjects. *Clin Pharmacokinet* 52: 783–792. doi:10.1007/s40262-013-0072-7
58. Wysocki J, Ye M, Rodriguez E, González-Pacheco FR, Barrios C, Evora K, Schuster M, Loibner H, Brosnihan KB, Ferrario CM, et al (2010) Targeting the degradation of angiotensin II with recombinant angiotensin-converting enzyme 2: Prevention of angiotensin II-dependent hypertension. *Hypertension* 55: 90–98. doi:10.1161/hypertensionaha.109.138420
59. Trembl B, Neu N, Kleinsasser A, Gritsch C, Finsterwalder T, Geiger R, Schuster M, Janzek E, Loibner H, Penninger J, et al (2010) Recombinant

- angiotensin-converting enzyme 2 improves pulmonary blood flow and oxygenation in lipopolysaccharide-induced lung injury in piglets. *Crit Care Med* 38: 596–601. doi:[10.1097/ccm.0b013e3181c03009](https://doi.org/10.1097/ccm.0b013e3181c03009)
60. Gawish R, Starkl P, Pimenov L, Hladik A, Lakovits K, Oberndorfer F, Cronin SJ, Ohradanova-Repic A, Wirnsberger G, Agerer B, et al (2022) ACE2 is the critical in vivo receptor for SARS-CoV-2 in a novel COVID-19 mouse model with TNF- and IFN $\gamma$ -driven immunopathology. *Elife* 11: e74623. doi:[10.7554/eLife.74623](https://doi.org/10.7554/eLife.74623)
  61. Moreau GB, Burgess SL, Sturek JM, Donlan AN, Petri WA, Jr, Mann BJ (2020) Evaluation of K18-hACE2 mice as a model of SARS-CoV-2 infection. *Am J Trop Med Hyg* 103: 1215–1219. doi:[10.4269/ajtmh.20-0762](https://doi.org/10.4269/ajtmh.20-0762)
  62. Rathnasinghe R, Strohmeier S, Amanat F, Gillespie VL, Krammer F, García-Sastre A, Coughlan L, Schotsaert M, Uccellini MB (2020) Comparison of transgenic and adenovirus hACE2 mouse models for SARS-CoV-2 infection. *Emerging microbes & infections* 9: 2433–2445. doi:[10.1080/22221751.2020.1838955](https://doi.org/10.1080/22221751.2020.1838955)
  63. Ye M, Wysocki J, Naaz P, Salabat MR, LaPointe MS, Battle D (2004) Increased ACE 2 and decreased ACE protein in renal tubules from diabetic mice: A renoprotective combination? *Hypertension* 43: 1120–1125. doi:[10.1161/01.hyp.0000126192.27644.76](https://doi.org/10.1161/01.hyp.0000126192.27644.76)
  64. Ye M, Wysocki J, Gonzalez-Pacheco FR, Salem M, Evora K, Garcia-Halpin L, Poglitsch M, Schuster M, Battle D (2012) Murine recombinant angiotensin-converting enzyme 2: Effect on angiotensin II-dependent hypertension and distinctive angiotensin-converting enzyme 2 inhibitor characteristics on rodent and human angiotensin-converting enzyme 2. *Hypertension* 60: 730–740. doi:[10.1161/hypertensionaha.112.198622](https://doi.org/10.1161/hypertensionaha.112.198622)
  65. Wysocki J, Lores E, Ye M, Soler MJ, Battle D (2020) Kidney and lung ACE2 expression after an ACE inhibitor or an ang II receptor blocker: Implications for COVID-19. *J Am Soc Nephrol* 31: 1941–1943. doi:[10.1681/asn.2020050667](https://doi.org/10.1681/asn.2020050667)



**License:** This article is available under a Creative Commons License (Attribution 4.0 International, as described at <https://creativecommons.org/licenses/by/4.0/>).

From: Hassler et al (1), Intranasal soluble ACE2 improves survival and prevents brain SARS-CoV-2 infection. Life Science Alliance, Volume 6, No. 7, page 13, (not modified) <https://doi.org/10.26508/lsa.202301969> licensed under CC BY 4.0 <https://creativecommons.org/licenses/by/4.0/>

**CV**

Mein Lebenslauf wird aus datenschutzrechtlichen Gründen in der elektronischen Version meiner Arbeit nicht veröffentlicht.



---

## Complete list of publications

### Paper:

1. Cianfarini C, Hassler L, Wysocki J, Hassan A, Nicolaescu V, Elli D, ... & Batlle D. Soluble Angiotensin-Converting Enzyme 2 Protein Improves Survival and Lowers Viral Titers in Lethal Mouse Model of Severe Acute Respiratory Syndrome Coronavirus Type 2 Infection with the Delta Variant. *Cells*. 2024;13(3):203.
2. Hassler, L., Wysocki, J., Ahrendsen, J. T., Ye, M., Gelarden, I., Nicolaescu, V., ... & Batlle, D. (2023). Intranasal soluble ACE2 improves survival and prevents brain SARS-CoV-2 infection. *Life Science Alliance*, 6(7).
3. Hassler, L., Penninger, J. & Batlle, D. (2022). On the essentiality of the angiotensin converting enzyme 2 receptor for SARS-CoV-2 infection and the potential of soluble angiotensin converting enzyme 2 proteins as universal approach for variants causing COVID-19. *Clinical and Translational Medicine*, 2022;12:e1080.
4. Lin, H., Geurts, F., Hassler, L., Batlle, D., Colafella, K. M. M., Denton, K. M., ... & Danser, A. J. (2022). Kidney Angiotensin in Cardiovascular Disease: Formation and Drug Targeting. *Pharmacological Reviews*, 74(3), 462-505.
5. Batlle, D., Monteil, V., Garreta, E., Hassler, L., Wysocki, J., Chandar, V., ... & Penninger, J. M. (2022). Evidence in favor of the essentiality of human cell membrane-bound ACE2 and against soluble ACE2 for SARS-CoV-2 infectivity. *Cell*, 185(11), 1837-1839.
6. Hassler, L., Wysocki, J., Gelarden, I., Sharma, I., Tomatsidou, A., Ye, M., ... & Batlle, D. (2022). A Novel Soluble ACE2 Protein Provides Lung and Kidney Protection in Mice Susceptible to Lethal SARS-CoV-2 Infection. *Journal of the American Society of Nephrology* 33 (7) 1293-1307
7. Hassler, L. and Batlle, D. "Potential SARS-CoV-2 kidney infection and paths to injury." *Nature Reviews Nephrology* 18.5 (2022): 275-276.

8. Hassler, L., Reyes, F., Sparks, M. A., Welling, P., & Battle, D. (2021). Evidence for and against direct kidney infection by SARS-CoV-2 in patients with COVID-19. *Clinical Journal of the American Society of Nephrology*, 16(11), 1755-1765.
9. Wysocki, J., Ye, M., Hassler, L., Gupta, A. K., Wang, Y., Nicoleascu, V., ... & Battle, D. (2021). A novel soluble ACE2 variant with prolonged duration of action neutralizes SARS-CoV-2 infection in human kidney organoids. *Journal of the American Society of Nephrology*, 32(4), 795-803.

## **Acknowledgements**

I would like to express my gratitude to Prof. Dr. Daniel Battle, my supervisor at Northwestern University, Chicago, for the opportunity to be a part of his laboratory. His passion for research continues to inspire me and I am very grateful to have such a supportive mentor nurturing my interest in research. Moreover, I would like to give special thanks to Dr. Jan Wysocki, M.D./PhD, for his constant encouragement and support while teaching me how to work in the lab; his kindness and patience were much appreciated. I would also like to express my gratitude to Prof. Dr. Michael Bader, my supervisor at Max-Delbrück-Centrum, Berlin, for his support during the completion of my dissertation and always answering any upcoming questions promptly. I would also like to thank Dr. Jack Henkin, PhD, for productive and helpful discussions during my time in the Battle lab. Additionally, I would like to thank Minghao Ye, Fernando Marmol, Atthar Baig and Mohammed Badaruddin for their support during my time in the Battle lab. I would also like to thank the Biomedical exchange program (BMEP) for providing a stipend that supported a part of my stay in Chicago. Finally, I would like to thank my personal support system: Oscar Guzman for his love and understanding during our time together in Chicago; and most importantly Almut, Thomas and Klara Hassler for their continuous love, support and encouragement from the very beginning to the very end of this dissertation.